# *Hox* genes and the regulation of programmed cell death in the embryonic central nervous system of *Drosophila melanogaster*

Dissertation
zur Erlangung des Grades
**Doktor der Naturwissenschaften**

**Am Fachbereich Biologie**
**der Johannes Gutenberg-Universität Mainz**

Ana Rogulja-Ortmann
Mainz, März 2009

Dekan:

1. Berichterstatter:
2. Berichterstatter:

Datum der mündlichen Prüfung: 30.04.2009

# Chapter index

1. Introduction ..... 1
1.1. Development of the *Drosophila* central nervous system ..... 1
1.2. *Hox* genes in CNS development ..... 5
1.2.1. Early function of *Hox* genes ..... 6
1.2.2. Late functions of *Hox* genes ..... 8
1.3. Programmed cell death ..... 8
1.4. Aims ..... 11

2. Materials and methods ..... 12
2.1. Fly food media ..... 12
2.1.1. Fly stock maintenance ..... 12
2.1.2. Apple juice agar ..... 12
2.2. Fly stocks ..... 12
2.3. Genetic crosses ..... 14
2.4. Ectopic gene expression ..... 14
2.4.1. The Gal4/UAS system ..... 14
2.4.2. The heat shock system ..... 15
2.5. Embryo collection ..... 15
2.6. Heat-shock procedure ..... 16
2.7. Immunohistochemistry ..... 16
2.7.1. Antibodies ..... 16
2.7.2. Fixation of embryos for antibody staining and *in situ R*NA hybridization ..... 18
2.7.3. Preparation and fixation of L1 larval CNS ..... 19
2.7.4. Incubation in antibody solutions ..... 19
2.7.4.1. Fluorescent staining ..... 19
2.7.4.2. Color staining ..... 20
2.8. RNA *in situ* hybridization ..... 20
2.8.1. Generation of a *reaper* riboprobe ..... 21
2.8.2. Hybridization ..... 21
2.8.3. Signal detection ..... 22

2.9. Image detection and documentation ..... 23
2.10. Chemicals and solutions ..... 23
2.11. Equipment and software ..... 25

3. Results ..... 27
A. Programmed cell death in the developing embryonic central nervous system ..... 27
3.1. CNS morphology of apoptosis-deficient embryos ..... 28
3.2. Identification of apoptotic cells in the CNS of wild type embryos ..... 31
3.2.1. Markers with broad expression domains ..... 33
3.2.2. Markers expressed in small groups of cells ..... 35
B. Regulation of apoptosis in identified dying neurons in the embryonic CNS ..... 42
3.3. Segment-specific apoptosis of U motoneurons ..... 42
3.3.1. Expression of *Antennapedia* in U motoneurons ..... 42
3.3.2. Expression of the *bithorax* complex genes in U motoneurons ..... 43
3.4. Segment-specific apoptosis of the GW and the NB2-4t anterior motoneuron ..... 45
3.4.1. The NB7-3 lineage ..... 45
3.4.2. The NB2-4t lineage ..... 50
3.5. Expression pattern of *Ultrabithorax* in the NB7-3 and NB2-4t lineages ..... 53
3.5.1. *Ubx* expression in NB7-3 ..... 53
3.5.2. *Ubx* and *abdA* determine segment-specific NB7-3 identity ..... 55
3.5.3. *Ubx* expression in NB2-4 ..... 58
3.5.4. How is the differential regulation of *Ubx* in the NB7-3 lineage of segment T2 achieved? ..... 58
3.6. *Ubx* is necessary and sufficient to induce apoptosis in the GW and MNa motoneurons ..... 61
3.6.1. Exploring the cell context-specific effect of *Ubx* ..... 66
3.7. Initiation of apoptosis is a late function of *Ubx* ..... 70
3.8. *Antp* is necessary and sufficient for survival of the GW motoneuron ..... 73
3.9. *Ubx* prevents *Antp* from promoting survival of the GW motoneuron ..... 77

4. Discussion ..... 86
4.1. The CNS of apoptosis-deficient embryos does not appear grossly perturbed ..... 87
4.2. Specification of supernumerary neural cells in apoptosis-deficient embryos ..... 87
4.2.1. Supernumerary cells cannot be specified as glia ..... 87
4.2.2. Some supernumerary cells can differentiate into neurons ..... 88
4.2.3. On the origins of supernumerary cells in apoptosis-deficient embryos ..... 89
4.3. Involvement of *Hox* genes in developmental apoptosis in the CNS ..... 90
4.3.1. *Abdominal-B* may be involved in apoptosis of U motoneurons ..... 91
4.4. A dual requirement for *Ubx* in the development of the NB7-3 and NB2-4 lineages ..... 92
4.5. The ability of *Ubx* to induce apoptosis is context dependent ..... 93
4.6. *Ubx* counteracts *Antp* to induce programmed cell death ..... 96
4.7. *Hox* gene dependent apoptosis as a mechanism for CNS patterning ..... 98

5. Summary ..... 100

6. References ..... 102

7. Appendix ..... 112
Abbreviation index ..... 112
Declaration ..... 114

# 1. Introduction

The body plan of many animals is composed of groups of homologous structures (e.g. somites in vertebrates or body segments in the fruitfly *Drosophila melanogaster*) that, over the course of development, achieve amazing morphological and functional diversity along the body axis. The organ with the highest degree of complexity and cellular diversity is the central nervous system, as here diverse regional requirements for control of locomotion, respiration, reproduction etc. need to be fulfilled. Understanding how this morphological and functional pattern diversity arises during development is one of the fundamental challenges in biology. We know today that it requires a precisely controlled balance between cell proliferation, differentiation and death. However, the regulatory mechanisms controlling these processes and how they are integrated to allow regional specification are not well understood.

*Drosophila melanogaster* represents a widely used model organism for investigations into patterning mechanisms. During my thesis work, I have attempted to add a small piece to the puzzle of central nervous system patterning by examining what role programmed cell death, or apoptosis, plays in the generation of segmental diversity in the *Drosophila* embryonic central nervous system, and by investigating which developmental regulators are involved in controlling it.

## 1.1. Development of the *Drosophila* central nervous system

The nervous system of *Drosophila* is composed of the central nervous system (CNS), comprising the ventral nerve cord (VNC) and the brain proper, and the peripheral nervous system (PNS). Each part of the CNS develops from a specific region of the ectoderm: the VNC from the ventral neurogenic region (vNR) and the brain from the procephalic neurogenic region (pNR) (Fig. 1-1A). The vNR can be

further subdivided into two regions, the mesectoderm and the neuroectoderm (Fig. 1-1B). The mesectoderm gives rise to the midline precursors (Poulson, 1950), which in turn generate the midline neurons and glia. The neuroectoderm gives rise to neural precursor cells, the so-called neuroblasts (NBs) that generate the neurons and glia of the VNC (Campos-Ortega, 1993) (Fig. 1-1C). The VNC is organized in 14 bilaterally symmetrical ganglia, also referred to as neuromeres: three gnathal (head), three thoracic and eight abdominal ones.

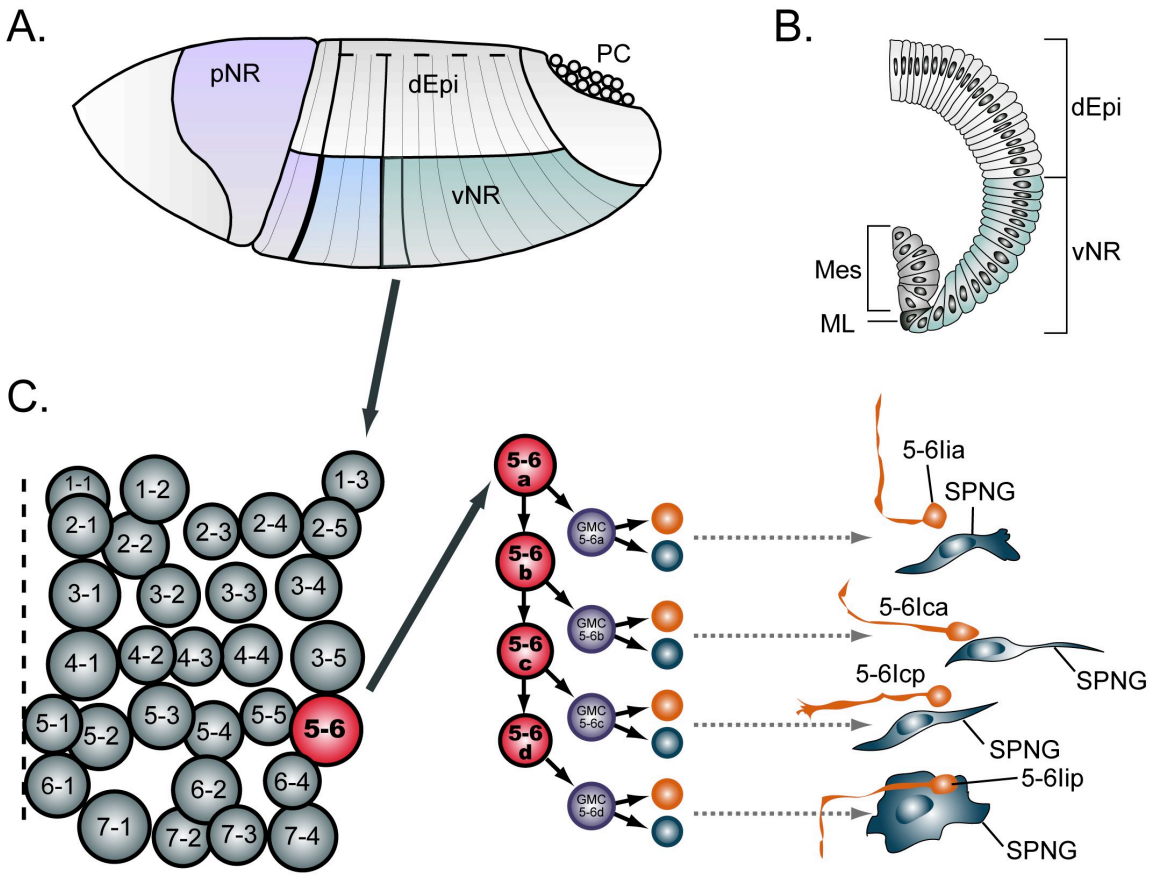


**Fig. 1-1. Scheme of neurogenesis in the *Drosophila* embryo.**

A. Fatemap of the early embryo (gastrula stage). The procephalic neurogenic region (pNR, lilac) of the neuroectoderm gives rise to the brain. The thoracic (blue) and abdominal (green) parts of the ventral nerve cord originate from the ventral neurogenic region (vNR). dEpi = dorsal epidermis; PC = pole cells. Anterior is left.
B. Cross-section of a gastrulating embryo showing two regions of the vNR: the midline (ML), deriving from the mesectoderm, and the neurogenic region (vNR), deriving from the ectoderm. Mes = mesoderm.
C. 30 neuroblasts (NBs) per hemineuromere delaminate in a segmentally repeated pattern. Each NB generates a characteristic, invariant lineage by dividing in a stem-cell mode. One ganglion mother cell (GMC) is generated with each division and divides only once. The progeny cells differentiate into neurons (orange) and/or glia (blue). Shown is the lineage of the NB5-6. Each neuron develops characteristic projections (5-6lia, 5-6lca, 5-6lcp, 5-6lip). The glial cells differentiate into subperineurial glia (SPNG). Anterior is up. The dashed line marks the midline.
Kindly provided by C. Berger and C. Rickert.

The patterning of the neuroectoderm is underway already in the early gastrula (Udolph et al., 1995), and appears to be set up by the expression of pair-rule and segment polarity genes along the anteroposterior (AP) axis, and the dorso-ventral patterning genes along the dorsoventral (DV) axis (Hassan and Vaessin, 1996; Skeath, 1999). These control expression of proneural genes of the *achaete-scute* complex (AS-C) (Martin-Bermudo et al., 1991; Skeath and Carroll, 1992; Villares and Cabrera, 1987), which in turn promote the formation of proneural clusters in the neuroectoderm (Fig.1-2A). Proneural clusters are groups of five to seven neuroectodermal cells that all express AS-C genes and thus have the potential to become a NB. In the next phase of neurogenesis one cell out of this cluster is singled out in a process called lateral inhibition (Fig. 1-2B), which is controlled by neurogenic genes of the Notch signaling pathway. The presumptive NB expresses the Notch ligand Delta on its membrane and thus activates the Notch signaling pathway in its neighbors. This in turn results in downregulation of the AS-C genes and loss of neural potential in the neighboring cells (Artavanis-Tsakonas and Simpson, 1991; Campos-Ortega, 1993), rendering the presumptive NB the only neural cell in the cluster. It then delaminates into the interior of the embryo, whereas the other cells remain in the neuroectoderm and develop into epidermoblasts. Once delaminated, the NB undergoes a series of asymmetric, stem cell-like divisions through which the NB is regenerated and a chain of smaller ganglion mother cells (GMCs) is produced. Each GMC then typically divides only once to generate two daughter cells that differentiate into neurons and/or glia (Campos-Ortega and Hartenstein, 1997) (Fig. 1-1C).

In each neuromere, about 30 NBs delaminate in 5 sequential waves (S1-S5). The number of divisions and the type of cell lineage that each individual NB generates are unique and almost invariant (Bossing et al., 1996; Schmid et al., 1999; Schmidt et al., 1997). This reflects the specific identity that a NB has acquired through its positional information within the segment and the timing of formation in the neuroectoderm (Fig. 1-2C,D), and through the combination of regulatory genes it expresses (Fig. 1-3). As this information is almost identical in the thoracic and abdominal segments, NBs delaminating at the same position in different segments along the AP axis are considered serial homologs. However, NBs also receive information about their position on the AP axis, which is mediated

by the expression of homeotic (*Hox*) genes. Thus, in addition to intrasegmental NB identity, determined by segmentation and dorsoventral patterning genes, a segment-specific identity is imposed on the NB through the expression of *Hox* genes (intersegmental specification).

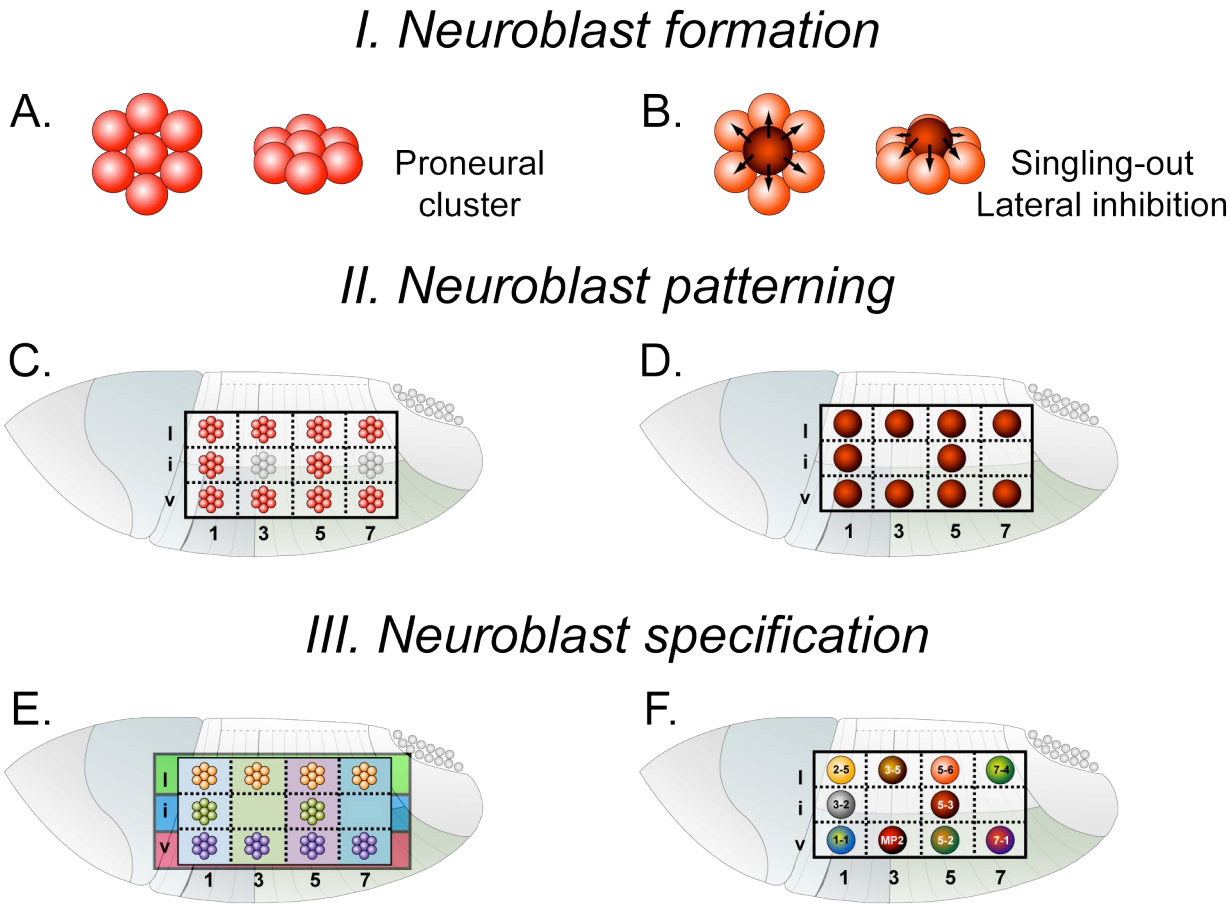


**Fig. 1-2. Formation, patterning and specification of neuroblasts.**
I. Neuroblast formation
A. Expression of proneural genes of the *achaete-scute* complex (AS-C, red) leads to the formation of a proneural cluster. In this phase all cells of the cluster have the competence to become neuroblasts (NB). B. The cell with the highest level of AS-C gene expression (dark red) is selected from the proneural cluster (singling-out) and inhibits proneural gene expression in its neighbors through lateral inhibition. The selected cell then enlarges and delaminates into the embryo as a NB.
II. Neuroblast patterning
C. Scheme of an early embryo, with one hemisegment enlarged. The S1 proneural cluster pattern is shown in red. Each hemisegment is thus divided into four rows (1, 3, 5, 7) and three columns (v, ventral; i, intermediate and l, lateral). D. One NB (dark red) delaminates out of each proneural cluster. This results in an NB pattern that exactly mirrors the earlier pattern of proneural clusters. Anterior is to the left, ventral is down in both images.
III. Neuroblast specification
E. The ventral (v), intermediate (i) and lateral (l) columns are defined by the expression of columnar genes (light red, blue and green, respectively) whereas the rows are defined by expression of segment polarity genes (1, light blue; 3, light green; 5, lilac; 7, turquoise). Each proneural cluster thus expresses a unique combination of genes. F. Based on the unique set of genes expressed in each proneural cluster and on the time of delamination, each NB acquires a unique identity (indicated by color codes). Anterior is to the left, ventral is down in both images.
Modified after Skeath (1999) and kindly provided by C. Berger.

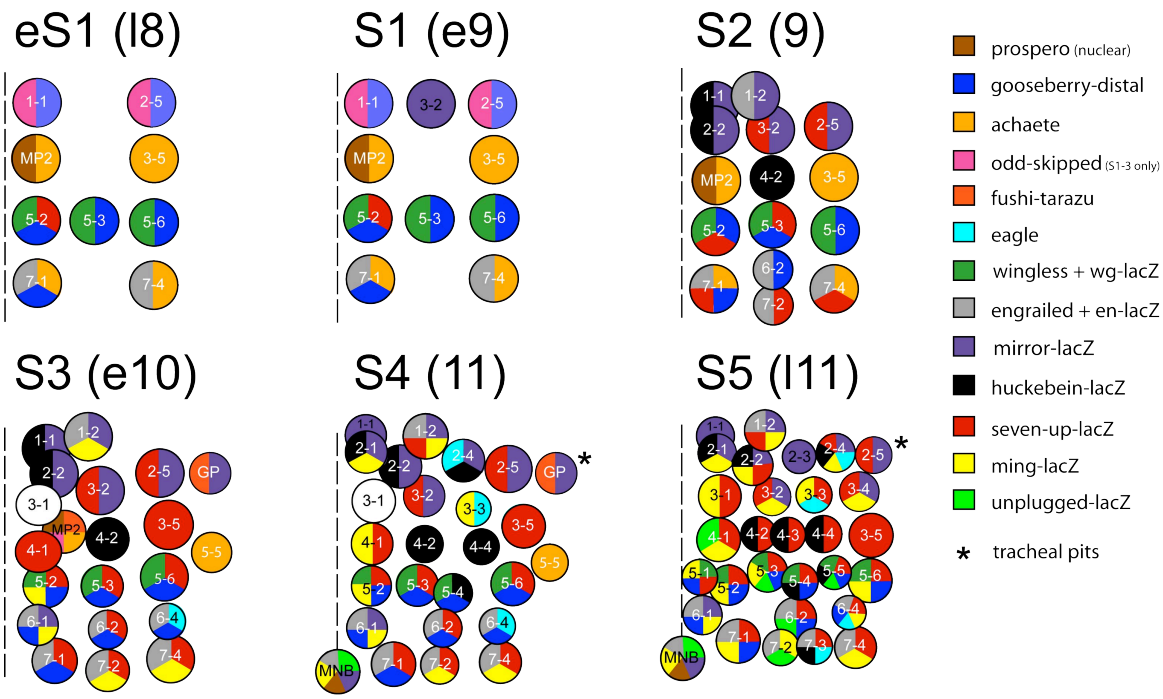


**Fig. 1-3.The neuroblast map.**
Each NB delaminates in a specific delamination wave (S1-S5) which also determines the combination of markers it expresses. This marker combination, the position in the hemineuromere and the time of delamination give each NB its unique identity and allow its identification. Anterior is up. The dashed line marks the midline, the asterisk the position of the tracheal pits. Modified after Doe (1992) and Broadus et al. (1995), and kindly provided by C. Rickert.

## 1.2. *Hox* genes in CNS development

Many studies over the years have shown that Hox proteins, a conserved group of homeodomain transcription factors, function in the morphological diversification of segments along the AP body axis of both vertebrates and invertebrates, and that they do so through regulation of transcriptional networks and signaling pathways (Mann and Morata, 2000; McGinnis and Krumlauf, 1992). *Drosophila Hox* genes are grouped in two complexes, whose members regulate the different segment identities: the *Antennapedia* complex (ANT-C) and the *bithorax* complex (BX-C) (Kaufman et al., 1990; Lewis, 1978). ANT-C contains the *Hox* genes *labial* (*lab*), *proboscipedia* (*pb*), *Deformed* (*Dfd*), *Sex combs reduced* (*Scr*) and *Antennapedia* (*Antp*), which specify segment identities in the head and anterior thorax (Kaufman et al., 1990). The posterior thorax and abdomen are specified by the genes of the BX-C, *Ultrabithorax* (*Ubx*), *abdominal-A* (*abdA*) and *Abdominal-B* (*AbdB*) (Lewis, 1978).

### 1.2.1. Early function of *Hox* genes

*Hox* genes have also been shown to dictate segment specific NB division patterns and progeny specification in the early *Drosophila* CNS. There are at least seven serially homologous NBs that generate different lineages in the thorax and abdomen (Bossing et al., 1996; Schmidt et al., 1997) (Table 1-1). For example, NB1-1 generates both neurons and glia in the thorax and a purely neuronal lineage in the abdomen (Fig. 1-4A). The tagma-specific identity of NB1-1 is determined already in the neuroectoderm, at the early gastrula stage (Prokop and Technau, 1994), with the thoracic identity probably being the "ground" state, as it requires no *Hox* gene input. The *Hox* genes *Ubx* and *abdA* are required to specify its abdominal identity. Similarly, the thoracic lineage of NB6-4, composed of neurons and glia (Schmidt et al., 1997), appears to develop without input of *Hox* genes, but requires *abdA* or *AbdB* to induce the abdominal fate, consisting exclusively of glia (Berger et al., 2005) (Fig. 1-4B). Both of these lineages, and a few others (Table 1-1), differ between thorax and abdomen in the composition of cell types. Other NBs, e.g. NB2-4 or NB5-4 (Schmidt et al., 1997) (Fig. 1-4C,D), produce lineages composed only of neurons in both tagmata, but the number of progeny they generate differs considerably between thorax and abdomen. It remains to be seen whether *Hox* genes influence the tagma specific NB proliferation patterns as well.

| NBs generating different cell types | NBs generating different cell numbers |
|---|---|
| NB1-1 | NB2-4 |
| NB2-2 | NB3-1 |
| NB5-6 | NB5-4 |
| NB6-4 | |

Table 1-1. NBs showing tagma-specific differences in cell type or cell number.

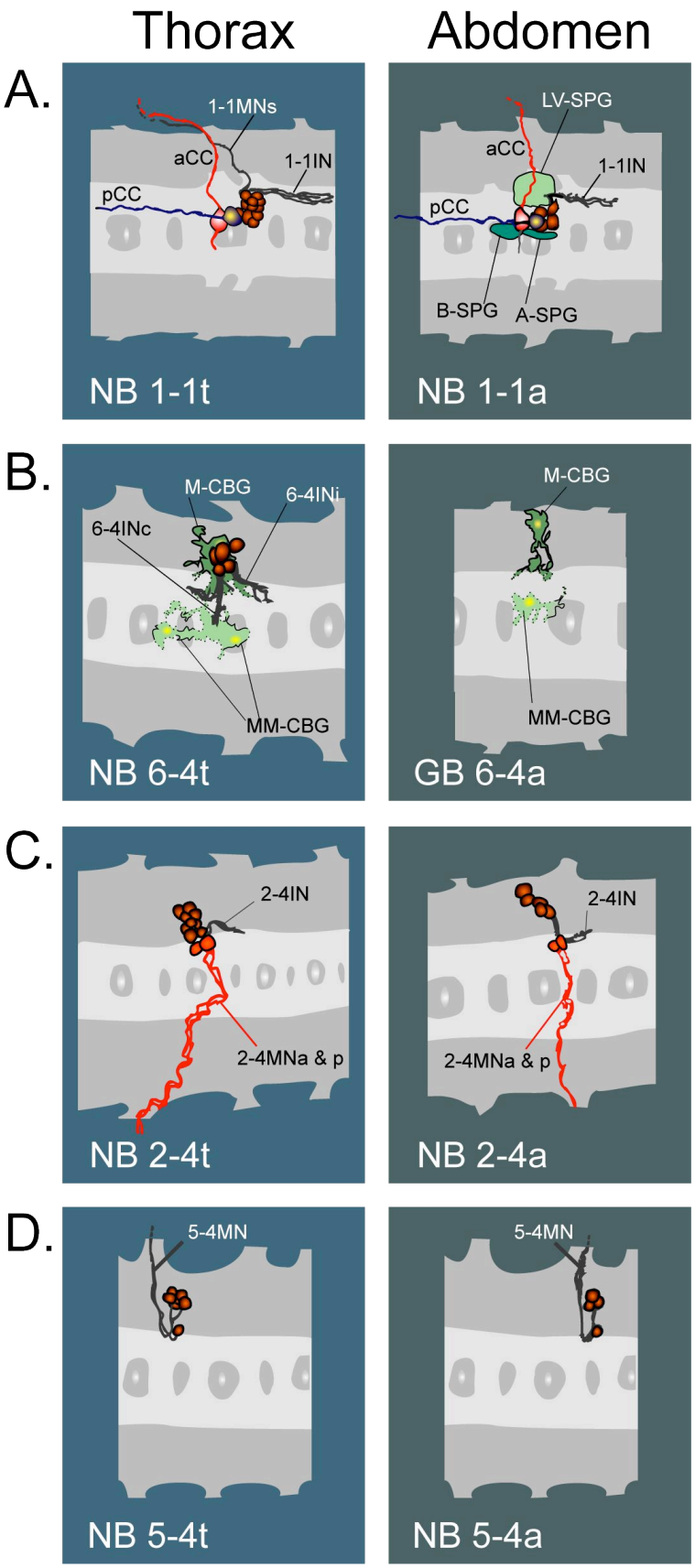


**Fig. 1-4. Some NBs generate tagma-specific lineages.**
These can comprise different types of cells (A,B) or different numbers of the same type of cells (C,D).
A. NB1-1 comprises only neurons in the thorax, and neurons and glia in the abdomen.
B. NB6-4 generates neurons and glia in the thorax and only glia in the abdomen.
C. NB2-4 generates only neurons, but in a greater number in the thorax than in the abdomen.
D. NB5-4 is a purely motoneuronal lineage, comprising more cells in the thorax.
Kindly provided by C. Rickert.

### 1.2.2. Late functions of *Hox* genes

In addition to their early role as master regulators of segment diversity, the *Hox* 'selector' genes can directly affect the so-called 'realizator genes' which regulate e.g. cell adhesion, migration, proliferation and apoptosis (Garcia-Bellido, 1975; Hombria and Lovegrove, 2003; Pearson et al., 2005). In *Drosophila* larvae, *Hox* genes have been suggested to orchestrate the assembly of neuromuscular networks that control region-specific peristaltic movements in crawling (Dixit et al., 2008). In the embryonic CNS, Hox proteins continue to be expressed throughout development, and are present in neurons at the time when they begin growing out axons and dendrites and making synaptic connections with their targets (Hirth et al., 1998). In chick embryos, a *Hox* regulatory network has been shown to regulate identities of different pools of spinal cord motoneurons (Dasen et al., 2003) and, later in development, to direct connectivity of the same motoneurons to specific muscle targets in the limb (Dasen et al., 2005).

Within the last decade, several reports have emerged describing an involvement of *Hox* genes in regulating developmental programmed cell death in various tissues and organs including the CNS (Economides et al., 2003; Liu et al., 2006; Lohmann et al., 2002). In the *Drosophila* embryo, *Dfd* directly induces transcription of the proapoptotic gene *reaper* (*rpr*) to sculpt the border between two head segments (Lohmann et al., 2002). *AbdB* expression ensures survival of differentiated pioneer neurons in the posterior neuromeres of the embryo (Miguel-Aliaga and Thor, 2004), and *abdA* is required to induce apoptosis of larval abdominal neuroblasts, thus limiting neuronal numbers in abdominal segments (Bello et al., 2003). These reports also reveal programmed cell death as one of the mechanisms through which *Hox* genes act to control morphogenesis and organogenesis at the single cell level.

## 1.3. Programmed cell death

The above studies also underscore the importance of programmed cell death or apoptosis in patterning the nervous system, as it enables selective removal of misplaced cells or of cells that have fulfilled their role in development and may

disturb the highly refined circuitry required for control of locomotion. Apoptosis is abundant also in the embryonic CNS of *Drosophila* and occurs both in apparently random cells, and in a regular, segmentally repeated pattern (Abrams et al., 1993; Rogulja-Ortmann et al., 2007). This kind of pattern implies, at least in part, a strict spatio-temporal regulation of apoptosis. The developmental factors involved are, however, still largely unknown.

In contrast, more is known about the downstream effectors of apoptosis, most of which have functional homologs in vertebrates (Fig. 1-5). The execution of apoptosis is mediated by an evolutionarily conserved class of cysteine proteases called Caspases, which are widely expressed throughout development in the form of inactive zymogens (pro-Caspases) (Cryns and Yuan, 1998). In *Drosophila*, there are two effector Caspases, Dcp-1 and DrICE (Fig. 1-5). Their activation through proteolytic cleavage by so-called initiator Caspases, e.g. Dronc in *Drosophila*, is critical for execution of apoptosis. Once cleaved, effector Caspases proteolytically cleave a number of substrates, such as structural proteins and enzymes involved in DNA replication, gene expression and cellular metabolism. As a result, the cell eventually fragments into apoptotic bodies which are then engulfed by macrophages and/or neighboring cells (Bangs et al., 2000; Bangs and White, 2000; Bergmann et al., 1998b). Involvement of Caspases in non-apoptotic processes such as spermatid individualization in *Drosophila* (Arama et al., 2003) or muscle differentiation in mouse (Maelfait and Beyaert, 2008; Murray et al., 2008) have also been reported.

In healthy cells, initiator Caspases are held inactive by a conserved group of molecules, the Inhibitor of Apoptosis Proteins (IAPs) (Deveraux et al., 1997). IAPs are E3 ubiquitin ligases that interact physically with Caspases and mediate their ubiquitination and subsequent degradation, thereby suppressing apoptosis (Wilson et al., 2002) (Fig. 1-5). In *Drosophila*, activation of practically all developmental apoptosis depends on the physical interaction of *Drosophila* IAPs (DIAPs) with one of the three proapoptotic factors (Vucic et al., 1997; Vucic et al., 1998): Head involution defective (Hid) (Grether et al., 1995), Reaper (Rpr) (White et al., 1994; White et al., 1996) or Grim (Chen et al., 1996). These three genes are clustered together on one chromosome and are subject to both transcriptional (*hid*, *rpr*, *grim*) (Chen et al., 1996; White et al., 1996) and posttranslational regulation (Hid only)

(Bergmann et al., 1998a; Kurada and White, 1998). While posttranslational regulation by phosphorylation of the Hid protein via the Ras/MAPK pathway has been described in some detail (Bergmann et al., 1998a; Kurada and White, 1998), only a few factors are known that directly activate or inhibit transcription of any of the three proapoptotic genes (Brodsky et al., 2000; Jiang et al., 2000; Lohmann et al., 2002). More recently three additional genes have been identified in *Drosophila* that can induce ectopic cell death when overexpressed: *jafrac2* (Tenev et al., 2002), *sickle* (*skl*) (Christich et al., 2002; Srinivasula et al., 2002; Wing et al., 2002) and *dOmi/HtrA2* (Challa et al., 2007; Igaki et al., 2007; Khan et al., 2008).

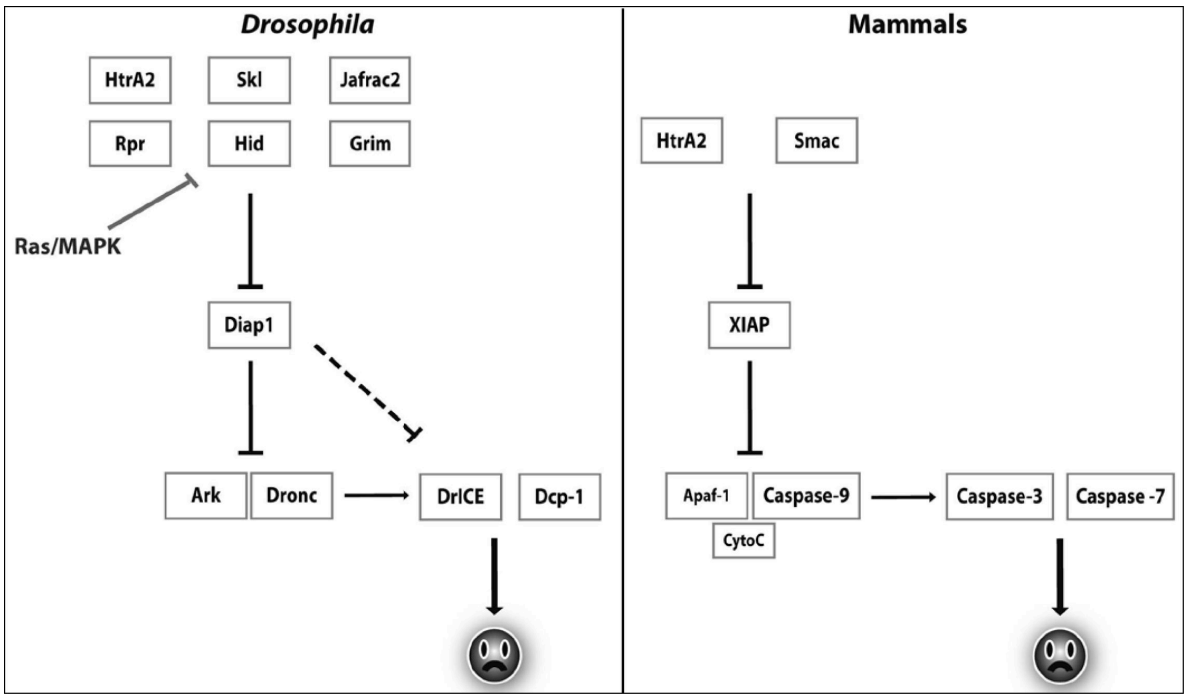


**Fig. 1-5. Members of the cell death pathways are conserved in *Drosophila* and mammals.**
The upstream proapoptotic proteins Reaper (Rpr), Head involution defective (Hid), Grim, Sickle (Skl), HtrA2/Omi and Jafrac2 are regulated by death or survival signals. Upon cell death signals, these proteins release the initiator caspase Dronc from inhibition by Diap1. Released Dronc binds to Ark and forms the apoptosome, which activates the effector caspases Dcp-1 and DrICE, triggering apoptotic processes by cleaving many cellular substrates. In mammals, Smac and HtrA2, released from mitochondria, promote cell death by binding to XIAP and releasing initiator caspases such as Caspase-9. In contrast to *Drosophila*, apoptosome formation requires Cytochrome *c* release from mitochondria, which binds to Apaf-1 and then recruits Caspase-9 for activation. Thereafter, effector caspases, such as Caspase-3 and Caspase-7, are activated to trigger downstream apoptotic reactions. Taken from (Xu et al., 2009).

## 1.4. Aims

Considering the significance of apoptosis for the morphogenetic processes that occur during development, including proper patterning and wiring of the CNS, the identification of the developmental signals involved in regulating apoptosis is an important prerequisite to understanding how it is integrated into CNS patterning during development. As no detailed analysis of apoptosis in the *Drosophila* embryonic CNS had been undertaken, the first aim of my thesis work was to analyze the role and pattern of apoptosis in the developing embryonic CNS, with a particular focus on segment-specific neural apoptosis, and on the precise identification of apoptotic cells. The identified cells were then used as models in the second part of the work, which focused on revealing the developmental mechanisms that regulate segment-specific apoptosis in the CNS.

# 2. Materials and methods

## 2.1. Fly food media

### 2.1.1. Fly stock maintenance

Fly stocks were maintained on a standard food medium composed of yeast flakes, soy flour, corn flour, malt extract and sugar beets syrup. Agar was added for solidification, and Nipagin and propionic acid for conservation. Stocks were maintained at 25°C and transferred to fresh medium every two weeks. Stocks not currently used for experiments were maintained at 18°C, and transferred every four to six weeks.

### 2.1.2. Apple juice agar

For egg collections, apple juice solidified with 2% agar was used. 26-28 g agar was resuspended in 1L of commercially available apple juice and heated to boiling. The mixture was stirred and heated repeatedly until the agar dissolved. After pouring into vials, the agar was allowed to cool down and solidify. Shortly before use, dry yeast was sprinkled onto the surface.

## 2.2. Fly stocks

The fly stocks used in the course of this work are listed in Table 2-1. Lethal mutations were maintained over balancer chromosomes that carry a “blue” (lacZ) or “green” (*GFP*) reporter gene. The reporter genes are carried on P-elements that drive the expression of lacZ or *GFP* under control of a specific promoter. Homozygous mutant embryos could thus be identified via antibody staining by their lack of β-galactosidase or GFP expression.

| Denotation | Genotype | Reference |
|---|---|---|
| WT | *Oregon-R-C* | Bloomington (BL 5) |
| *H99* | *Df(3L)H99*/TM3,*Sb,Ser,e* | Bloomington (BL 1576) |
| $hb^{P1}$,$hb^{15}$ | $hb^{P1}$,$hb^{15}$ / TM6b,$Antp^{Hu}$,*e,hb*-lacZ | C. Doe (Isshiki et al., 2001) |
| $Ubx^{1}$ | $Ubx^{1}$ / TM6b,*Tb,Sb,e,Dfd*-lacZ | AG Technau (Sanchez-Herrero et al., 1985) |
| $hth^{P2}$ | $hth^{P2}$ / TM6b,$Antp^{Hu}$,*abdA*-lacZ | Sun et al., 1995 |
| $exd^{B108}$ | $exd^{B108}$ / FM7,*ftz*-lacZ | C. Berger (Rauskolb et al., 1993) |
| $abdA^{MX1}$ | $abdA^{MX1}$ / TM3,*Sb,e,Kr*-Gal4,UAS-*GFP* | Bloomington (BL 3057) (Sanchez-Herrero et al., 1985) |
| $numb^{1}$ | $numb^{1}$ / *CyO,wg*-lacZ | AG Technau (Uemura et al., 1989) |
| $zfh1^{5}$ | $zfh1^{5}$ / TM3, *Sb,e,Kr*-Gal4,UAS-*GFP* | Z. C. Lai |
| $Antp^{W10}$ | $Antp^{W10}$ / TM6b,$Antp^{Hu}$,*abdA*-lacZ | AG Technau (Wakimoto et al., 1984) |
| $Antp^{W10}$,$Ubx^{1}$ | $Antp^{W10}$,$Ubx^{1}$ / TM6b,*Tb,Sb,e,Dfd*-lacZ | Bloomington (BL 2031) |
| *Def(109); Ubx;abdA* | *Df(3R)Ubx109/* TM6b,$Antp^{Hu}$,*abdA*-lacZ | AG Technau (Sanchez-Herrero et al., 1985) |
| *hs-Ubx* | *hs-Ubx /* TM6b,*Tb,Sb,e,Dfd*-lacZ | G. Struhl (Mann and Hogness, 1990) |
| **Gal4 lines** | | |
| *eg*-Gal4 | *w;;eg*-Gal4 | J. Urban (Dittrich et al., 1997) |
| *en*-Gal4 | *w;en*-Gal4 | AG Technau (Tabata et al., 1995) |
| *poxN*-Gal4,UAS-*GFP* | *w;; poxN*-Gal4,UAS-*GFP /* TM6b,*Tb* | M. Noll (Boll and Noll, 2002) |
| **UAS lines** | | |
| UAS-*mCD8::GFP* | *w;* UAS-*mCD8::GFP;* UAS-*mCD8::GFP* | O. Vef |
| UAS-e$GFP^{nuclear}$ | *w;* UAS-*GFP;* UAS-*GFP* | O. Vef |
| UAS-*hb*;UAS-*hb* | *w;* UAS-*hb;* UAS-*hb* | J. Urban (Wimmer et al., 2000) |
| UAS-*Ubx* | *w;*;UAS-*Ubx* | L. Shashidara |
| UAS-*abdA* | *w;* UAS-*abdA* | A. Michelson |
| UAS-*Antp* | *w;* UAS-*Antp* | Bloomington (BL 7301) |

| Balancer stocks | |
|---|---|
| TM3,*Sb,e,K*r-Gal4, UAS-*GFP* / TM6b, *Antp$^{Hu}$,e,abdA*-lacZ | O. Vef |
| *Dr* / TM6b,*Tb,Sb,e,Dfd*-lacZ | O. Vef |
| *N / F*M7*,ftz*-lacZ | O. Vef |

Table 2-1. *Drosophila* stocks used in the course of this work.

## 2.3. Genetic crosses

To set up crosses between two fly strains, freshly eclosed female virgins of one strain were collected every 4 hours at 25°C or overnight at 12°C. They were then crossed to males of the other strain and allowed to mate for three to four days. For collecting F1 generation progeny from crosses, flies were transferred to fresh medium every three to four days. Vials with eggs were kept at 25°C for about 10 days, around which point the F1 progeny begun to eclose. Flies of the wanted genotype were then collected for further crosses or experiments.

## 2.4. Ectopic gene expression

### 2.4.1. The Gal4/UAS system

The Gal4/UAS system (Brand and Perrimon, 1993) was used for tissue- or cell-targeted gene expression in a number of experiments. The system consists of two components, both originating from the yeast *Saccahromyces cerevisiae*: the transcriptional activator Gal4 and its target sequence, the “upstream activating sequence” (UAS) (Fig. 2-1). The Gal4 gene is under regulation of an endogenous enhancer on a transposable element (P-element), and the P-element is carried by transgenic flies (driver strain or Gal4-strain). Another strain of transgenic flies carries a P-element in which the transgene of interest is placed downstream of several UAS sequences (UAS-strain). Crossing flies of the Gal4-strain to flies of the UAS-strain results in expression of the transgene of interest under control of the selected endogenous enhancer. This method allows, through selection of

appropriate driver strains, analysis of the function of a gene of interest in a specific tissue and at a specific developmental time.

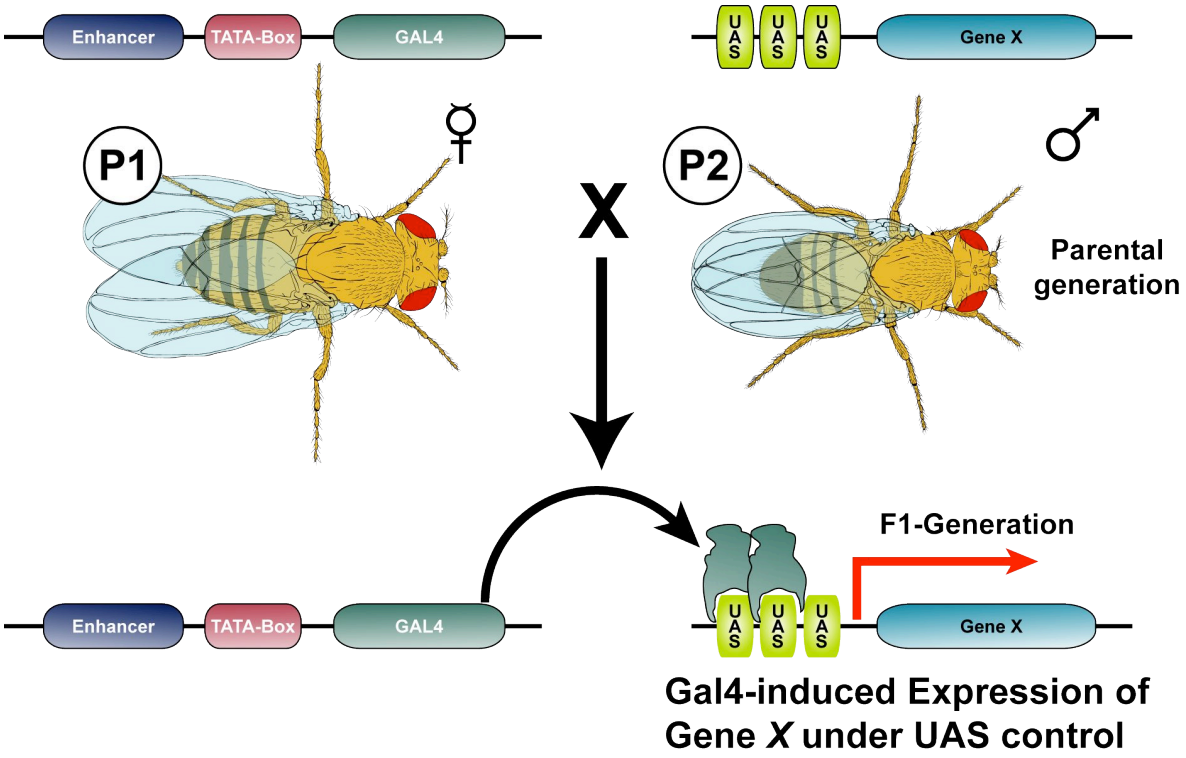


**Fig. 2-1. The Gal4/UAS system.**
Flies of the Gal4-strain (P1) express Gal4 under control of an endogenous enhancer. These flies are crossed with flies of the UAS-strain (P2), which carry the transgene of interest downstream of several UAS sequences. In the progeny (F1 generation), the Gal4 protein can bind to the UAS sequences and drive transcription of Gene *X* in the spatio-temporal pattern of endogenous enhancer expression. Kindly provided by C. Berger and C. Rickert.

### 2.4.2. The heat shock system

The heat shock system was used to ectopically drive expression of the *Ultrabithorax* (*Ubx*) gene. In this case, the *Ubx* gene is under regulation of the heat shock (*hs*) promoter. The promoter is activated when a heat pulse is given at 35°C.

## 2.5. Embryo collection

For embryo collections, flies were first transferred to fresh medium sprinkled with dry yeast and allowed to feed for two days. They were then transferred to vials containing apple juice agar sprinkled with dry yeast. For timed collections (time "after egg laying", abbreviated "AEL"), flies were allowed to lay eggs for a certain

period of time, and the embryos then allowed to develop to the desired developmental stage.

## 2.6. Heat-shock procedure

For the heat-shock experiment, two time points were chosen: 3.5 hours (hrs) and 12 hrs AEL. For the 3.5 hr experiment, eggs were collected for 30 minutes (min) and allowed to develop for another 3.5 hrs. At 3.5 hrs AEL, embryos were dechorionated in 6% bleach and rinsed into a mesh. The heat shock was given by placing the mesh for 30 min into a beaker with PBS prewarmed to 35$^{o}$C in a water bath. For the 12 hr experiment, 60 min egg collections were made and the embryos allowed to develop for another 12 hrs. The embryos were then dechorionated as above and the heat shock was performed for 60 min at 35$^{o}$C. After the heat shock, embryos from both experiments were allowed to develop at 25$^{o}$C until late stage 16, and were then fixed as described below.

## 2.7. Immunohistochemistry

### 2.7.1. Antibodies

| Primary antibodies | | | |
|---|---|---|---|
| **Antibody** | **Donor** | **Dilution** | **Source** |
| BP102 | mouse | 1:20 | DSHB |
| anti-FasII (ID4) | mouse | 1:10 | DSHB |
| anti-Repo (4$\alpha$3) | rabbit | 1:500 | J. Urban |
| anti-Repo (8D12) | mouse | 1:10 | DSHB |
| anti-En/Inv () | mouse | 1:4 | DSHB |
| anti-Gsb-d | rat | 1:2 | R. Holmgren |
| anti-Gsb-p | rat | 1:2 | R. Holmgren |
| anti-dHb9 | guinea pig | 1:1000 | J. Skeath |

| | | | |
|---|---|---|---|
| anti-Lbe | mouse | 1:2 | K. Jagla |
| anti-Eve (3C10) | mouse | 1:2 | DSHB |
| anti-Eve | rabbit | 1:1000 | M. Frasch |
| anti-Eagle | mouse | 1:10 | C. Doe |
| anti-Eagle | rabbit | 1:500 | J. Urban |
| anti-activated Caspase 3 | rabbit | 1:50 | Cell Signaling Technology |
| anti-Scr | mouse | 1:20 | DSHB |
| anti-Antp | mouse | 1:20 | DSHB |
| anti-Ubx | mouse | 1:20 | R. White |
| anti-AbdA | mouse | 1:50 | I. Duncan |
| anti-AbdB | mouse | 1:50 | DSHB |
| anti-Hb | guinea pig | 1:500 | J. Urban |
| anti-Zfh1 | guinea pig | 1:1000 | J. Skeath |
| anti-Hth | rabbit | 1:500 | A. Salzberg |
| anti-Exd | mouse | 1:5 | G. Morata |
| anti-β-gal | mouse | 1:750 | Promega |
| anti-β-gal | rabbit | 1:2000 | Cappel |
| anti-GFP | mouse | 1:250 | Promega |

Table 2-2. Primary antibodies used.

| **Secondary antibodies** | | | |
|---|---|---|---|
| **Antibody** | **Donor** | **Dilution** | **Source** |
| anti-mouse-biotin | donkey | 1:500 | Jackson Labs. |
| anti-rat-biotin | donkey | 1:500 | Jackson Labs. |
| anti-rabbit-biotin | donkey | 1:500 | Jackson Labs. |
| anti-guinea pig-biotin | donkey | 1:500 | Jackson Labs. |
| anti-mouse-FITC | donkey | 1:500 | Jackson Labs. |

| | | | |
|---|---|---|---|
| anti-rat-FITC | donkey | 1:500 | Jackson Labs. |
| anti-rabbit-FITC | donkey | 1:500 | Jackson Labs. |
| anti-mouse-Cy3 | donkey | 1:500 | Jackson Labs. |
| anti-rabbit-Cy3 | donkey | 1:500 | Jackson Labs. |
| anti-guinea pig-Cy3 | donkey | 1:500 | Jackson Labs. |
| anti-mouse-Cy5 | goat | 1:500 | Jackson Labs. |
| anti-rat-Cy5 | donkey | 1:500 | Jackson Labs. |
| anti-rabbit-Cy5 | donkey | 1:500 | Jackson Labs. |
| anti-guinea pig-Cy5 | donkey | 1:500 | Jackson Labs. |
| anti-mouse-Alexa488 | donkey | 1:500 | Molecular Probes |

Table 2-3. Secondary antibodies used.

### 2.7.2. Fixation of embryos for antibody staining and *in situ R*NA hybridization

Embryos were collected either overnight or over a fixed period of time (e.g. 30-minute or 60-minute collections for the heat-shock experiments). The collected eggs were dechorionated in 6% household bleach (sodium hypochloride) for 3 minutes, poured into a funnel with mesh and rinsed thoroughly with tap water. The embryos were then transferred into an Eppendorf vial containing the two-phased fixing solution, consisting of heptane (damages the vitelline membrane) and formaldehyde (fixative), and incubated with vigorous shaking for 22 mins at room temperature (RT). The two phases were allowed to separate, and the lower phase containing formaldehyde was replaced with an equal volume of methanol. The vial was vortexed for 1 min during which the surface tension between the phases caused the damaged vitelline membrane to be stripped from the embryos, allowing them to sink to the bottom of the vial. The lower phase containing the methanol was removed, replaced with a new aliquot and the devitellinization step repeated one more time. Next, all of the heptane and methanol was removed and the embryos rinsed several times in pure methanol to remove the rest of the heptane. Finally, the embryos were dehydrated by a 10 min wash in methanol, and rehydrated by rinsing several times and washing twice for 10 min in PBT.

### 2.7.3. Preparation and fixation of L1 larval CNS

Young *Drosophila* larvae which have just hatched are referred to as first instar larvae (L1 larvae). By this developmental stage, they have secreted a cuticula which impairs access of outside agents such as fixative or antibodies to the inner tissues. Therefore the larvae have to be dissected prior to fixation. To this purpose, L1 larvae were transferred from apple juice agar into a well containing Broadie and Bate (B&B) buffer (Broadie and Bate, 1993). Using forceps to hold the head on one end and the abdomen on the other, each larva was opened by pulling at both ends. Care was taken to leave the two halves attached at the gut. The buffer solution containing thus opened larvae was transferred into an Eppendorf vial equilibrated with a Bovine serum albumine (BSA) solution to prevent the larvae from sticking to the walls of the vial. After the larvae have sunk to the bottom, the buffer was replaced with 1 ml 4% paraformaldehyde and fixed with gentle mixing for 50 min at RT. After rinsing several times with PBT, the larvae were washed twice for 15 min in PBT.

### 2.7.4. Incubation in antibody solutions

All antibodies used were diluted accordingly in PBT (Table 2-2). Incubations in primary antibody dilutions were performed overnight at 4$^{o}$C, with gentle mixing. Following incubation, the antibody solution was removed, the embryos/larvae rinsed 3 times and then washed several times with PBT. After washing, the secondary antibody, diluted in PBT, was added (for dilutions see Table 2-3) and incubated for 2 hours at RT (or overnight at 4$^{o}$C) with gentle mixing. The secondary antibody was removed, and the embryos/larvae rinsed and washed several times in PBT. Many of the primary antibodies were stored at 4$^{o}$C and reused. To prevent contamination of the stored antibody solutions, sodium-azide was added to a final concentration of 0.03%.

#### *2.7.4.1. Fluorescent staining*

For fluorescent staining, secondary antibodies conjugated with various fluorescent dyes (FITC, Alexa488, Cy3 or Cy5) were used (Table 2-3). The incubation with such antibodies was performed in the dark. Following the usual washing steps, the embryos/larvae were rinsed once in PBS, embedded in 70% glycerol and stored at 4$^{o}$C in the dark. For analysis of the staining, the embryos

were transferred into a drop of Vectashield quenching medium on a microscope slide, fillet ("flat") preparations were made to expose the CNS, the preparations covered and the cover slip sealed with nail polish. For L1 larvae, after transfer into a drop of the Vectashield quenching medium, tweezers were used to dissect the CNS from the rest of the tissue. The dissected CNS were covered with a cover slip and sealed with nail polish. The stained preparations were imaged using a fluorescence or a confocal microscope.

#### *2.7.4.2. Color staining*

Biotin-conjugated secondary antibodies were used for color (visible) staining of embryos. Following incubation with the secondary antibody, embryos were washed as above. During this time, equal amounts of Avidin and Horseradish-peroxidase (HRP)-coupled Streptavidin (Vectastain Elite ABC Kit, Vector Laboratories) were diluted in PBT (further referred to as AB solution) and incubated for 60 mins at RT with mixing, allowing Avidin to complex with multiple Streptavidin-HRP molecules. The AB solution was then added to the embryos and incubated for 60 mins at RT with mixing. This step allowed multiple Avidin molecules, bound in the Avidin-Streptavidin-HRP complex, to bind to Biotin, thus significantly amplifying the signal from the secondary antibody. The embryos were then washed again as above, and the staining solution, containing $H_2O_2$-activated Diaminobenzidine (DAB), added. The horseradish peroxidase catalyzes the oxidation of DAB into a brown pellet, thus visualizing the location of the bound antibodies. The staining was monitored through a binocular and stopped by washing with PBT when it reached a satisfying level. After rinsing once in PBS, the embryos were embedded in 70% glycerol and stored at 4$^{o}$C. For analysis of the staining, the embryos were transferred into a drop of 70% glycerol on a microscope slide, fillet ("flat") preparations were made to expose the CNS, covered and the cover slip sealed with nail polish. The stained preparations were imaged using a light microscope.

## 2.8. RNA *in situ* hybridization

In order to detect mRNA transcripts in the tissue, RNA probes were made. All steps in the protocol were performed under RNAse-free conditions, using gloves

and RNAse-free disposables and glassware. All solutions used were made with DEPC (diethylpyrocarbonate) treated water. To this purpose, 0.1% DEPC was added to double distilled water and allowed to stand for a minimum of 12 hrs at RT. The DEPC-water was then autoclaved and stored at RT.

### 2.8.1. Generation of a *reaper* riboprobe

The pBluescript plasmid containing the *reaper* (*rpr*) cDNA (kindly provided by H. Steller) was linearized with the restriction endonuclease EcoRV, purified, precipitated and dissolved in DEPC-treated water. In the *in vitro* labeling reaction, the antisense RNA probe was synthesized and labeled with digoxigenin (DIG)-labeled UTP (DIG-RNA Labeling Mix, Boehringer) using the T3 RNA polymerase. The reaction mixture contained 14μl (3μg) linearized plasmid DNA, 2μl 10x transcription buffer, 2μl 10x DIG-labeling mix, 0,5μl (20 units) RNase inhibitor and 2μl T3 RNA polymerase, and was allowed to run for 2 hrs at 37°C. The reaction was stopped by adding 2μl DNaseI and incubating further 15 min at 37°C to remove the plasmid DNA template. The T3 RNA polymerase was then inactivated by adding 2μl 0,2M ethylenediaminetetraacetic acid (EDTA, pH 8,0). To precipitate the labeled RNA probe, 2,5μl 4M lithium chloride (LiCl) and 70μl cold ethanol were added and the solution kept at -20°C for 2 hrs. It was then centrifuged at 14000 rpm for 45 min at 4°C, the pellet washed in cold 70% ethanol and centrifuged again at 14000 rpm and 4°C for 10 min. The supernatant was decanted and the pellet dried for 2 min in the vacuum dryer to remove traces of ethanol. The dry pellet was finally dissolved in 50μl of DEPC-water.

The *rpr* probe was tested on wild type embryos and a dilution of 1:600 was found to produce the best signal with a minimal amount of background staining. All further experiments were carried out with this dilution.

### 2.8.2. Hybridization

Embryo fixation was performed as in section 2.7.2. Following washes in PBTw, embryos were incubated for 10 min in sodiumborohydrid (NaBH4, 1 mg/ml in PBS) to remove excess fixation products and reduce autofluorescence. The embryos were washed several times in PBTw, and then a 1:1 mixture of PBTw and Hybridization buffer (PBTw/Hyb buffer) was added and the embryos incubated for

10 min at RT with gentle mixing. The PBTw/Hyb buffer mixture was replaced with pure Hyb buffer and incubated another 10 min. During this time, the prehybridization solution was prepared (1ml Hyb buffer containing 10μl of 10 mg/ml sonicated salmon sperm DNA [ssDNA]) and heated for 5 min at 100°C. After cooling on ice, the prehybridization solution was added to the embryos and incubated for 2 hrs at 55°C.

The DIG-labeled rpr probe was diluted 1:600 in Hyb buffer containing 10% ssDNA and heated for 5 min at 95°C. After cooling on ice for a minimum of 5 min, the probe was added to the embryos and incubated overnight at 55°C. The probe was removed and the embryos washed in Hyb buffer for 30 min at 65°C, and then in a 1:1 PBTw/Hyb buffer mix for another 30 min at 65°C. PBTw/Hyb buffer was replaced with pure PBTw and washed four times for 20 min at 65°C and then 10 min in PBTw at RT.

### 2.8.3. Signal detection

Following the washes, embryos were blocked for 30 min at RT in TNB buffer, and the anti-DIG-POD antibody, diluted in TNB buffer, was added and incubated for 2 hrs at RT. The embryos were washed four times for 10 min with PBTw and then twice for 5 min in TNT buffer. For signal amplification, the Perkin-Elmer TSA Kit was used. The embryos were incubated for 10 min in the Tyramide-Cy3 solution (Tyramide-Cy3 was diluted 1:50 in 1x amplification diluent provided in the kit), rinsed and washed several times for 10 min in TNT buffer to stop the reaction. The staining was checked under the fluorescence microscope and the embryos rinsed and washed once for 10 min in PBT. Antibody staining for additional markers was then performed as in sections 2.7.4. and 2.7.4.1. Following the staining, the embryos were embedded in 70% glycerol and stored at 4°C in the dark. For analysis of the staining, the embryos were transferred into a drop of Vectashield quenching medium on a microscope slide, fillet (“flat”) preparations were made to expose the CNS and the cover slip was sealed with nail polish.

## 2.9. Image detection and documentation

The Leica TCS SPII confocal microscope was used for fluorescent imaging, and the images were processed using Leica Confocal Software and Adobe Photoshop. For color staining, images were made using an Axiophot light microscope with a Kontron camera and also processed with Adobe Photoshop.

## 2.10. Chemicals and solutions

The chemicals used in this work were obtained from the following companies: Merck, Roth, Roche, Sigma-Aldrich, MBI Fermentas and Vector laboratories. Exceptions are mentioned where appropriate.

Fixative for antibody staining and *in situ* hybridization

| | |
|---|---|
| 430 µl | PEMS buffer |
| 70 µl | Formaldehyde (37%) |
| 500 µl | Heptane |

PEMS buffer

| | |
|---|---|
| 0,1 M | Pipes |
| 1 mM | $MgSO_4$ |
| 1 mM | EGTA |
| 1,2 M | Sorbitol |

20x PBS (pH 7,4)

| | |
|---|---|
| 151,94 g | NaCl |
| 19,88 g | $Na_2HPO_4 \cdot 0\ H_2O$ |
| 8,28 g | $NaH_2PO_4 \cdot 1\ H_2O$ |
| 1000 ml | $H_2O$ |

PBT

1x PBS

0.1% Triton X-100

PBTw

1x PBS

0.1% Tween-20 (Riedel-de Haën)

Broadie & Bate buffer (pH7,15)

135 mM NaCl

5 mM KCl

4 mM $MgCl_2$

0,5 mM $CaCl_2$

5 mM TES (N-Tris[hydroxymethyl]methyl-2-aminoethanesulfonic acid)

36 mM D+Saccharose

4% paraformaldehyde fixative for L1 larval CNS

18 ml buffer A

25 ml $H_2O$

2 g paraformaldehyde

dissolve at 65°C

7 ml buffer B

store at -20°C in 2 ml aliquots

Buffer A

2,84 g $Na_2HPO_4 \cdot 0\ H_2O$

100 ml $H_2O$

Buffer B

2,76 g $NaH_2PO_4 \cdot 1\ H_2O$

100 ml $H_2O$

DAB staining solution

1 Tablet 3,3'-Diaminobenzidine (10 mg)

20 ml 1x PBS

store at -20°C in 1 ml aliquots

Hybridization buffer

20 ml formamide

50 µl Tween-20

17,5 ml DEPC-$H_20$

12,5 ml 20x saline sodium citrate (SSC) buffer

TNB buffer

0,1 M Tris-HCl (pH7,5)

0,15 M NaCl

0,5% blocking reagent

TNT buffer

0,1 M Tris-HCl (pH7,5)

0,15 M NaCl

0,05% Tween-20

## 2.11. Equipment and software

| Equipment | Producer |
|---|---|
| Binocular MS5 | Leica |
| Light microscope Axioplan | Zeiss |
| CCD Camera ProgRes 3012 | Kontron |
| Fluorescence microscope BX 50 WI | Olympus |
| CCD Camera Axiocam MRm | Zeiss |
| Confocal laser scanning microscope TCS SPII | Leica |
| Centrifuge 5417R | Eppendorf |

| | |
|---|---|
| Thermomixer compact | Eppendorf |
| Vacuum Centrifuge SpeedVac | Savant |
| Agarose Gel Unit HE33 | Hoefer |
| Gene Power Supply GPS 200/400 | Pharmacia |
| Printer P91 Video Copy Processor | Mitsubishi |
| UV Transilluminator | MS -Laborgeräte |
| Vortex Vibrofix VF1 | Janke & Kunkel |
| Incubator Friocell | MMM Medcenter |
| Incubator WTB Binder | Labotec |
| Mixer TPM2 | Sarstedt |
| Scale PM4600 | Mettler |
| Scale AM50 | Mettler |
| pH Meter CG840 | Schott |
| **Software** | **Producer** |
| Axiovision 4.1.1 | Zeiss |
| Leica Confocal Software 2.00 | Leica |
| Endnote 9 | Thomson |
| Photoshop CS2 | Adobe |
| Illustrator CS | Adobe |
| Office 2003 | Microsoft |

Table 2-4. Equipment and software used in the course of this work.

# 3. Results

## A. Programmed cell death in the developing embryonic central nervous system

Despite the obvious importance of programmed cell death in *Drosophila* development, only a very general overview of the occurrence of apoptosis in the developing embryonic CNS has been provided to date (Abrams et al., 1993). In this work, the authors used the vital dye acridine orange to visualize apoptotic cells in living embryos. They found drastic variation in the number and location of apoptotic cells over the course of embryonic development, but the patterns in each developmental stage were reproducible. In the central nervous system, they found both segmental repeated patterns, indicating spatio-temporal control of apoptosis, and random patterns, which suggested a certain amount of plasticity during development. However, a systematic analysis of the number, segmental pattern and identity of dying cells has not been made, although it would be an important foundation for further research on mechanisms regulating developmental cell death. Therefore, three approaches were taken in our laboratory to gain insight into the occurrence and role of apoptosis in the *Drosophila* embryonic central nervous system:

1) Comparison of the embryonic CNS structure and cell number in wild type and apoptosis-deficient embryos, as well as counts of apoptotic cells in the developing wild type CNS (conducted by Karin Lüer-Kirsch and myself).

2) Examination of the clonal origin, development and axonal projection patterns of additional cells in apoptosis-deficient embryos by DiI labelling of neuroblast lineages (conducted by Janina Seibert in the course of her Diploma thesis).

3) Analysis of specific cell subpopulations in apoptosis-deficient embryos using various cell markers, and determination of the timing of apoptosis and the identity of some of these cells in order to establish models for studying mechanisms of apoptosis regulation (conducted by myself).

The concerted efforts on this part of the work resulted in a publication in the journal *Development* 134 (1), 2007.

## 3.1. CNS morphology of apoptosis-deficient embryos

To begin investigations into programmed cell death in embryonic CNS development, I compared the CNS morphology of wild type (wt) and apoptosis-deficient embryos, homozygous for the deficiency *Df(3L)H99* (from here on referred to as *H99*). The deficiency removes *head involution defective (hid)*, *reaper* (*rpr*) and *grim*, three genes responsible for inducing virtually all developmental cell death in *Drosophila* embryos (Chen et al., 1996; Grether et al., 1995; White et al., 1994; White et al., 1996). One typical feature of *H99* embryos is a variably penetrant defect in morphogenetic reorganization of the head region, termed head involution, detectable from a late developmental stage until the end of embryogenesis (Abbott and Lengyel, 1991). In other tissues, these embryos show a range of phenotypes, from problems with germ-band retraction, over defects in gut development and central nervous system condensation, to hardly any macroscopically visible phenotype. In order to maximize the chances for observing differences between the wt and *H99* CNS, I analyzed embryos at late developmental stages (late 16 or early 17), considering cases with and without defects in CNS condensation, as this did not seem to affect the observations.

I examined the general morphology of the CNS, and subsequently performed immunostaining to visualize the axon tracts and the pattern of glial cells. As a consequence of the lack of apoptotic cell death, the CNS in late *H99* embryos is wider than in wt, but otherwise has a rather normal appearance. The ventral midline is widened and disrupted due to the survival of several midline glia (Sonnenfeld and Jacobs, 1995; Zhou et al., 1995) (Fig. 3-1A,B). Axonal projections were examined by immunostaining against BP102, which visualizes the neuropil (Seeger et al., 1993), the region of axonal and dendritic branches and synapses. In each truncal segment of a wt embryo, the neuropil exhibits a typical scaffold comprising an anterior and a posterior commissure, and a pair of longitudinal connectives (Fig. 3-1A). As earlier publications showed, in homozygous *H99* mutants the commissures and longitudinal connectives are broadened, and the

junctions between them thickened due to additional axons (Dong and Jacobs, 1997; Zhou et al., 1995) (Fig. 3-1B). However, their pattern still closely resembles the pattern in wt embryos. This indicates that at least some of the supernumerary neurons differentiate and extend axonal projections, but they remain within the regular commissures and longitudinal connectives. A smaller subset of axonal bundles was visualized by immunostaining against Fasciclin II (FasII), a surface glycoprotein required for selective axon fasciculation (Bastiani et al., 1987). In the wt CNS, FasII is expressed in three longitudinal bundles on each side of the neuropil, in a subset of glial cells and in most motoneuronal axons (Grenningloh et al., 1991). In this comparison I examined FasII expression in the longitudinal bundles (Fig. 3-1C,D) and in the motoneuronal projections, which exit the CNS through the transverse (TN), segmental (SN) and intersegmental (ISN) nerves (Fig. 3-1E,F). In *H99* embryos, the axons generally seem to find and follow their normal pathways, as I observed no obvious phenotype in the FasII expression pattern. The three longitudinal fascicles form and, apart from a variably “bumpy” appearance, look similar to wt (Fig. 3-1D). The TN and ISN also appear normal, as well as the four branches of the segmental nerve (SNa-d) (Fig. 3-1F). The nerves all appear of normal thickness, although it is difficult to tell whether they contain supernumerary axons.

I also examined by immunostaining the pattern of glial cells that show expression of the *reversed polarity* (*repo*) gene. *repo* encodes a homeodomain transcription factor required for proper differentiation of all lateral glia in the CNS and PNS (Halter et al., 1995; Xiong et al., 1994). At late developmental stages, wt embryos show a stereotyped pattern of Repo expression. In the VNC, all but the midline glia are Repo-positive, and they are associated with the CNS surface, the cortex or the neuropil (Ito et al., 1995) (Fig. 3-1G). Peripheral glia are associated with the SN and ISN at the CNS exit area (Halter et al., 1995; Klambt and Goodman, 1991; Schmidt et al., 1997; von Hilchen et al., 2008), and in the periphery itself with the TN, ISN and SN (Carlson et al., 1997; von Hilchen et al., 2008) (Fig. 3-1I). In the ventral nerve cord of *H99* homozygotes, the Repo expression pattern is surprisingly normal, apart from a moderate misplacement of some cells (Fig. 3-1H). The slight shift in the positioning of some glia is most likely not due to defects in glial development, but rather a consequence of too many cells

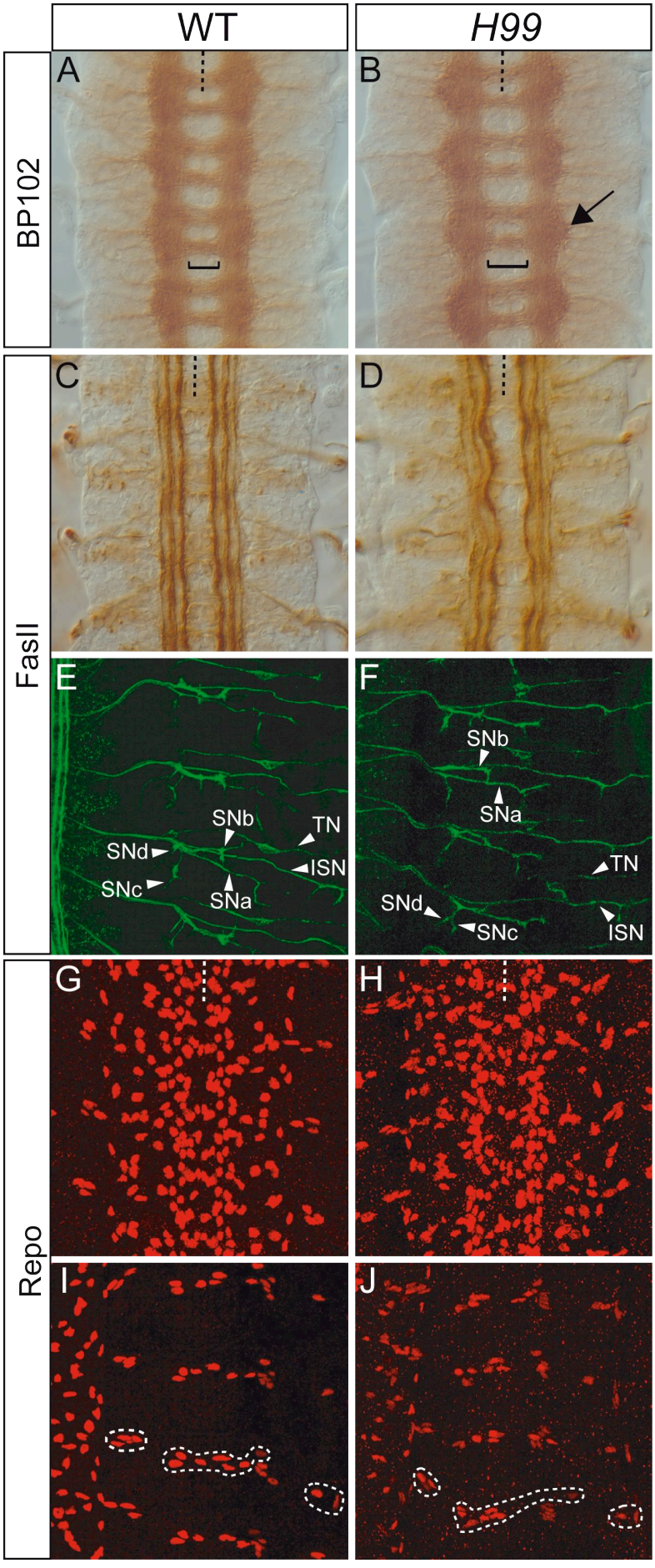


**Fig. 3-1. The CNS of homozygous *H99* embryos is not grossly deformed.**
A,B. Axon tracts are visualized using the BP102 antibody (brown) in wt (A) and *H99* (B) embryos. Their pattern is similar, although thickened junctions between the longitudinal connectives and the commissures (arrow), and a widened midline (bracket) are visible in *H99*. Note that the CNS of *H99* embryos is generally wider than that of wt due to additional cells.
C-F. FasII staining (brown in C,D; green in E,F) of axons reveals a variably altered pattern. C,D show the longitudinal axon tracts in the ventral nerve cord. The *H99* embryo shown in D has a more extreme phenotype in that the longitudinal fascicles are somewhat disordered and fuzzy. E,F show the peripheral nerves (SNa-d, ISN, TN). They do not appear altered in *H99* (F).
G-J. Glial cells, visualized with the anti-Repo antibody (red). A stack of scans was made throughout the CNS and the scans then projected together to show all Repo-positive cells. G,H show the ventral nerve cord glia and I,J the peripheral glia (stippled outline). The positioning of glia is only slightly affected in *H99*.
All images show abdominal segments (A3 to A6) of late stage 16 embryos. Stippled line marks the midline, anterior is up.

persisting in the CNS. The exit glia are often located at the inner CNS border instead of the outer one (Fig. 3-1J). Considering the greater CNS width of these embryos, these cells probably require more time to reach the outer border, but they eventually do so. In the periphery itself they also occupy their typical positions, although, like for the exit glia, a slight lag in migration can be seen in some cases (Fig. 3-1J).

These observations indicate that the overall CNS structure in late homozygous *H99* embryos is not drastically affected at the macroscopic level, although there must be a large number of additional cells present.

## 3.2. Identification of apoptotic cells in the CNS of wild type embryos

To gain a general overview of the occurrence of apoptosis in the wild type embryonic CNS, a polyclonal antibody raised against the activated form of the human Caspase-3 protein was used. It has been shown that an antiserum raised against the same epitope reacts specifically with the cleaved form of the *Drosophila* Caspase Drice and labels apoptotic cells (Yu et al., 2002). In addition, the activated Caspase-3 antibody used for the experiments described here has been used in numerous studies to monitor apoptosis in *Drosophila* tissues, and it did not show any staining in homozygous *H99* embryos (Brennecke et al., 2003; Giraldez and Cohen, 2003; Marois et al., 2006; Martin and Baehrecke, 2004; Primrose et al., 2007; Ryoo et al., 2004; Wichmann et al., 2006).

In the CNS of wt embryos, Caspase-3 activation was first observed around the beginning of stage 11, and was then continually visible until the end of embryonic development (Rogulja-Ortmann et al., 2007) (Fig. 3-2). The number of activated Caspase-3-positive cells per abdominal hemisegment (hs) increased steadily from stage 11 to reach a peak in mid-development (stage 14). After this point, the number of activated Caspase-3-positive cells stayed more or less constant until the end of embryonic development (Rogulja-Ortmann et al., 2007). As has been reported previously (Abrams et al., 1993), the spatial distribution of activated Caspase-3-positive cells at any stage shows both a regular, segmental repetitive

distribution, as well as a random one (Fig. 3-2). In addition, the most posterior segments continually show higher concentrations of apoptotic cells from stage 13 until the end of embryonic development.

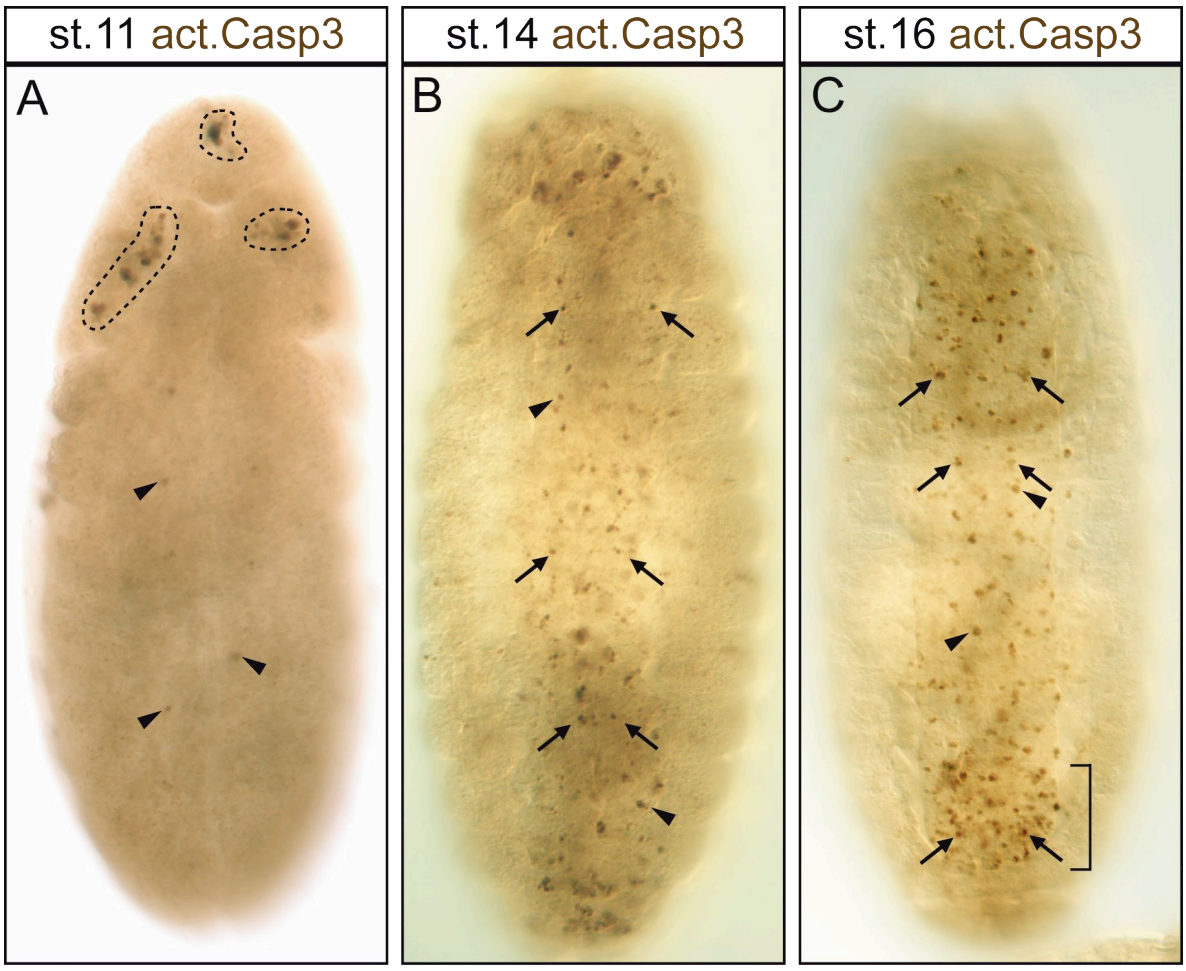


**Fig. 3-2. Visualization of apoptotic cells in *Drosophila* embryos with the activated Caspase-3 antibody.**
A. Dorsal view of a stage 11 embryo. First cells positive for activated Caspase 3 (act.Casp3, brown) are most obvious in the head region (stippled outline). Weakly stained cells also begin to appear at random positions in the developing CNS (arrowheads).
B. Ventral view of an embryo at mid-embryogenesis (stage 14). Many apoptotic cells are visible in the CNS, both at regular, segmentally repeated positions (arrows) and at random ones (arrowheads).
C. Ventral view of a late embryo (stage 16). There are still many cells positive for activated Caspase-3. Repeated patterns are visible (arrows) as well as random ones (arrowheads). The most posterior neuromeres exhibit particularly high amounts of apoptotic cells (square bracket).
Anterior is up in all images.

In order to identify some of the dying cells in the CNS more precisely, I selected a number of molecular markers that are known to be expressed in larger or smaller groups of cells in the ventral nerve cord. I compared the extent of expression of these markers in late developmental stages in wt and homozygous

*H99* embryos. The reasoning behind this approach was that any cell which is born and expresses one of these markers, but undergoes apoptosis at some point in development, would likely continue to express this marker until the end of embryogenesis if apoptosis is prevented. Such a persistence of molecular marker expression following inhibition of apoptosis has been shown for midline glia (Sonnenfeld and Jacobs, 1995; Zhou et al., 1995) and other apoptotic cells in the CNS (Miguel-Aliaga and Thor, 2004; Novotny et al., 2002). I therefore expected to see all the additional cells in *H99* embryos which continued to express a particular marker. The chosen markers, most of which are transcription factors, included those expressed in large groups of CNS cells, such as Engrailed/Invected (En/Inv) (DiNardo et al., 1985; Kornberg et al., 1985), Gooseberry proximal (Gsb-p) and Gooseberry distal (Gsb-d) (Bopp et al., 1986; Zhang et al., 1994) and dHb9 (Broihier and Skeath, 2002), and those expressed in smaller groups of cells such as Repo (Halter et al., 1995; Xiong et al., 1994), Ladybird early (Lbe) (De Graeve et al., 2004; Jagla et al., 1997), Even-skipped (Eve) (Frasch et al., 1987) and Eagle (Eg) (Dittrich et al., 1997; Higashijima et al., 1996).

Determining the time of death of some of these cells was another prerequisite for establishing models for studies on regulation of developmental apoptosis. Therefore, in a parallel set of experiments, I looked for activation of Caspase-3 by immunostaining in cells that express the chosen molecular markers. I chose embryos in mid-development for this analysis as the observations on apoptosis distribution indicated that it is most frequent in these stages (Rogulja-Ortmann et al., 2007). In addition, I examined embryos at a late developmental stage (late stage 16) in order to identify cells which are removed at the end of embryogenesis.

### 3.2.1. Markers with broad expression domains

The difference between *H99* and wt embryos in the number of cells positive for broadly expressed markers was not very obvious (Fig. 3-3). In the late wt embryo, En/Inv is expressed in a posterior stripe of cells comprising progeny of all NBs delaminating from rows 6 and 7, and one NB delaminating from row 1 of the neuroectoderm (Doe, 1992; Patel et al., 1989) (Fig. 3-3A). In the CNS of *H99* embryos, the pattern of En/Inv-positive cells is similar to the wt one, although occasional segments appear to contain more stained cells (Fig. 3-3B). This is in agreement with observed increased proliferation of some NBs in *H99* embryos at

the end of embryogenesis, and with a significant increase in surviving progeny numbers within the lineages of some row 6 NBs and of all row 7 NBs labelled by DiI in the same mutant (Rogulja-Ortmann et al., 2007). The double-staining with the activated Caspase 3 antibody showed apoptosis of En/Inv-positive cells in wt embryos of all examined stages (Fig. 3-4A-C).

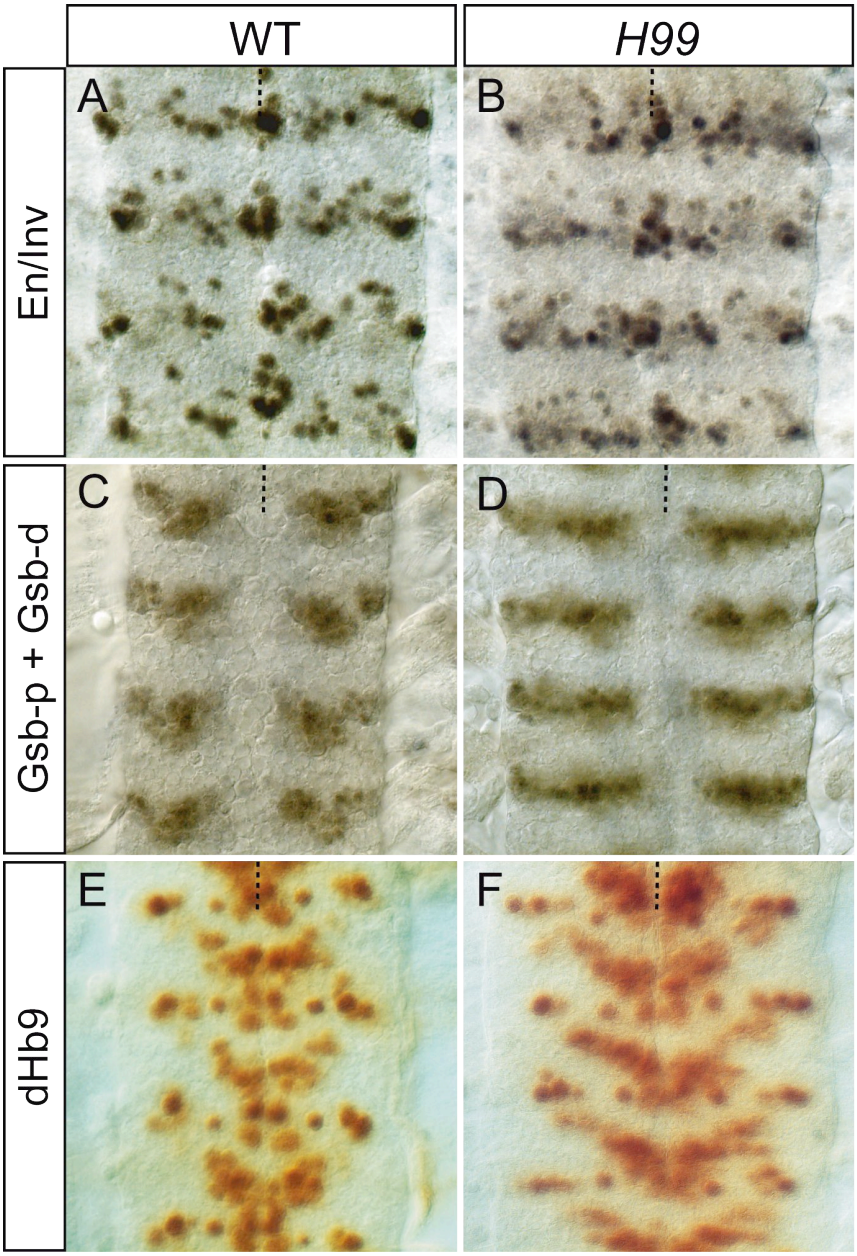


**Fig. 3-3. Comparison of markers with broad expression domains.**
A,B. Engrailed/Invected expression (brown) does not show obvious differences between in wt (A) and *H99* (B) embryos.
C,D. Gooseberry-proximal and -distal expression (brown) domain appears somewhat wider in *H99* (D) than in wt (C). This may, however, be due to the fact that the CNS of *H99* (D) embryos is generally wider than that of wt ones (C).
E,F. dHb9 (brown) is expressed in more cells in *H99* embryos (F) than in wt ones (E).
Segments A3 to A6 of late stage 16 embryos are shown. Stippled line marks the midline, anterior is up in all images.

Similar to the En/Inv expression, Gooseberry-proximal (Gsb-p) and -distal (Gsb-d) are expressed in a posterior stripe of cells in the CNS of late embryos (Fig. 3-3C). This stripe comprises progeny of the NBs delaminating from rows 5 and 6 (Gutjahr et al., 1993). In *H99* embryos the cluster of Gsb-positive cells appears more elongated than in the wt (Fig. 3-3D), which again agrees with increased cell numbers of all row 5 and some row 6 NBs in *H99* embryos (Rogulja-Ortmann et al., 2007). Activated Caspase-3 staining on wt embryos shows single apoptotic Gsb-expressing cells per hemisegment in all stages examined (Fig. 3-4D-F).

Expression of dHb9, a homeodomain-containing protein, in wt embryos has been found in specific subsets of neurons (Broihier and Skeath, 2002) (Fig. 3-3E), including the medial RP motoneurons (Goodman et al., 1984; Sink and Whitington, 1991), two serotonergic interneurons, and a lateral cluster of about six neurons (Broihier and Skeath, 2002). In *H99* embryos some of these subsets contain additional cells (Fig. 3-3F). Accordingly, a few dHb9-expressing cells showed Caspase-3 activation in each developmental stage examined (Fig. 3-4G-I).

As mentioned above, most of these markers showed, at least in some of the developmental stages examined, overlap with activated Caspase-3 staining in a few cells in wt embryos (Fig. 3-4). In most cases it was difficult to identify these cells due to the extent of marker expression, and closer identification was possible only for dHb9-positive cells. At late stage 16 for example, cells that most likely correspond to one of the RP motoneurons (RP 1, 3, 4 or 5) or one of their siblings, were co-labelled with activated Caspase-3. This cell death was not segment-specific, and occurred in 27.3% of analysed hemisegments (n=22; Fig. 3-4D-F).

### 3.2.2. Markers expressed in small groups of cells

For Repo-expressing cells I performed precise cell counts, as I observed no obvious difference in the extent of this glia-specific marker expression between wt and *H99* embryos (Fig. 3-1G-J). I counted cells at late stage 16, and both CNS glia and the peripheral glia, that are born in the CNS and then migrate out along the nerves, were included. Among the peripheral glia only those that migrate out up to the chordotonal organ were counted. Wt embryos showed an average total of 34.17±0.65 cells/hemisegment (hs) (n=30). *H99* embryos exhibited on average 34.77±0.73 cells/hs (n=30). These results show that the number of glial cells is not

significantly changed in *H99* embryos, and indicate that the great majority of dying cells in the embryonic CNS are neurons or undifferentiated cells.

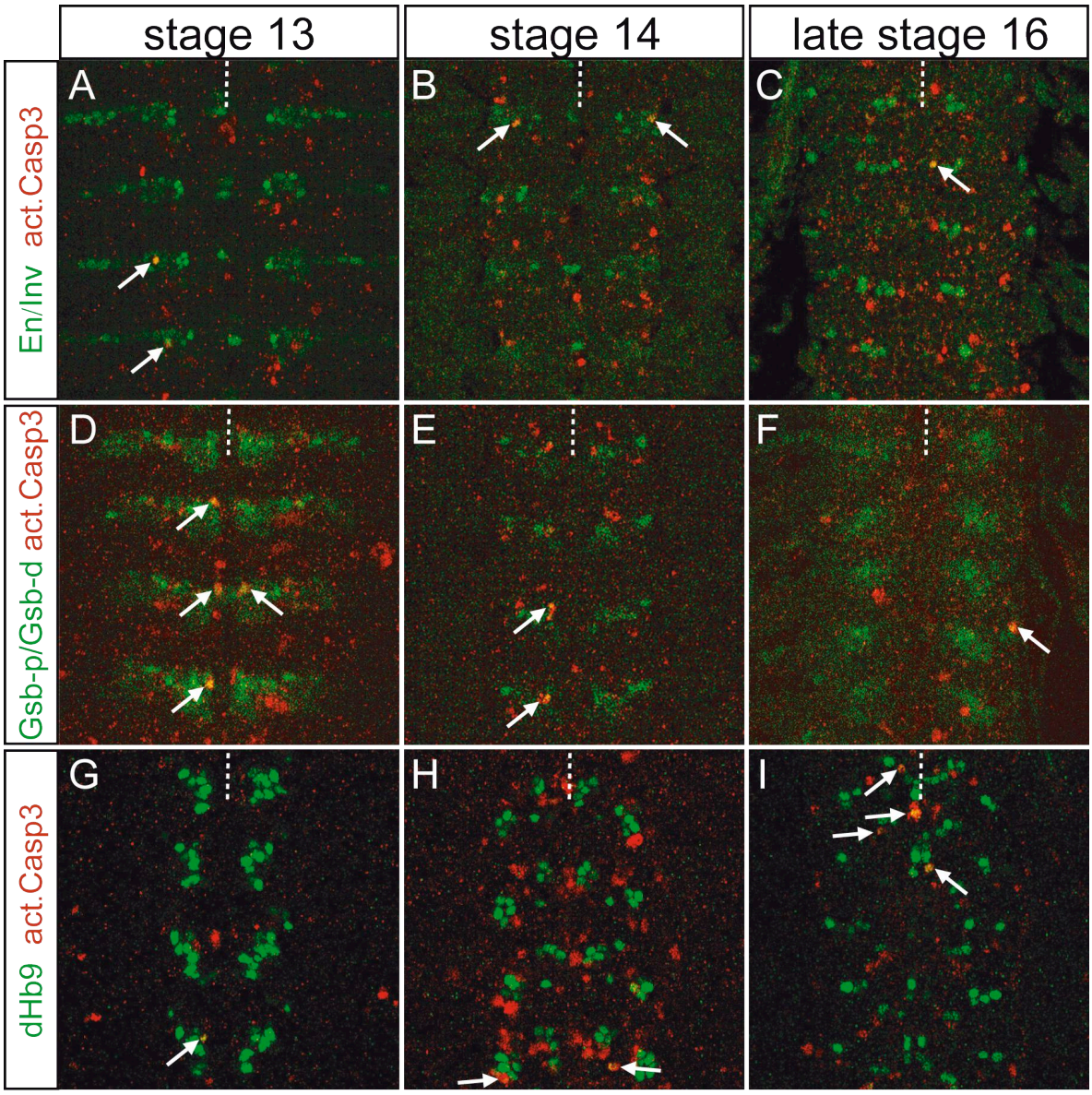


**Fig. 3-4. Caspase-dependent apoptosis of cells labeled by broadly expressed markers.**
A-C. Activated Caspase 3 (red) positive cells in the En/Inv expression (green) domain (arrows) are found throughout development.
D-F. Gsb-p and Gsb-d (green) positive cells also show Caspase-3 activation (red) at all examined stages (arrows). At stages 13 (D) and 14 (E) apoptotic cells appear in segmentally repeated positions.
G-I. Activated Caspase-3 staining (red) in dHb9-expressing cells (green) (arrows). Apoptosis of dHb9-positive cells appears to be most abundant at late stage 16 (I).
Four abdominal segments are shown in each image. Stippled line marks the midline, anterior is up.

Some molecular markers which are expressed in small subsets of cells in the ventral nerve cord showed, as has already been reported (De Graeve et al., 2004; Novotny et al., 2002), interesting pattern changes in *H99* embryos (Fig. 3-5).

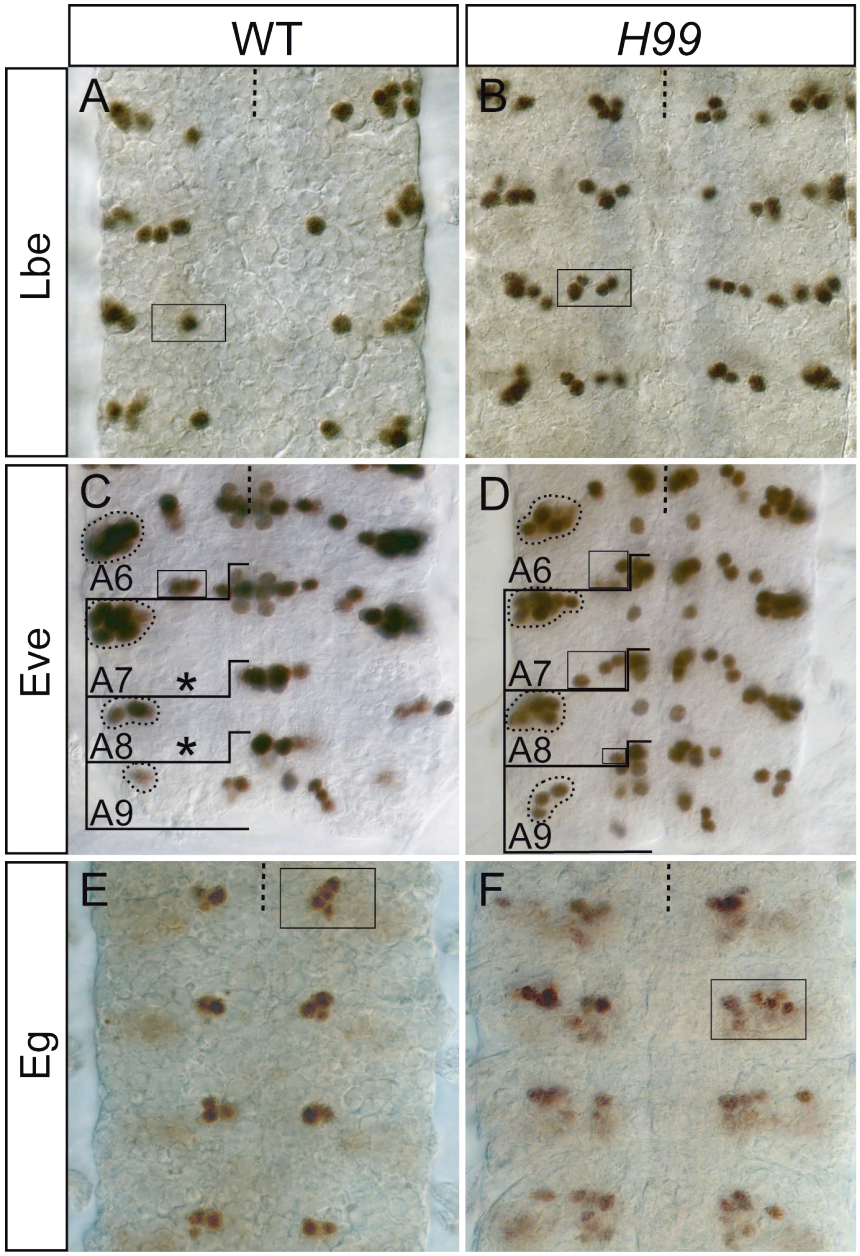


**Fig. 3-5. Comparison of markers expressed in small groups of cells.**
A,B. Ladybird-early-positive cells (brown) in the wt abdominal segments (A) form a lateral cluster. One additional cell, most likely from the NB5-3 lineage, is found more medially (square). In *H99* mutants (B), the lateral cluster appears unchanged. A cluster of 4 cells is found at the medial position (square).
C,D. Even-skipped expression (brown) in a wt embryo (C) marks three groups of cells: the medial cluster, U3, U4 and U5 motoneurons (squared in segment A6) and the EL cluster (dotted outline). The U3-U5 motoneurons are missing in A7 and A8 (asterisks). The EL clusters in A8 and A9 (dotted outline) are clearly smaller than those in more anterior segments. In *H99* embryos (D), U3-U5 motoneurons (square) are still present in A7, as well as U3 in A8 (square). The EL cluster in A8 (dotted outline) appears as big as those in more anterior segments. In A9 the EL cluster (dotted outline) comprises fewer cells than A8 in *H99*, but more than A9 in the wt.
E,F. The Eagle-positive (brown) NB7-3 cluster (square) comprises 4 cells in the wt abdominal segments (E). In *H99* embyos (F) the clusters contain 8 to 10 cells (square).
Shown are four abdominal segments of late stage 16 embryos. Stippled line marks the midline, anterior is up.

Ladybird early (Lbe) is a homeobox transcription factor involved in several processes such as heart and muscle development (Jagla et al., 1997; Jagla et al., 1994; Jagla et al., 1998). In the embryonic CNS it is required for the correct development of glial cells derived from NB5-6 and of neurons derived from NB5-3 (De Graeve et al., 2004). De Graeve et al. also showed that late *H99* embryos have additional Lbe-positive neurons in the ventral nerve cord. I could confirm this observation (Fig. 3-5A,B), and in addition could show by immunostaining with the activated Caspase 3 antibody that these Lbe-positive cells die in stages 13 and 14 (Fig. 3-6A-C). Caspase 3 activation in Lbe-expressing cells also occurred at late stage 16. Due to a lack of additional markers that would allow discrimination between the Lbe-positive cells in each hemisegment, I could not precisely identify the apoptotic cells.

Even-skipped (Eve), another marker used, is a homeodomain-containing transcription factor expressed in a very restricted and well-described pattern in the embryonic CNS (Doe et al., 1988; Frasch et al., 1987). Eve-expressing cells in each hemisegment include the medially lying aCC motoneuron and pCC interneuron, first-born progeny of NB1-1, the 8-10 Eve-lateral (EL) neurons descending from NB3-3, the RP2 motoneuron belonging to the lineage NB4-2 and the 5 U motoneurons descending from NB7-1 (Broadus et al., 1995; Doe et al., 1988; Jacobs and Goodman, 1989; Patel et al., 1989) (Fig. 3-5C). At late stage 16, the Eve expression pattern in the thorax and in abdominal segments A1 to A6 did not reveal any difference between wt and H99 embryos (Fig. 3-5C,D). However, the posteriormost segments (A7-A9) showed two clear differences in the Eve pattern. First, the EL clusters in A8 and A9 of wt embryos comprised fewer cells than in *H99* embryos. Second, a part of the U motoneurons (from here on referred to as Us) in segments A7 to A8 of wt embryos were missing, whereas they were still present in homozygous *H99* embryos (Fig. 3-5C,D). To determine how the differences in EL and U neuron numbers between wt and *H99* embryos come about, I compared their numbers in the relevant segments. Cell counts in wt late stage 16 embryos revealed that A8 and A9 EL clusters contain 3.42±0.64 and 1.35±0.49 cells/hs, respectively. In *H99* embryos, these numbers increased to 7.17±0.70 (A8) and 2.96±0.20 (A9) cells/hs (Table 3-1). In the wt, EL clusters in more anterior abdominal segments contain 8 to 10 neurons (Patel et al., 1989),

which suggests that the reduction in A8 and A9 is achieved through two mechanisms: 1. generating fewer EL neurons in A8 and especially A9. This could be a consequence of NB3-3 undergoing fewer divisions in these segments, or of keeping Eve expression off in some of the NB3-3 progeny, or a combination of both. 2. removal of a part of the EL neurons through apoptosis. Stage 14 and 15 wt embryos show activation of Caspase 3 in the A8 and A9 EL clusters, indicating that apoptosis indeed contributes to the adjustment of EL neuron numbers in these segments.

| Genotype | Number of EL neurons per segment | |
|---|---|---|
| | A8 | A9 |
| WT | 3.42 ± 0.64 (n=26) | 1.35 ± 0.49 (n=26) |
| *H99* | 7.17 ± 0.70 (n=24) | 2.96 ± 0.20 (n=24) |

Table 3-1. Cell counts of A8 and A9 EL neurons in late stage 16 wild type (WT) and *H99* embryos. n indicates the number of counted hemisegments.

Counts of U motoneurons revealed that, in late stage 16 wt embryos, there were 2.1±0.32 Us/hs in segment A7. Segment A8 contained 2.4±0.52 Us/hs. In *H99* embryos, segment A7 always comprised 5 Us/hs, and segment A8 3 Us/hs. Based on their medial position, the surviving Us in both segments are probably U1 and U2, whereas the more lateral and ventral U3, U4 and U5 underwent apoptosis in A7. In A8, the one dying U is probably U3. U4 and U5 do not seem to be born in this segment, as I have observed these neurons neither in earlier stages of wt embryos, nor in *H99* embryos (Fig. 3-5D). Alternatively, they may be present but not express Eve. The immunostaining against activated Caspase 3 showed that the U3, U4 and U5 motoneurons in A7 and U3 in A8 die at stages 14 and 15 (Fig. 3-6D,E). In addition, I observed apoptotic neurons in A8 at late stage 16 (Fig. 3-6F). As their dorsal and medial position reveals, these are the aCC and RP2 motoneurons.

A further marker, the zinc-finger protein Eagle, has been described to be required for proper differentiation of cells in 4 neuroblast lineages, NB2-4, NB3-3, NB6-4 and NB7-3 (Dittrich et al., 1997; Higashijima et al., 1996). Due to the downregulation of Eg protein in late development, I could reliably analyze only the NB7-3 lineage. It consists of four neurons, 3 interneurons (EW1-3) and one moto-

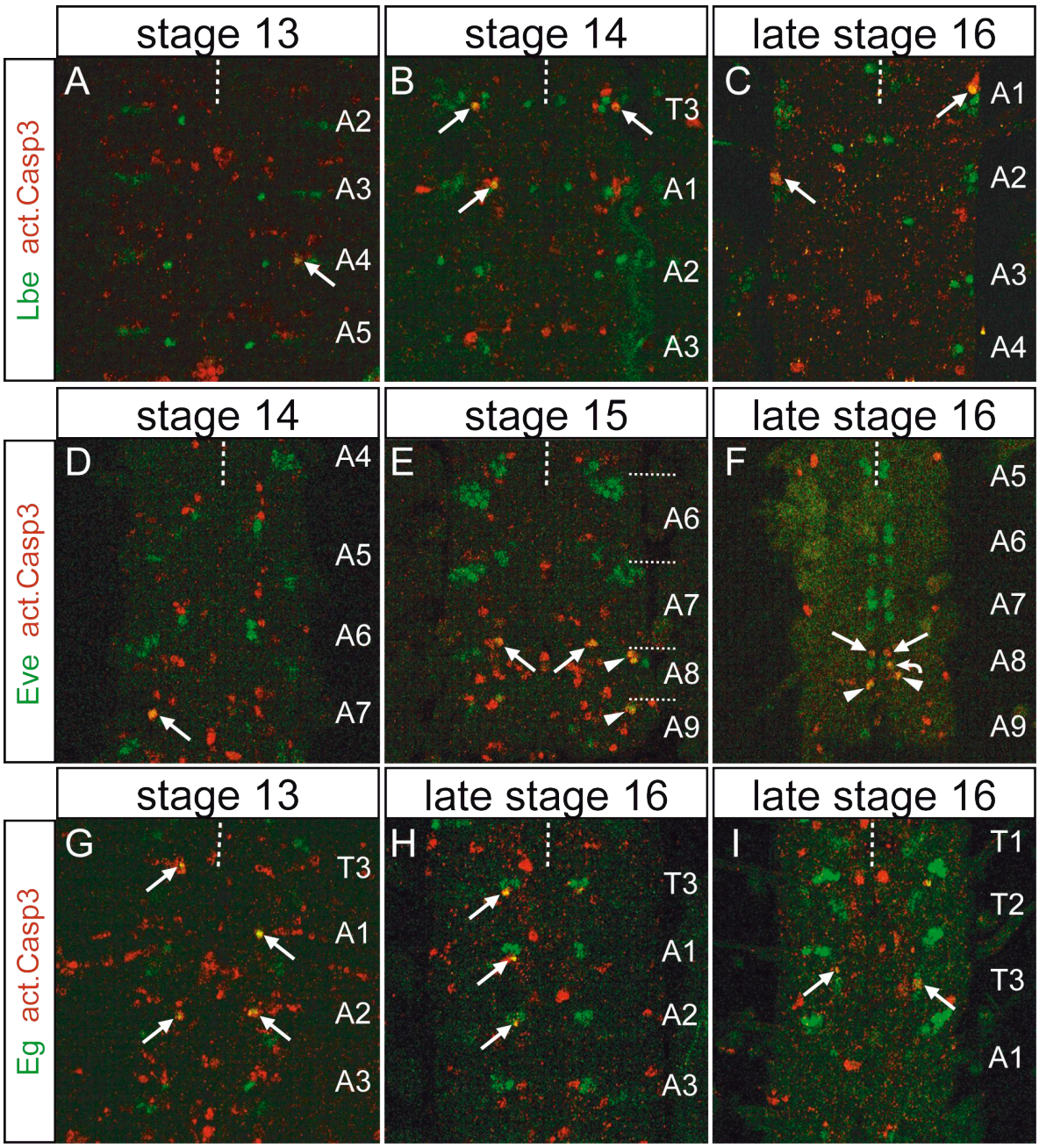


**Fig. 3-6. Caspase-dependent apoptosis of cells expressing markers that label small groups of cells.**

A-C. Lbe-positive (green) cells showing Caspase 3 activation (act.Casp3, red) are found at stages 13 (A), 14 (B) and late 16 (C) (arrows).

D-F. Activation of Caspase 3 (red) in Eve-expressing cells (green). At stage 14 (D) apoptotic U motoneurons are first visible in segment A7 (arrow). More apoptotic Us are found at stage 15 (arrows in E), as well as dying EL neurons in A8 and A9 (arrowheads in E). Dotted lines delineate approximate segment borders. At late stage 16 (F), segment A8 shows dying aCC motoneurons (arrows), pCC interneuron (curved arrow) and RP2 motoneurons (arrowheads).

G-I. Eg-positive cells (green) showing act.Casp3 staining (red). At stage 13 (G) the presumptive NB7-3 neuroblast shows Caspase-3 activation (arrows). Apoptosis of the NB7-3 GW motoneuron (H) takes place at late stage 16 and in segments T3 to A2 (arrows). The anterior NB2-4t motoneuron in segment T3 (arrows) also dies at late stage 16 (I).

Segments shown are indicated in each image. Stippled line marks the midline, anterior is up.

neuron (GW) (Fig. 3-5E, 3-9), and previously published data suggest that apoptosis is involved in the formation of this lineage, as it comprises additional cells in late *H99* embryos (Novotny et al., 2002) (Fig. 3-5F). It has also been shown that the death of some of these cells depends on Notch signalling activity (Lundell et al., 2003). In addition to the already described apoptosis in NB7-3, one of its cells per hemisegment was positive for activated Caspase 3 in all segments of stage 13 embryos (Fig. 3-6G). It was found at a very ventral position in the CNS, and showed activation of Caspase 3 in all thoracic and abdominal segments, which suggested it may be the neuroblast born in the third and last division in this lineage. These findings are in agreement with data obtained for DiI labeled lineages in *H99* embryos, where the last NB7-3 neuroblast appears to survive and to continue dividing both in the thoracic and abdominal segments (Rogulja-Ortmann et al., 2007). However, as no neuroblast-specific marker has been described in *Drosophila* to date, I could not unambiguously determine the identity of this cell. I found a further apoptotic cell in the NB7-3 lineage specifically in the third thoracic and all abdominal segments of late stage 16 embryos (Fig. 3-6H). Its posterior position in the cluster suggested it may be the GW motoneuron (from here on referred to as GW).

As Eg expression in the thorax is generally stronger than in the abdomen, an unexpected additional apoptotic cell was found exclusively in the third thoracic segment, in a very dorsal position in the CNS that corresponded to a motoneuron belonging to the NB2-4t lineage (Fig. 3-6I).

# B. Regulation of apoptosis in identified dying neurons in the embryonic CNS

In the second part of my thesis work, I focused on the identified apoptotic neurons. Most of these turned out to be presumptive motoneurons (U motoneurons, GW and the anterior NB2-4t motoneuron), and their removal only in specific body segments implies a role for apoptosis in the formation and/or refining of neuromuscular networks along the antero-posterior body axis. It was therefore of importance to investigate the developmental mechanisms involved in regulating survival versus death decisions in these cells. The results from this part of the work were published in the journals *Development* 135(20), 2008 and *Fly* 2(6), 2008.

## 3.3. Segment-specific apoptosis of U motoneurons

A part of the U motoneurons in segments A7 and A8 were found to be positive for activated Caspase 3 at developmental stages 14 and 15. More precise analysis revealed that U3, U4 and U5 undergo apoptosis in A7, as well as U3 in A8. By the end of embryonic development (late stage 16), these cells can no longer be detected using the anti-Eve antibody. Interestingly, the pattern of death of these neurons showed correlations to the expression pattern of homeotic genes, known to specify the identity of segments along the antero-posterior body axis both in vertebrates and invertebrates. The apoptotic U motoneurons were found in the domain where expression of a posterior *Hox* gene, *Abdominal-B* (*AbdB*), is strongest (Casanova et al., 1986; Sanchez-Herrero and Crosby, 1988), and that of more anterior ones, *Antennapedia* (*Antp*)*, Ultrabithorax* (*Ubx*) and *Abdominal-A* (*abdA*), very weak (Hirth et al., 1998). I therefore examined the expression of these genes in the U motoneurons.

### 3.3.1. Expression of *Antennapedia* in U motoneurons

*Antp* is expressed in the embryonic CNS from the posterior half of the labial segment through to the anterior half of A8 (Carroll et al., 1986; Hirth et al., 1998) (Fig. 3-7), with strongest expression from the posterior half of T1 to the anterior half

of T3. In abdominal segments A5 and A6 of stage 14 embryos, all Us strongly expressed *Antp* (Fig. 3-8A). In segment A7, U1 was Antp-negative, U2 and U3 showed very weak *Antp* expression, and U4 and U5 showed weak to moderate *Antp* levels. In A8, U1 was mostly very weakly Antp-positive, and occasionally it was devoid of *Antp* expression. U2 and U3 were weakly Antp-positive.

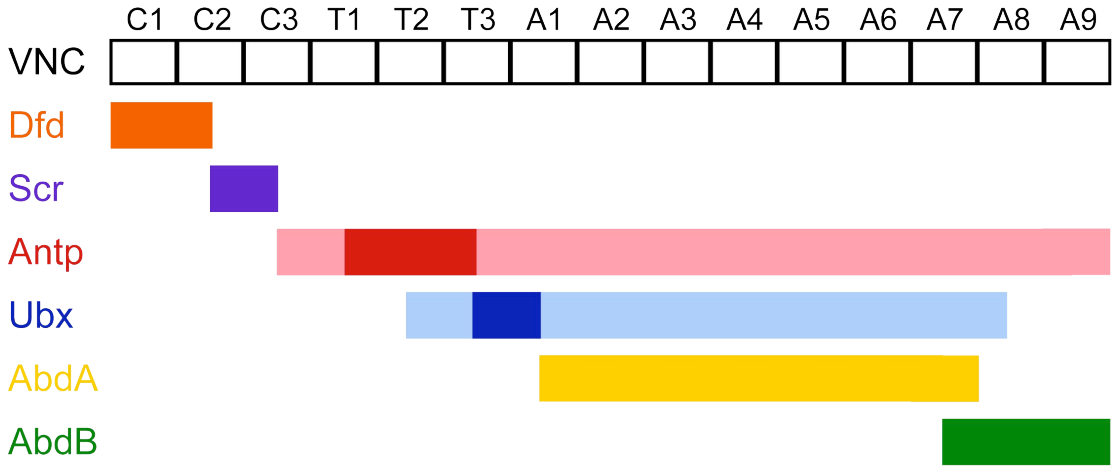


**Fig. 3-7. Scheme of *Hox* gene expression in early stages of embryonic development.**
*Hox* genes are expressed in a parasegmental fashion, with the anterior border of expression localized in the middle of a segment. C1-C3 denotes the gnathal segments, T1-T3 the thoracic, and A1-A9 the abdominal ones. Anterior is to the left.

### 3.3.2. Expression of the *bithorax* complex genes in U motoneurons

*Ubx* expression stretches from the posterior half of segment T2 to the anterior half of segment A7, with strongest expression in posterior T3 and anterior A1 (Beachy et al., 1985; Carroll et al., 1988; White and Wilcox, 1985) (Fig. 3-7). At stage 14, U1 and U2 showed strong and U3 weak *Ubx* expression in A5 and A6 (Fig. 3-8B). U4 and U5 were free of Ubx in both segments. In segments A7 and A8, none of the Us expressed *Ubx*.

*abdA* is expressed from the posterior half of segment A1 to the anterior half of A8 (Hirth et al., 1998; Karch et al., 1990) (Fig. 3-7). However, it was not expressed in the Us of any of the posterior body segments of stage 14 embryos (A5 to A8) (Fig. 3-8C).

*AbdB* is expressed in segments A5 to A9, with strongest expression in A7 to A9 (Delorenzi and Bienz, 1990; Hirth et al., 1998; Sanchez-Herrero and Crosby,

1988) (Fig. 3-7). In segment A5 at developmental stage 14, when the Us begin to undergo apoptosis, two of these cells, U1 and U2, showed very weak *AbdB* expression (Fig. 3-8D). The other three (U3-U5) did not express *AbdB*. In segment A6, U1 and U2 showed moderate *AbdB* expression, U3 and U4 showed traces of staining, whereas U5 either showed traces or was devoid of *AbdB*. In contrast, in A7 and A8 all 5 Us exhibited very high *AbdB* levels.

Considering the fact that none of the examined *Hox* genes was consistently present in, or excluded from, the apoptotic Us, none of these genes alone appears to be responsible for their fate. As *AbdB* levels were very high in A7 and A8, the possibility remains that it affects U motoneuron survival in a cell context-dependent manner.

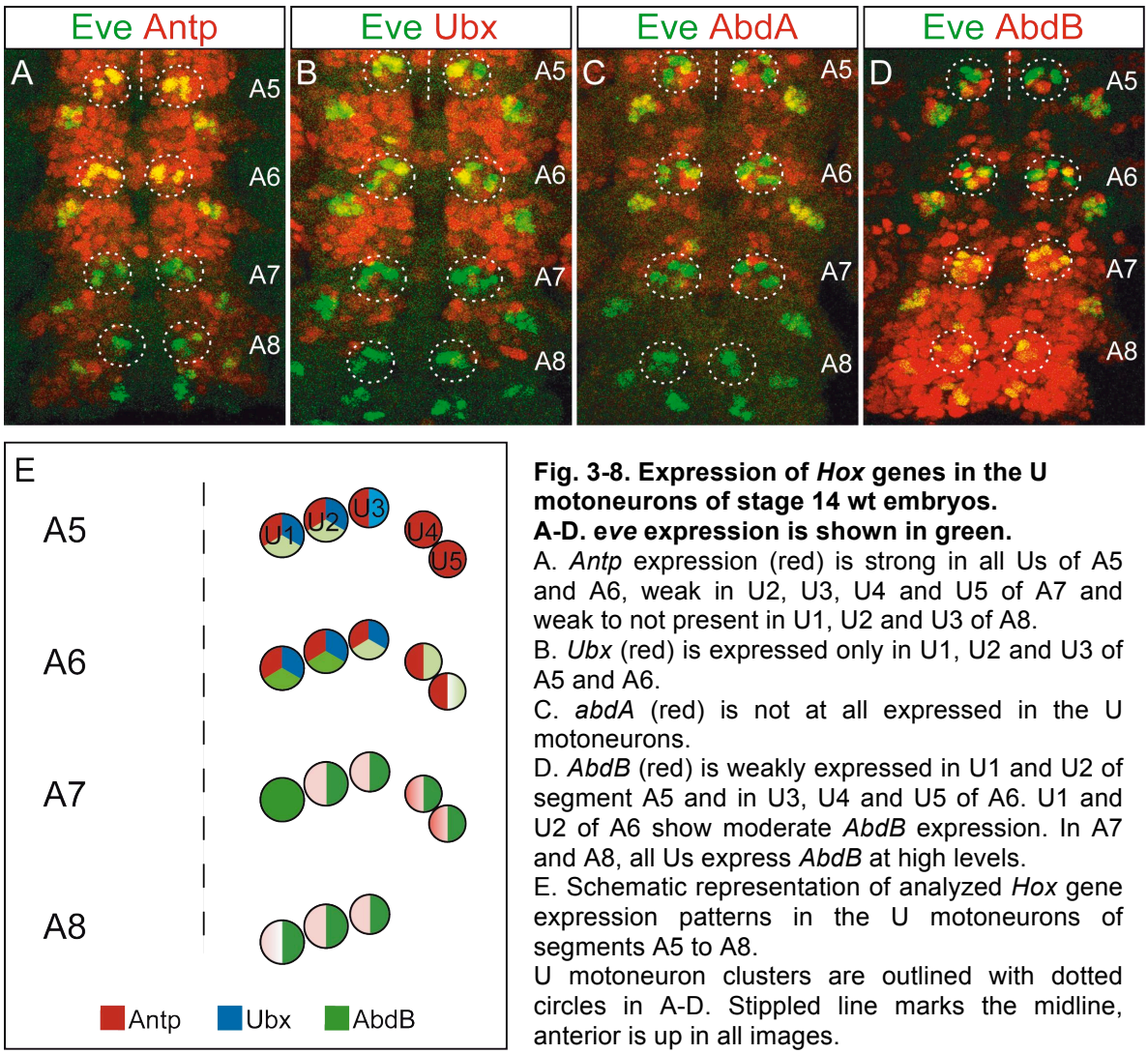


**Fig. 3-8. Expression of *Hox* genes in the U motoneurons of stage 14 wt embryos.**
**A-D. *eve* expression is shown in green.**
A. *Antp* expression (red) is strong in all Us of A5 and A6, weak in U2, U3, U4 and U5 of A7 and weak to not present in U1, U2 and U3 of A8.
B. *Ubx* (red) is expressed only in U1, U2 and U3 of A5 and A6.
C. *abdA* (red) is not at all expressed in the U motoneurons.
D. *AbdB* (red) is weakly expressed in U1 and U2 of segment A5 and in U3, U4 and U5 of A6. U1 and U2 of A6 show moderate *AbdB* expression. In A7 and A8, all Us express *AbdB* at high levels.
E. Schematic representation of analyzed *Hox* gene expression patterns in the U motoneurons of segments A5 to A8.
U motoneuron clusters are outlined with dotted circles in A-D. Stippled line marks the midline, anterior is up in all images.

## 3.4. Segment-specific apoptosis of the GW and the NB2-4t anterior motoneuron

Using the transcription factor (Eagle) Eg as a marker, the GW motoneuron descending from NB7-3 was found to undergo apoptosis in segments T3 to A8, and the anterior motoneuron of NB2-4t was found to die in T3 only. Both of these motoneurons die near the end of embryogenesis, at late stage 16. As Eg labels the whole NB7-3 lineage in all segments throughout development, and the whole NB2-4 lineage only in early developmental stages, the extent of our knowledge about the development of each of these lineages is rather different. The lineages and my further investigations on them are therefore described separately below.

### 3.4.1. The NB7-3 lineage

The NB7-3 lineage generally comprises 3 interneurons (EW1-3) and one motoneuron (GW) (Bossing et al., 1996; Dittrich et al., 1997; Higashijima et al., 1996; Novotny et al., 2002; Schmid et al., 1999) (Fig. 3-9). The exact birth order of these neurons and the molecular markers they express have been the subject of several studies in recent years. The focus of these studies was on the abdominal NB7-3 lineage and their results will be briefly presented here. The NB7-3 neuroblast delaminates at a rather late point in CNS development, and expresses the transcription factor *eg* directly after delamination (Dittrich et al., 1997; Higashijima et al., 1996). It undergoes three asymmetric divisions and generates three ganglion mother cells, GMCa, GMCb and GMCc (Fig. 3-9). Generally, upon each division NBs in the embryonic CNS undergo temporal identity changes through sequential expression of identity markers, most of which are transcription factors (Brody and Odenwald, 2002; Kambadur et al., 1998). These temporal identity markers are inherited by, and specify the fate of, each GMC and its progeny, thus ensuring that each NB produces a unique and invariant cell lineage. The NB7-3 GMCa thus expresses *hunchback* (*hb*), the first temporal identity gene (Fig. 3-9). It divides once to generate a serotonergic interneuron, EW1, and a motoneuron, GW, both of which are *hb*-positive. The second GMC, GMCb, expresses *Krüppel* (*Kr*), the second gene in the temporal identity cascade. GMCb

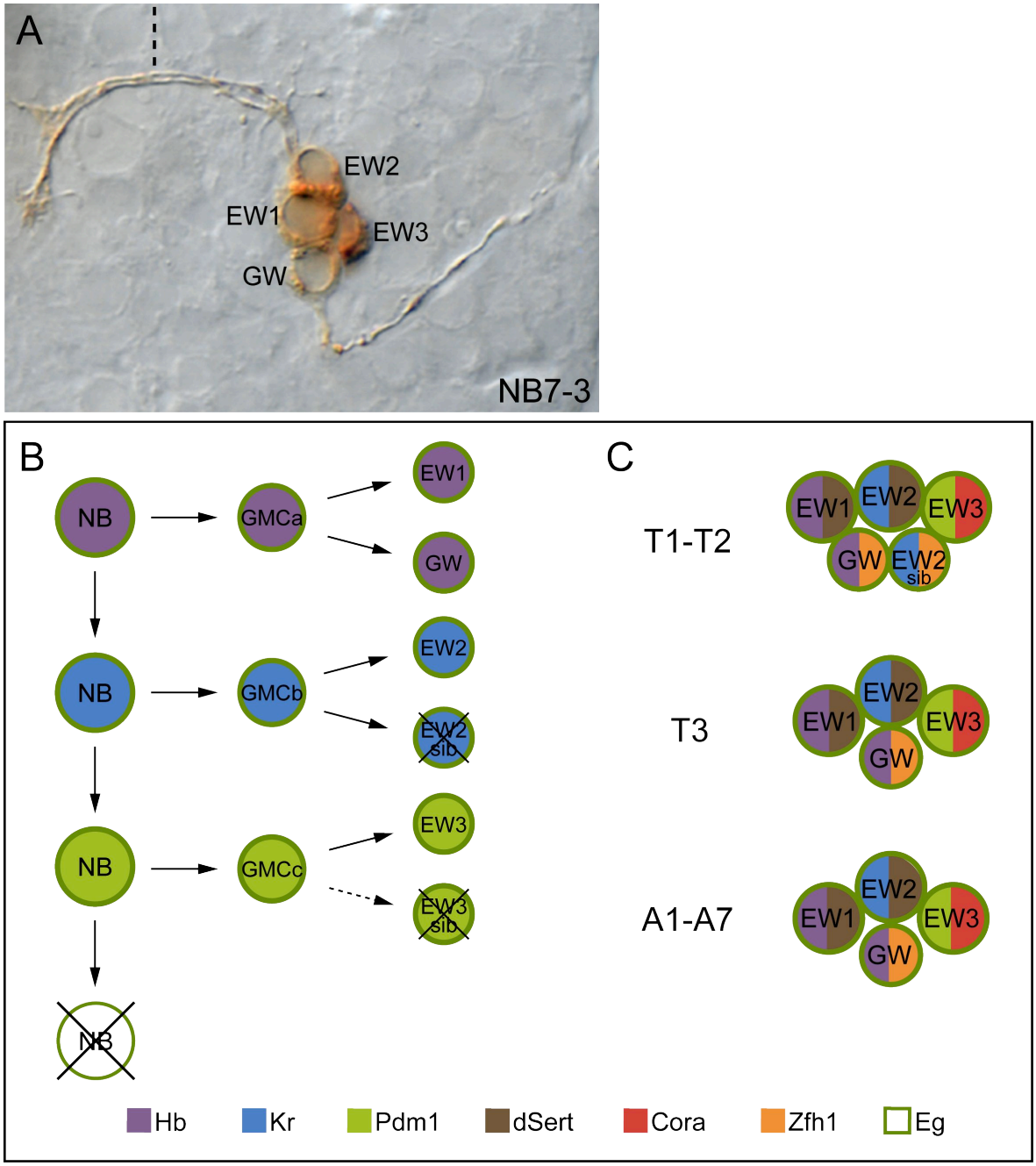


**Fig. 3-9. The NB7-3 lineage.**
A. A DiI-labeled clone of the NB7-3 lineage in a late stage 16 embryo. The three interneurons (EW1-3) projecting contralaterally, and the motoneuron (GW) with an ypsilateral outward projection are indicated. The stippled line marks the midline.
B. A scheme of the division pattern of NB7-3. The temporal identity markers are shown in the color code. Crosses indicate cells that undergo apoptosis in early stages of lineage development. The stippled arrow indicates the putative EW3 sibling cell.
C. The segment-specific NB7-3 lineages at late stage 16, showing marker genes that each cell expresses. 5 cells are mostly found in T1 and T2, whereas T3 to A7 mostly comprise 4 cells. Anterior is up in all images.

generates the second serotonergic interneuron, EW2, which maintains *Kr* expression (Isshiki et al., 2001; Novotny et al., 2002), and a sibling cell which undergoes apoptosis without differentiating (Lundell et al., 2003). GMCc is positive for the POU domain protein 1 (Pdm1) and produces a corazonergic interneuron, EW3, although it is still debated whether GMCc divides and the EW3 sibling cell undergoes apoptosis (Lundell et al., 2003), or if the GMCc directly differentiates into the EW3 interneuron (Karcavich and Doe, 2005) (Fig. 3-9B). The abdominal segments A7 and A8 lack the corazonin-expressing EW3 interneuron, and A8 also shows only one serotonin-producing interneuron. EW3 is only transiently Pdm1-positive (Isshiki et al., 2001; Novotny et al., 2002).

The Notch signalling pathway has been identified as the activator of apoptosis in the sibling cell of EW2 (Lundell et al., 2003). During asymmetric division of the second (and possibly third) GMC, the surviving sibling cell receives the asymmetrically distributed protein Numb (Karcavich and Doe, 2005; Lundell et al., 2003), which counteracts the apoptosis-inducing Notch signal, and thus allows it to survive and differentiate into an interneuron.

In our laboratory, a difference in cell number was observed in late embryos between anterior thoracic segments (T1 and T2) on the one side, and the posterior thoracic (T3) and the abdominal (A1 to A7) segments on the other. In T1 and T2, the NB7-3 cluster often contained a $5^{th}$ cell, which expresses *Kr* (J. Urban, personal communication). As *Kr* is the second gene in the temporal identity cascade, this cell was probably the EW2 sibling that dies right after birth in abdominal segments (Karcavich and Doe, 2005; Lundell et al., 2003). I found that this cell also underwent apoptosis in T1 and T2 but this took place at the end of embryogenesis (Fig. 3-10C). In addition, I observed activation of Caspase 3 in one interneuron in A7 (Fig. 3-10D). A lack of Corazonin expression has been reported for this abdominal segment (Novotny et al., 2002), suggesting that this is most likely the EW3 interneuron. The lateral position of the cell within the cluster also supports this notion. As the NB7-3 neurons can be individually identified based on marker gene expression and their position in the cluster (Fig. 3-9), I used the anti-Hb or anti-Zfh1 antibody to identify the GW motoneuron.

GW underwent Caspase-dependent cell death at late stage 16 specifically in segments T3 to A8 (Fig. 3-10A). Further analysis was restricted to the thorax and

the 7 abdominal segments A1-A7, as NB7-3 appears to develop differently in A8 and comprises only 2-3 cells. GW was either positive for activated Caspase 3, or already removed from the CNS, in 55.6% of analyzed T3 hemisegments (hs) (n=27) and in 81.2% of analyzed abdominal hs (A1-A7, n=69) (Table 3-2).

| Segment | Percentage of apoptotic GWs | |
|---|---|---|
| | mid stage 16 | late stage 16 |
| T1-T2 | 0 % (n=32) | 0 % (n=19) |
| T3 | 0 % (n=16) | 55.6 % (n=27) |
| A1-A7 | 12.5 % (n=112) | 81.2% (n=69) |

Table 3-2. Frequency of observed GW motoneuron apoptosis in thoracic and abdominal segments of wild type embryos at the indicated developmental stages. n indicates the number of hemisegments analyzed.

The considerable difference in the percentage of apoptotic GWs between T3 and the abdomen appeared to be a consequence of differential apoptosis timing, as wt embryos at mid stage 16 showed Caspase 3-positive GWs in 12.5% of analyzed A1-A7 hs (*n*=112) and I did not observe dying T3 GWs at this stage (*n*=16) (Table 3-2). In addition, Caspase 3 activation did not occur simultaneously in the GWs of all abdominal segments: late stage 16 embryos showed hemisegments where GW appeared intact, others where GW showed Caspase 3 activation, and a third group where it could no longer be visualized with the Eg marker. These observations are indicative of the dynamics of apoptosis, and show that the analyzed specimens can only be regarded as snapshots taken at the time of embryo fixation. In addition, they suggest that GW apoptosis in T3 is initiated slightly later than in the abdomen. I also tested which of the three *Drosophila* proapoptotic genes is involved in GW apoptosis, and found that only *reaper* (*rpr*) mRNA expression is upregulated (Fig. 3-10B), whereas I never observed *hid* or *grim* mRNA in this cell. Also, TUNEL staining in late stage 16 embryos revealed TUNEL-positive GWs, confirming apoptosis (Fig. 3-10E). In order to confirm its survival in T1 and T2, I examined the NB7-3 lineage in the CNS of first instar larvae just after hatching. Indeed, in the great majority of examined nerve cords, in T3 and in the abdominal segments NB7-3 comprised only 3 cells, whereas in T1 and T2 it contained 4 cells (Fig. 3-10F).

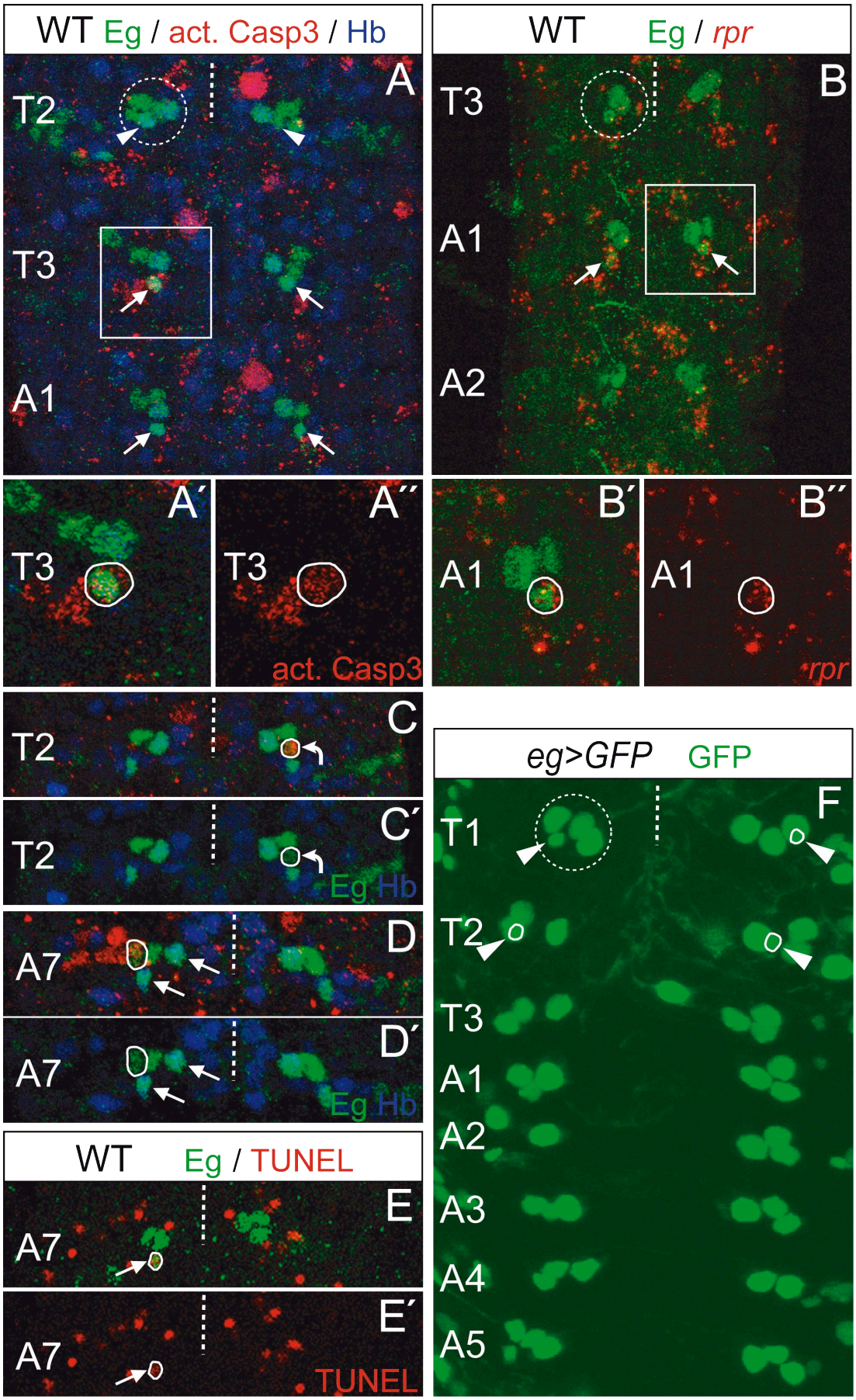
WT Eg / act. Casp3 / Hb
A
T2
T3
A1
WT Eg / rpr
B
T3
A1
A2
A´
T3
A´´
T3
act. Casp3
B´
A1
B´´
A1
rpr
C
T2
C´
T2
Eg Hb
D
A7
D´
A7
Eg Hb
WT Eg / TUNEL
E
A7
E´
A7
TUNEL
eg>GFP GFP
F
T1
T2
T3
A1
A2
A3
A4
A5

**Fig. 3-10.**

### 3.4.2. The NB2-4t lineage

The thoracic NB2-4 lineage comprises 8 to 12 neurons, two of which are motoneurons (Schmid et al., 1999; Schmidt et al., 1997) (Fig. 3-11). Later in development, from about stage 14, these two motoneurons lie in a dorso-medial position, separate from the other NB2-4t neurons. In the abdomen the motoneurons lie slightly apart from one another on the dorso-ventral axis, whereas in the thorax they occupy the same dorso-ventral position, with one lying anterior to the other (Fig. 3-12). Unfortunately, little is known about the division pattern of NB2-4, except that it generates 2 *hb*-positive GMCs, and thus 4 *hb*-positive progeny, including the two dorsal motoneurons (Mettler et al., 2006).

In segment T3, and only in this segment, the anterior NB2-4t motoneuron (from here on referred to as MNa) underwent Caspase-dependent apoptosis at late stage 16 (Fig. 3-12A). As *eg* expression was low in the NB2-4 lineage, I used the *eg*-Gal4 driver combined with UAS-*mCD8::GFP* for easier identification of NB2-4 cells. MNa either showed Caspase activation, or was already removed from the CNS, in 64.7% of analyzed T3 hs (n=17) (Table 3-3). As in the case of GW, only *rpr* mRNA expression was detectable in this cell (Fig. 3-12B). I confirmed apoptosis of this motoneuron by TUNEL staining (Fig. 3-12C). Identification and examination of the NB2-4t lineage in the CNS of first instar larvae was not possible due to the complexity of the *eg* expression pattern in the thorax.

**Fig. 3-10. The GW motoneuron undergoes *rpr*-dependent apoptosis.**
A. NB7-3 (stippled circle) in a late stage 16 wild type embryo is visualized with anti-Eagle (Eg) staining (green). GW motoneurons in T3 and A1 (arrows) and in T2 (arrowheads) also show Hunchback (Hb) staining (blue). In T3, one GW motoneuron is also positive for activated Caspase 3 (act. Casp3, red), indicating it is undergoing apoptosis. A´ shows a magnified single scan of the T3 NB7-3 lineage boxed in A. The apoptotic GW is outlined. A´´ shows only the activated Caspase 3 staining.
B. *rpr* mRNA (red) transcription is activated in apoptotic GWs (arrows). B´ shows a magnified single scan of the A1 NB7-3 lineage boxed in B. The GW expressing *rpr* mRNA is outlined. B´´ shows only the *rpr* mRNA staining.
C. A T2 NB7-3 shows a cell (curved arrow) positive for activated Caspase 3 (red). This cell does not express Hb (blue) and is thus not the GW motoneuron. C´ shows only the Eg and Hb staining.
D. An A7 NB7-3 is shown, with one interneuron positive for activated Caspase 3 (red). The GW motoneuron and the EW1 interneuron (arrows) express Hb (blue). This suggests, together with its very lateral position, that the apoptotic cell is EW3. D´ shows only the Eg and Hb staining.
E. NB7-3 in an A7 segment of a wild type embryo is shown. The apoptotic GW (arrow) shows TUNEL staining (red). E´ shows only the TUNEL staining.
F. GFP staining (green) in the CNS of an L1 larva expressing *GFP* in the Eg pattern. NB7-3 is outlined in T1 (stippled circle). GW is present only in segments T1 and T2 (arrowheads). The white outline marks GWs located underneath the interneurons.
Stippled line marks the midline, anterior is up in all images.

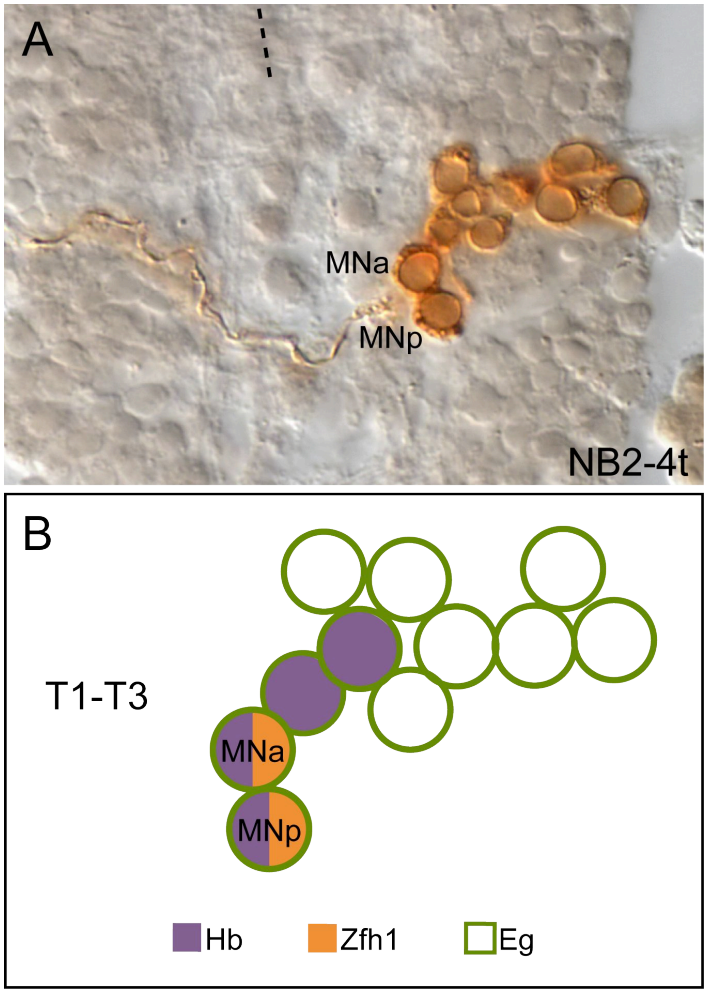


**Fig. 3-11. The NB2-4t lineage.**
A. A DiI-labeled clone of the NB2-4t lineage in a late stage 16 embryo. The two motoneurons (MNa and MNp) with contralateral outward projections are indicated. The stippled line marks the midline.
B. A scheme of NB2-4t. The currently known marker genes that its progeny cells express are shown in the color code.
Anterior is up in all images.

| Segment | Percentage of apoptotic MNas |
|---|---|
| T1-T2 | 0 % (n=29) |
| T3 | 64.7 % (n=17) |
| A1-A7 | 0 % (n=70) |

Table 3-3. Frequency of observed NB2-4t anterior motoneuron apoptosis in thoracic and abdominal segments of *eg>mCD8::GFP* embryos at late stage 16. n indicates the number of hemisegments analyzed.

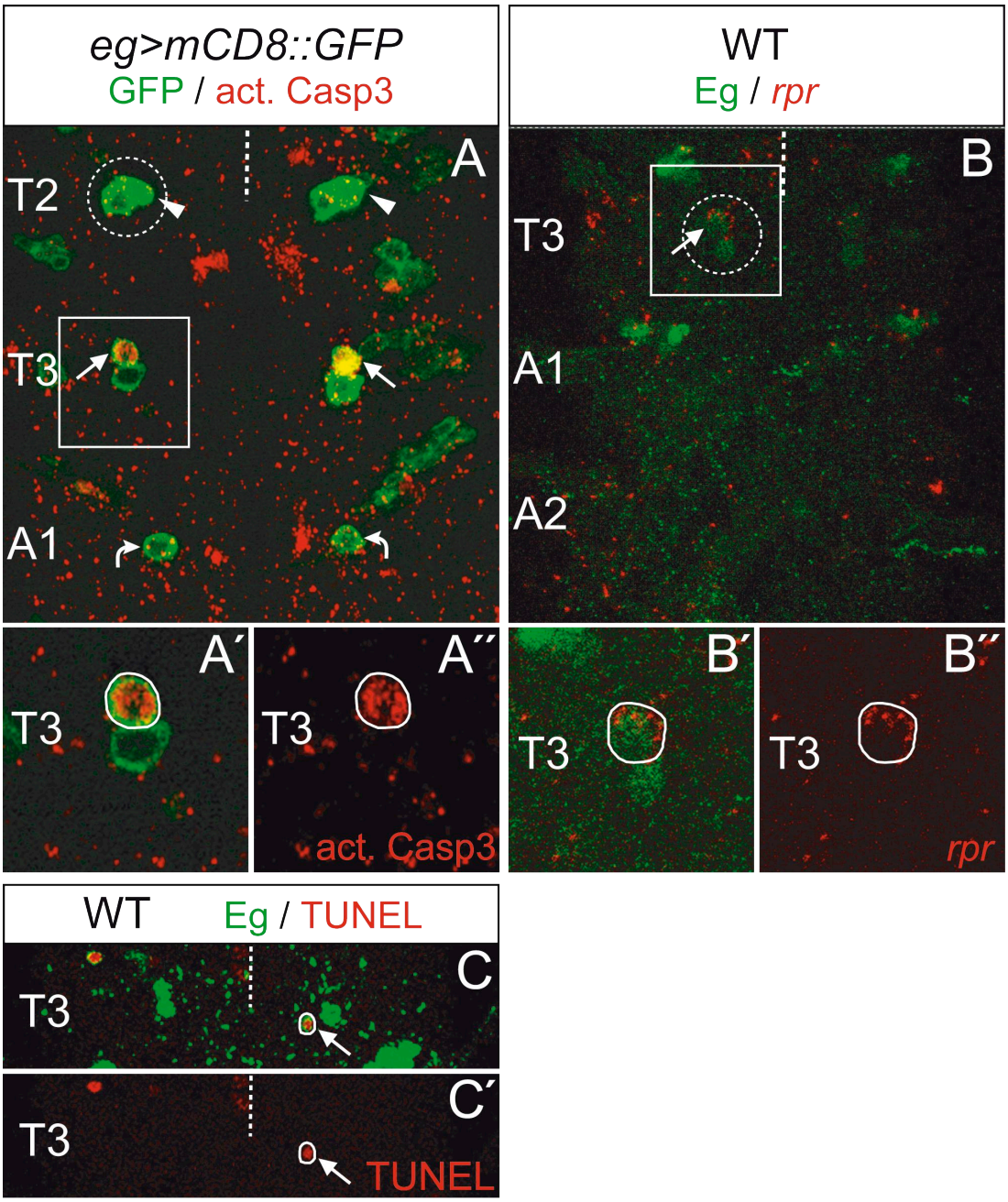


**Fig. 3-12. The MNa motoneuron undergoes *rpr*-dependent apoptosis.**
A. NB2-4t motoneurons (stippled circle) in a late stage 16 *eg>mCD8::GFP* embryo are visualized with anti-GFP staining (green). MNa motoneurons in T3 (arrows) are positive for activated Caspase 3 (act. Casp3, red), indicating they are undergoing apoptosis. Their counterparts in T2 (arrowheads) survive. In A1, only the anterior motoneuron is visible in this position (curved arrows). A´ shows a magnified single scan of the T3 NB2-4t MNs boxed in A. The apoptotic MNa is outlined. A´´ shows only the activated Caspase 3 staining.
B. *rpr* mRNA (red) transcription is activated in the apoptotic MNa (arrow). B´ shows a magnified single scan of the T3 NB2-4t lineage boxed in B. The MNa expressing *rpr* mRNA is outlined. B´´ shows only the *rpr* mRNA staining.
C. NB2-4t MNs in a T3 segment of a wild type embryo are visualized with anti-Eg staining (green). The apoptotic MNa (arrow) shows TUNEL staining (red). C´ shows only the TUNEL staining.
Stippled line marks the midline, anterior is up in all images.

## 3.5. Expression pattern of *Ultrabithorax* in the NB7-3 and NB2-4t lineages

The observed pattern of GW and MNa apoptosis showed an intriguing resemblance to the expression pattern of the *Drosophila Hox* gene *Ubx* (White and Wilcox, 1984). In the embryonic CNS, it is expressed from the posterior half of segment T2 to the anterior half of segment A7, with strongest expression in posterior T3 and anterior A1 (Beachy et al., 1985; Carroll et al., 1988; White and Wilcox, 1985) (Fig. 3-7). I therefore examined the expression of *Ubx* in the NB7-3 and NB2-4 lineages more closely.

### 3.5.1. *Ubx* expression in NB7-3

Ubx protein was present in the NB7-3 lineage from segment T2 to A7 (Figs. 3-13 and 3-14A). In T2, the early NB7-3 neuroblast did not express *Ubx*. Its progeny showed no or very low *Ubx* expression until stage 15, when *Ubx* was strongly upregulated, but only in the EWs. High *Ubx* levels were then maintained in the EWs at least until early stage 17, while the GW motoneuron and the presumable EW2sib remained devoid of *Ubx*. In segments T3 to A7 *Ubx* was expressed already in the newly delaminated NB7-3 neuroblast (Figs. 3-13 and 3-14A) and showed weak expression in all progeny cells until stage 15. In stage 15, it was strongly upregulated in all cells of the NB7-3 cluster. At late stage 16, *Ubx* was expressed at high levels in all NB7-3 cells of segments T3 to A7 (Figs. 3-14A and 3-17B). Thus, the pattern of *Ubx* expression in the GW motoneuron coincided with the timeline and pattern of apoptosis.

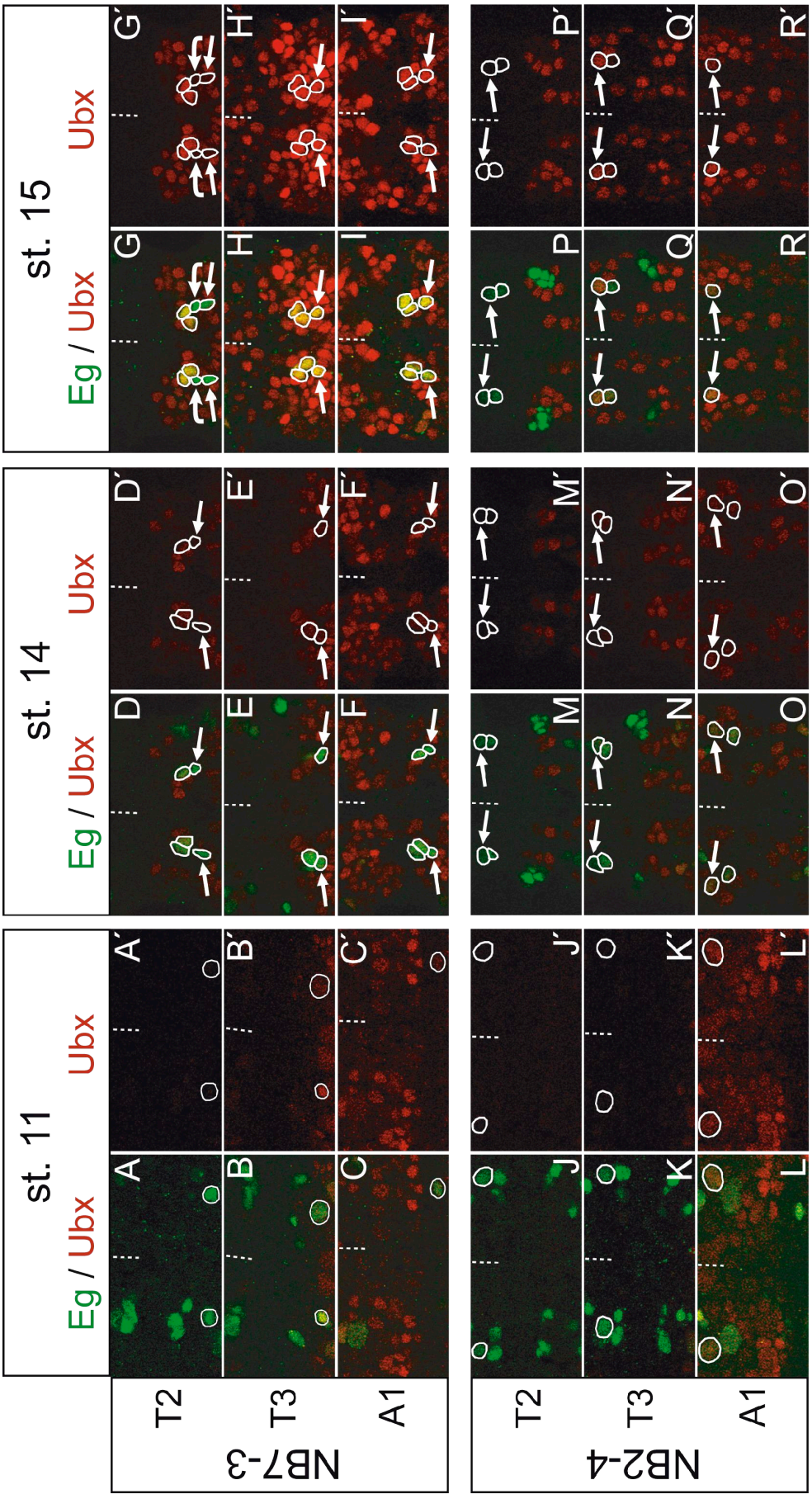
st. 11
Eg / Ubx
Ubx
st. 14
Eg / Ubx
Ubx
st. 15
Eg / Ubx
Ubx
T2
T3
A1
NB7-3
NB2-4

**Fig. 3-13.**

### 3.5.2. *Ubx* and *abdA* determine segment-specific NB7-3 identity

The difference in cell number between NB7-3 of T1-T2 and T3-A7 suggested a possible involvement of *Hox* genes in segment-specific identity of NB7-3. To test this, I examined cell numbers in NB7-3 of *Ubx* null mutants (*Ubx*$^{1}$) and indeed found that, only in segment T3, this lineage often comprised 5 cells instead of 4 (compare Fig. 3-15A and B), which would indicate a transformation into T2. To test whether *abdA* gives NB7-3 its identity in segments A1 to A7, I examined NB7-3 in *Df109*, a deficiency which removes both *Ubx* and *abdA*. Here, the NB7-3 lineage comprised 5 cells in all segments, indicating a transformation of NB7-3 into the T2 identity (Fig. 3-15D). The *abdA* mutant alone showed no phenotype (Fig. 3-15C), although it is possible that the abdominal NB7-3 lineage was transformed into T3. I would not have been able to see this effect, since there is no known difference between NB7-3 in T3 and the abdominal segments in the wild type. Nevertheless, these results show that the segment-specific identity of NB7-3 is determined by the *Hox* genes *Ubx* (in segment T3) and *abdA* (in segments A1 to A7).

**Fig. 3-13. Expression of Ubx in NB7-3 and NB2-4 in different developmental stages.**
A-C. Anti-Eg (green) and anti-Ubx (red) staining in wild type early NB7-3 neuroblasts (NBs) (outlined) at stage 11. In T2 (A), the NB shows no *Ubx* expression. In T3 (B) and A1 (C) the NB is *Ubx*-positive. A´-C´show only Ubx staining.
D-F. Stage 14 wild type embryos are shown. Only a part of the NB7-3 progeny is visible (outlined), including the GW motoneuron (arrows). In T2 (D), *Ubx* is expressed weakly or not at all in the progeny cells. GW shows no *Ubx* expression. In T3 (E) and in A1 (F), all progeny cells show weak *Ubx* expression at this stage. D´-F´show only Ubx staining.
G-I. Stage 15 wild type embryos show strong upregulation of *Ubx* expression. Some of the progeny cells are shown (outline), among them the GW motoneuron (arrows). In T2 (G) only the interneurons upregulate *Ubx*, whereas GW still shows no *Ubx* expression. The presumable EW2sib (curved arrows) is also devoid of Ubx. NB7-3 progeny of T3 (H) and A1 (I), including GW, all show strong *Ubx* expression. G´-I´show only Ubx staining.
J-L. Anti-Eg and anti-Ubx staining in wild type early NB2-4 neuroblasts (outlined) at stage 11. In T2 (J) and T3 (K) the NB shows no *Ubx* expression. In A1 (L) the NB is Ubx-positive. J´-L´show only Ubx staining.
M-O. Wild type embryos at stage 14 are shown. Only two motoneurons (outlined) are visible at this position, including MNa (arrows). In T2 (M), no *Ubx* expression can be seen. The T3 (N) and A1 (O) motoneurons show weak *Ubx* expression at this stage. M´-O´show only Ubx staining.
P-R. Wild type embryos at stage 15 are shown. The motoneurons (outlined) include MNa (arrows). The T2 motoneurons (P) are devoid of Ubx. In T3 (Q) *Ubx* is upregulated only in MNa (arrows). In A1 (R), only MNa is shown, and it has also upregulated *Ubx*. P´-R´show only Ubx staining.
Stippled lines mark the midline, anterior is up in all images.

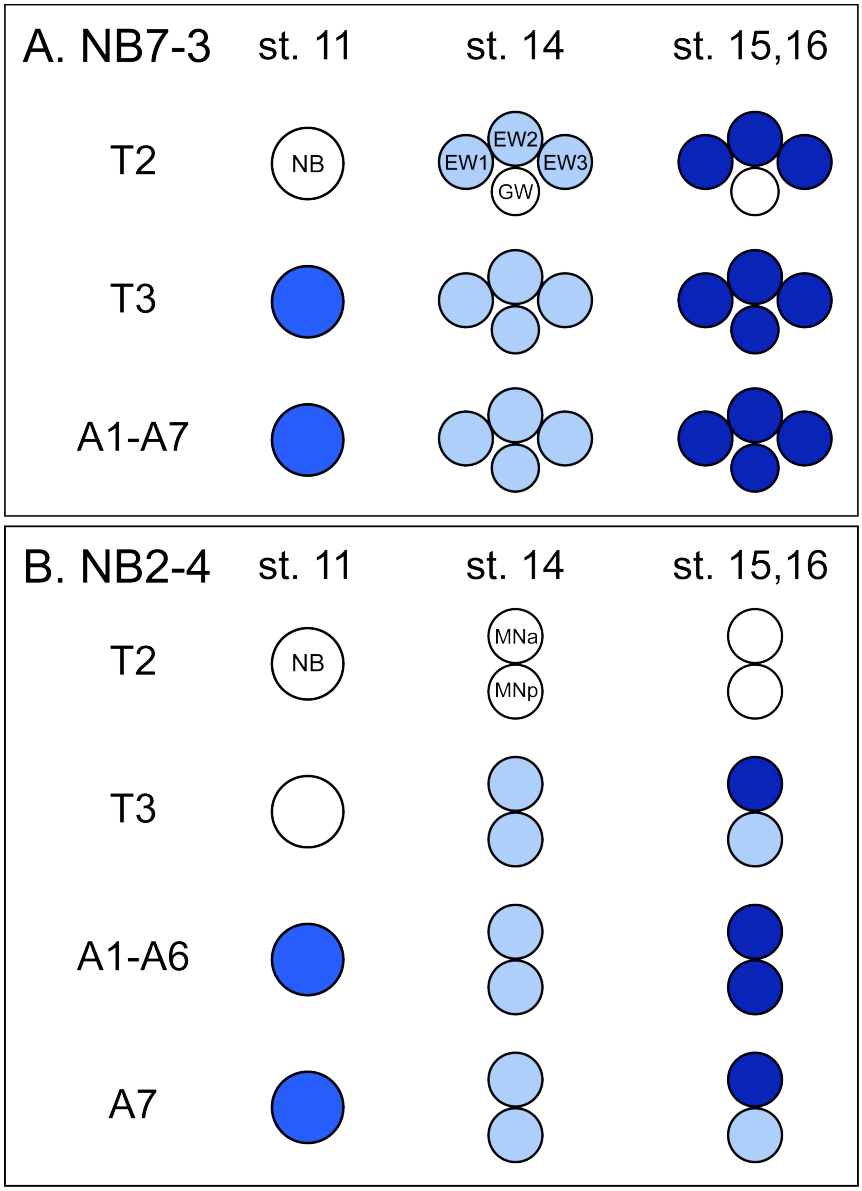


**Fig. 3-14. Summary of Ubx expression in the NB7-3 and NB2-4 lineages.**
A. The neuroblast and progeny of NB7-3. In segment T2 of stages 14-16, only GW and the interneurons are shown for clarity.
B. The neuroblast and the two motoneurons of NB2-4t.
The segmental pattern of Ubx expression is depicted at the indicated developmental stages. The intensity of the blue shading reflects the Ubx expression level; white indicates no expression. Anterior is up.

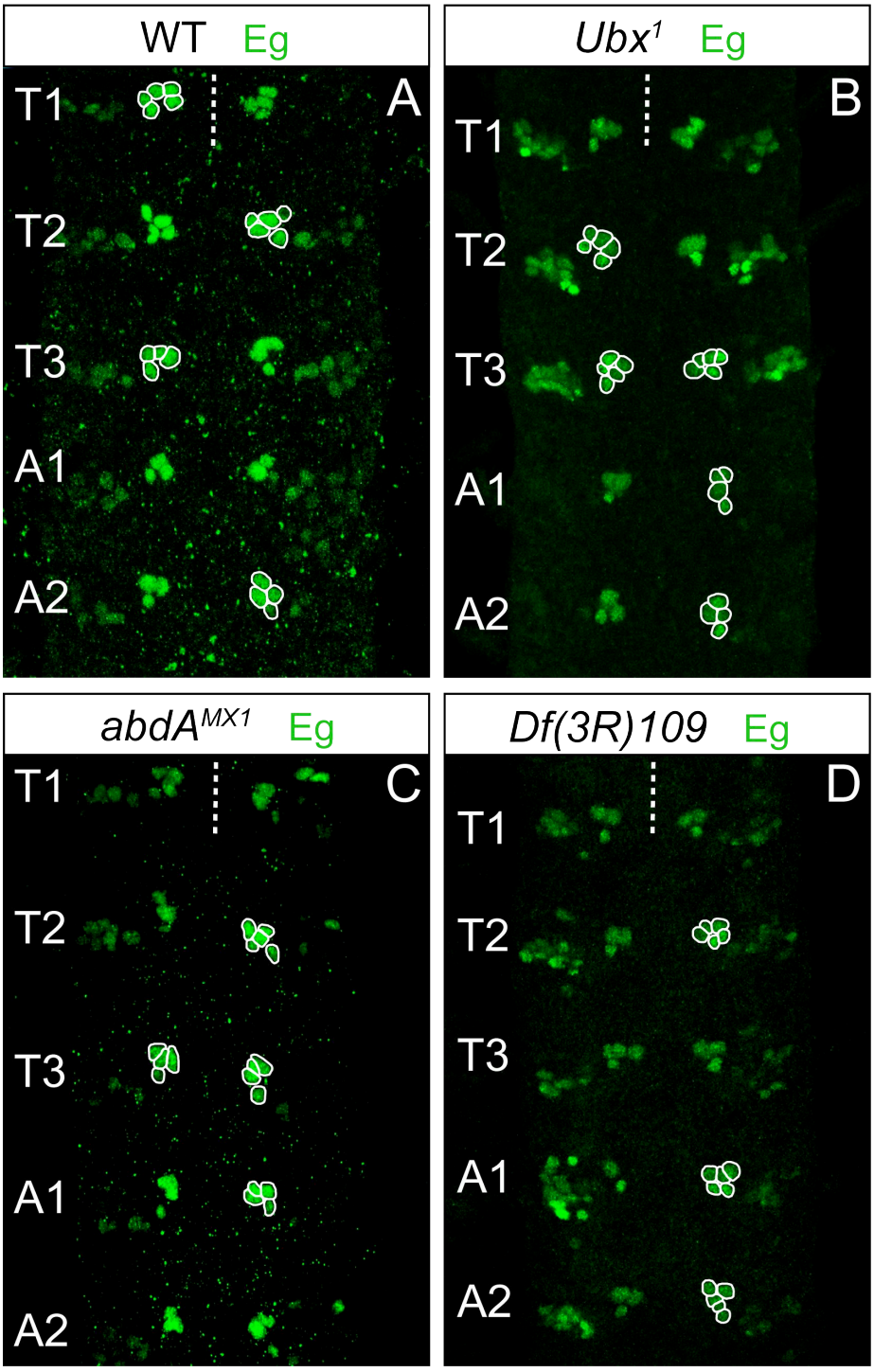


**Fig. 3-15. *Ubx* and *abdA* determine segment-specific NB7-3 identity.**
A. Anti-Eagle (Eg) staining (green) reveals that the wild type NB7-3 (outlined) comprises 5 cells in segments T1 and T2, and only four cells in T3 and the abdomen.
B. In an *Ubx* mutant, only NB7-3 of T3 appears to be transformed towards a T2 fate (5 cells), whereas the abdominal ones still show only 4 cells, presumably due to *abdA* function.
C. *abdA* mutants show no obvious transformation of NB7-3, although it is possible that abdominal lineages are transformed into T3.
D. In the *Df(3R)109* deficiency, where both *Ubx* and *abdA* are removed, NB7-3 in all segments shows 5 cells, indicating a transformation into T2.
The shown segments are indicated in the images, with cells of the NB7-3 lineage outlined. All images show the ventral nerve cord of developmental stage 16 embryos. Stippled lines mark the midline, anterior is up.

### 3.5.3. *Ubx* expression in NB2-4

As apoptosis in NB2-4t occured in segment T3 where Ubx levels are highest, I examined *Ubx* expression in this lineage as well. Here, *Ubx* was expressed from segment T3 to A8 (Figs. 3-13 and 3-14B). In T3, the early NB2-4t neuroblast did not express *Ubx*. First *Ubx*-positive cells in NB2-4t of T3 probably appeared around stage 12. However cells of NB2-4t and of the Eg-positive NB3-3 intermingle, making it difficult to distinguish between their progeny. From stage 14 on, the NB2-4t motoneurons were identifiable based on their dorsal position, and both showed weak *Ubx* expression. At stage 15 MNa strongly upregulated *Ubx*, whereas the posterior motoneuron (MNp) showed low *Ubx* levels (Figs. 3-13 and 3-14B). This difference was maintained at least until late stage 16 (Fig. 3-19B), when the motoneuron exhibiting high *Ubx* levels undergoes apoptosis. In segments A1 to A7, the young NB2-4 neuroblasts were all *Ubx*-positive (Figs. 3-13 and 3-14B). The progeny cells all seemed to show weak *Ubx* expression (although I could not tell them apart from progeny of NB3-3). At stage 14, where I could identify the motoneurons based on position, they still maintained weak *Ubx* expression levels. After this stage, and in contrast to segment T3, *Ubx* was strongly upregulated in both motoneurons in segments A1 to A6. In A7 *Ubx* expression in these cells resembled the one in segment T3: it was strong in MNa and weak in MNp (Fig. 3-14B). By late stage 16, *Ubx* levels were reduced only in MNp of all abdominal segments, whereas MNa maintained high *Ubx* expression but did not undergo apoptosis (Figs. 3-14B and 3-19B). The pattern of *Ubx* upregulation in the NB2-4t MNa of T3 thus correlated with apoptosis induction, although its counterparts in other segments also upregulated *Ubx* but did not undergo apoptosis.

### 3.5.4. How is the differential regulation of *Ubx* in the NB7-3 lineage of segment T2 achieved?

The differential late *Ubx* expression in the NB7-3 cells of segment T2 and in the NB2-4 motoneurons of T3 was intriguing. In NB7-3, EWs behaved like their counterparts in T3 and the abdominal segments. In contrast, GW did not upregulate *Ubx* like its counterparts in the more posterior segments. In NB2-4 of T3, MNa upregulated *Ubx* expression whereas MNp did not. In an attempt to identify the factor responsible for these differences in *Ubx* expression, I examined the gap gene *hunchback* (*hb*), a known regulator of *Ubx*. I focused on NB7-3 since

more is known about the development of this lineage, and there are more tools available for genetic manipulation. *hb* is known to repress *Ubx* in early embryonic development (White and Lehmann, 1986). Unfortunately, I could not assess whether *hb* has the same function in GW of T2, as it is required early in development to activate *Antp* expression and thereby specify the second thoracic segment (Wu et al., 2001). Consequently, in *hb* mutants the second thoracic segment does not develop. However, if *hb* were repressing *Ubx* in GW of T2, it may also be doing so in all cells of NB7-3 in the early developmental stages. The differentiation program of the NB7-3 neurons may then allow late *Ubx* upregulation despite the presence of Hb protein in the cells. Accordingly, *hb* mutants would show earlier upregulation of *Ubx* in the NB7-3 lineage. To test this hypothesis, I examined the NB7-3 lineage in *hb* null mutants and found that it did not show premature upregulation of *Ubx* (Fig. 3-16A,B). These results should be taken with caution, since the GW and EW1 neurons require *hb* for proper differentiation and, in its absence, undergo apoptosis by stage 15, hindering the analysis of *Ubx* expression after this stage.

Interestingly, *hb* overexpression using the *en*-Gal4 driver could suppress *Ubx* expression in the NB7-3 lineage of all segments (Fig. 3-16C,D). However, *hb* overexpression also keeps the NB in a so-called “young” state, meaning that the NB cannot make the transition to the next step in the specification cascade (Isshiki et al., 2001; Novotny et al., 2002). It therefore repeatedly generates ganglion mother cells of the GMCa identity, which in turn produce multiple EW1 and GW progeny (Fig. 3-16D). Some, but not all, of this progeny expressed differentiation markers such as Zfh1 (presumably GWs) and some of the progeny also showed Caspase-3 activation, but it was not possible to evaluate the numbers and compare them to wt values, since I could not unambiguously identify the differentiated GW motoneurons. I could thus not resolve the question of differential *Ubx* regulation in NB7-3 of T2.

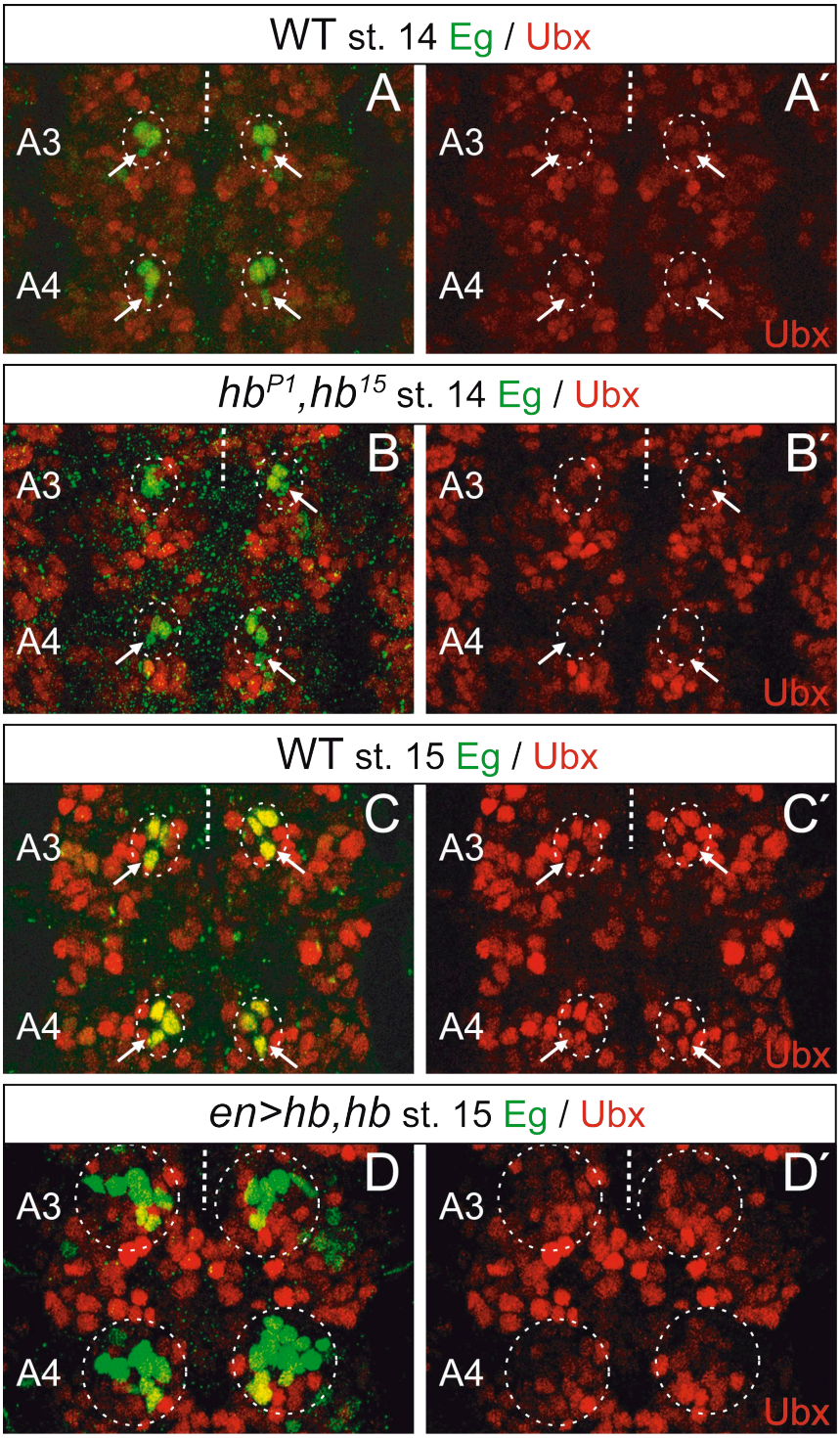


**Fig. 3-16. *hunchback* is not likely to regulate *Ubx* in the NB7-3 lineage.**
A. Co-expression of Eagle (Eg, green) and Ubx (red) in abdominal NB7-3 of a wild type stage 14 embryo. Only a part of the NB7-3 progeny is visible (stippled circles), including GW (arrows). At this stage *Ubx* expression is weak in all cells. A´ shows only the Ubx staining.
B. A stage 14 $hb^{P1},hb^{15}$ mutant embryo. Neither GW (arrows) nor any of the other NB7-3 progeny (stippled circles) show an increase in *Ubx* levels. B´ shows only the Ubx staining.
C. At stage 15, abdominal NB7-3 progeny (stippled circles) in the wild type all show strong *Ubx* expression. C´ shows only the Ubx staining.
D. Overexpression of *hb* (*en>hb,hb*) results in an increased number of NB7-3 progeny (stippled circles) at stage 15. These cells clearly show lower *Ubx* expression levels than in the wild type. D´ shows only the Ubx staining.
Stippled lines mark the midline, anterior is up in all images.

## 3.6. *Ubx* is necessary and sufficient to induce apoptosis in the GW and MNa motoneurons

To test whether *Ubx* is required for apoptosis of these cells, I analyzed their fate in *Ubx* null mutants. In the ventral nerve cord of $Ubx^1$ homozygous embryos, both motoneurons were rescued in 100% of cases (Figs. 3-17C and 3-19C; see also Tables 3-4 and 3-5), indicating that *Ubx* is required for apoptosis of the GW motoneuron in segments T3 to A7, and of MNa in segment T3. To answer the question whether *Ubx* is also sufficient to induce apoptosis of these cells, I used the *en*-Gal4 and *poxN*-Gal4,UAS-*GFP* lines to drive *Ubx* expression in the NB7-3 and NB2-4t lineages, respectively, in all segments in the CNS. The *poxN*-Gal4,UAS-*GFP* flies also express *GFP* in NB2-4, which allowed easier identification of the motoneurons. In segments T3 to A7 of *en>Ubx* embryos, the GW motoneuron showed Caspase-3 activation already at stage 15 (Fig. 3-17D). At late stage 16, it was removed from the CNS in 100% of analyzed abdominal hs (n=68), and in 90% of all analyzed T3 hs (n=10, see Table 3-4). Moreover, it also died in 80% of analyzed T1 and T2 hs (n=20) (Fig. 3-17D), suggesting that *Ubx* is sufficient to induce apoptosis in this cell. The earlier time point of apoptosis in *en>Ubx* embryos was most likely due to the fact that Ubx protein levels were high in NB7-3 from the point of NB delamination on. At late stage 16, I also observed occasional Caspase activation in an EW interneuron upon ectopic *Ubx* expression (Fig. 3-17E), however such cases were rather rare. *Ubx*-induced apoptosis appeared cell-specific, as I found no general increase in cell death in the posterior segmental stripe of these embryos, where the *en*-Gal4 driver is active (Fig. 3-18).

| Segment | Percentage of apoptotic GWs | | |
|---|---|---|---|
| | **WT** | ***Ubx*$^1$** | ***en>Ubx*** |
| T1-T2 | 0 % (n=19) | 0 % (n=28) | 80 % (n=20) |
| T3 | 55.6 % (n=27) | 0 % (n=14) | 90 % (n=10) |
| A1-A7 | 81.2% (n=69) | 0 % (n=98) | 100 % (n=68) |

Table 3-4. Frequency of observed GW motoneuron apoptosis in thoracic and abdominal segments of wild type, *Ubx* loss of function ($Ubx^1$) and *Ubx* gain of function (*en>Ubx*) embryos at late stage 16. n indicates the number of hemisegments analyzed.

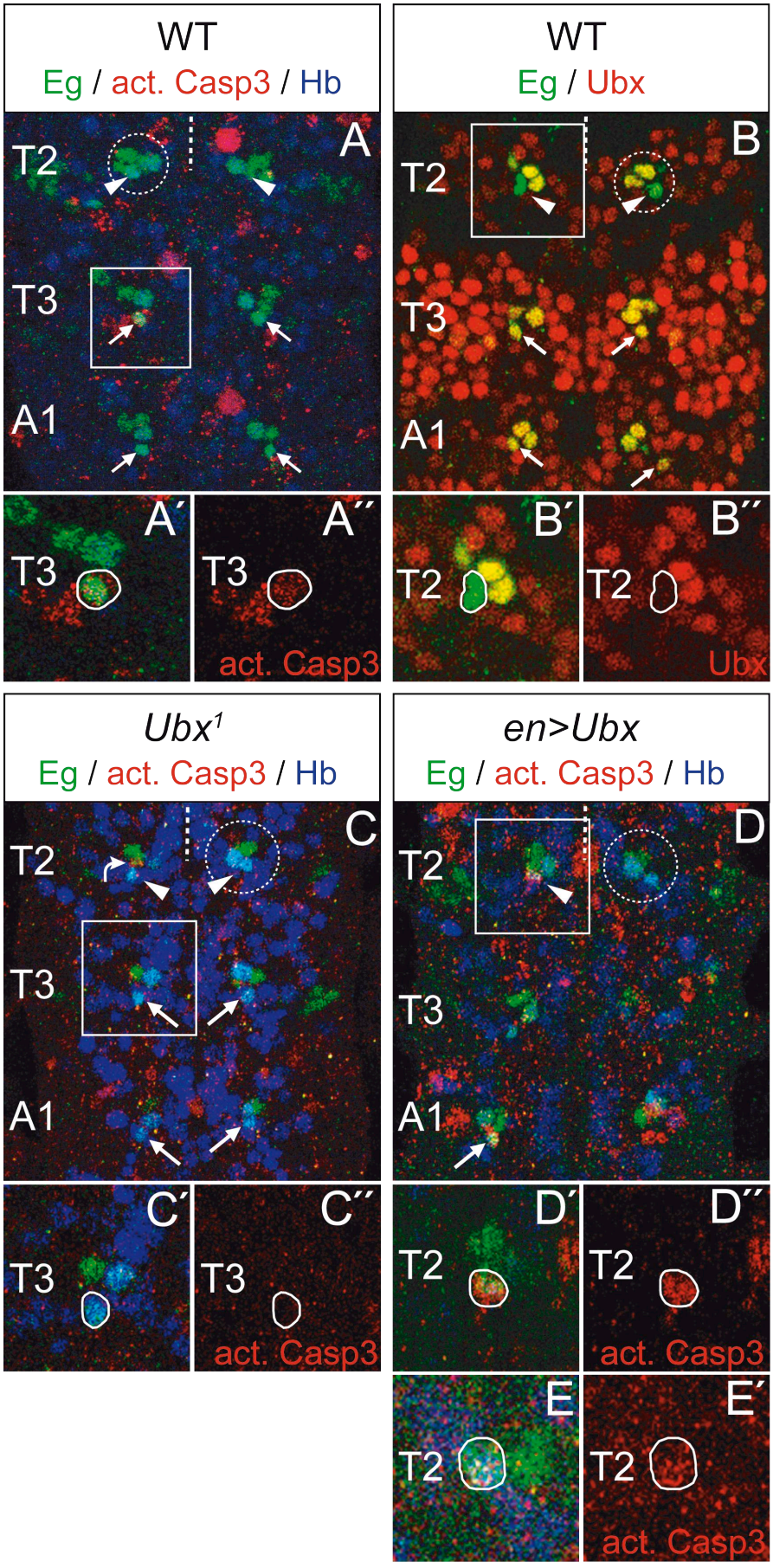
WT
Eg / act. Casp3 / Hb
A
T2
T3
A1
A′
T3
A″
T3
act. Casp3
WT
Eg / Ubx
B
T2
T3
A1
B′
T2
B″
T2
Ubx
Ubx1
Eg / act. Casp3 / Hb
C
T2
T3
A1
C′
T3
C″
T3
act. Casp3
en>Ubx
Eg / act. Casp3 / Hb
D
T2
T3
A1
D′
T2
D″
T2
act. Casp3
E
T2
E′
T2
act. Casp3

**Fig. 3-17.**

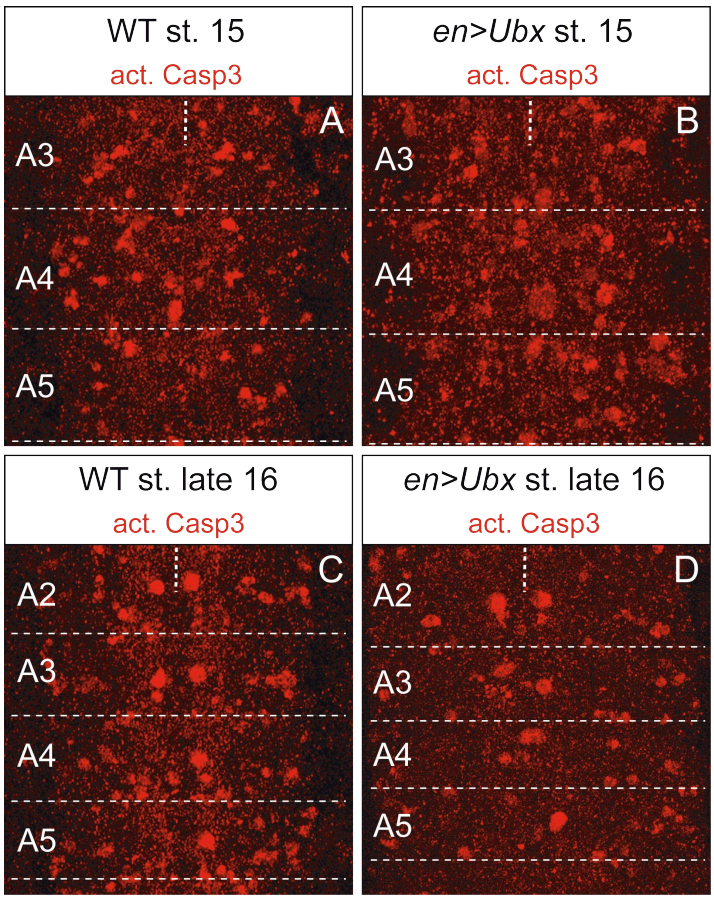


**Fig. 3-18. *Ubx* overexpression does not induce massive cell death in the CNS.**
A. A stage 15 wild type embryo stained for activated Caspase 3 (red).
B. Activated Caspase 3 staining in a stage 15 *en>Ubx* embryo. The amount of stained cells does not differ from that in the wild type.
C. A late stage 16 wild type embryo stained for activated Caspase 3.
D. Activated Caspase 3 staining in a late stage 16 *en>Ubx* embryo. The pattern of activated Caspase 3-positive cells is not changed compared to the wild type.
Each image shows a maximum projection of staining throughout the CNS. Stippled lines mark the midline, anterior is up in all images.

**Fig. 3-17. *Ubx* is necessary and sufficient for apoptosis of the GW motoneuron.**
A. NB7-3 (stippled circle) in a late stage 16 wild type embryo is visualized with anti-Eagle (Eg) staining (green). GW motoneurons in T3 and A1 (arrows) and in T2 (arrowheads) also show Hunchback (Hb) staining (blue). In T3, one GW motoneuron is also positive for activated Caspase 3 (act. Casp3, red), indicating it is undergoing apoptosis. A´ shows a magnified single scan of the T3 NB7-3 lineage boxed in A. The apoptotic GW is outlined. A´´ shows only the activated Caspase 3 staining.
B. Co-expression of Eg (green) and Ubx (red) in NB7-3 (stippled circle) of a late stage 16 wild type embryo. In T2 GW (arrowheads) does not express *Ubx*, whereas the interneurons show high *Ubx* levels. In T3 and A1 all progeny cells, including GW (arrows) show strong *Ubx* expression. B´ shows a magnified single scan of the T2 NB7-3 lineage boxed in B. GW is outlined. B´´ shows only the Ubx staining.
C. Co-expression of Eg (green), Hb (blue) and activated Caspase 3 (act. Casp3, red) in NB7-3 (stippled circle) of a late stage 16 $Ubx^{1}$ mutant embryo. In T2, one cell shows Caspase 3 activation (curved arrow). This is not GW (arrowheads), but rather the presumable EW2sib since it is not Hb-positive. GW in T3 and A1 (arrows) does not show Caspase 3 activation and appears large and intact. C´ shows a magnified single scan of the T3 NB7-3 lineage boxed in C. GW is outlined. C´´ shows only the activated Caspase 3 staining.
D. Co-expression of Eg (green), Hb (blue) and activated Caspase 3 (act. Casp3, red) in NB7-3 (stippled circle) of a stage 15 *en>Ubx* embryo. GW shows Caspase 3 activation in T2 (arrowhead), and in A1 (arrow). D´ shows a magnified single scan of the T2 NB7-3 lineage boxed in D. GW is outlined. D´´ shows only the activated Caspase 3 staining.
E. A magnified single scan of a T2 NB7-3 lineage in a late stage 16 *en>Ubx* embryo, stained for anti-Eg (green), anti-Hb (blue) and anti-activated Caspase 3 (red). The EW1 interneuron (outlined), identified by Hb staining and position, is also positive for activated Caspase 3. E´ shows only the activated Caspase 3 staining.
Stippled lines mark the midline, anterior is up in all images.

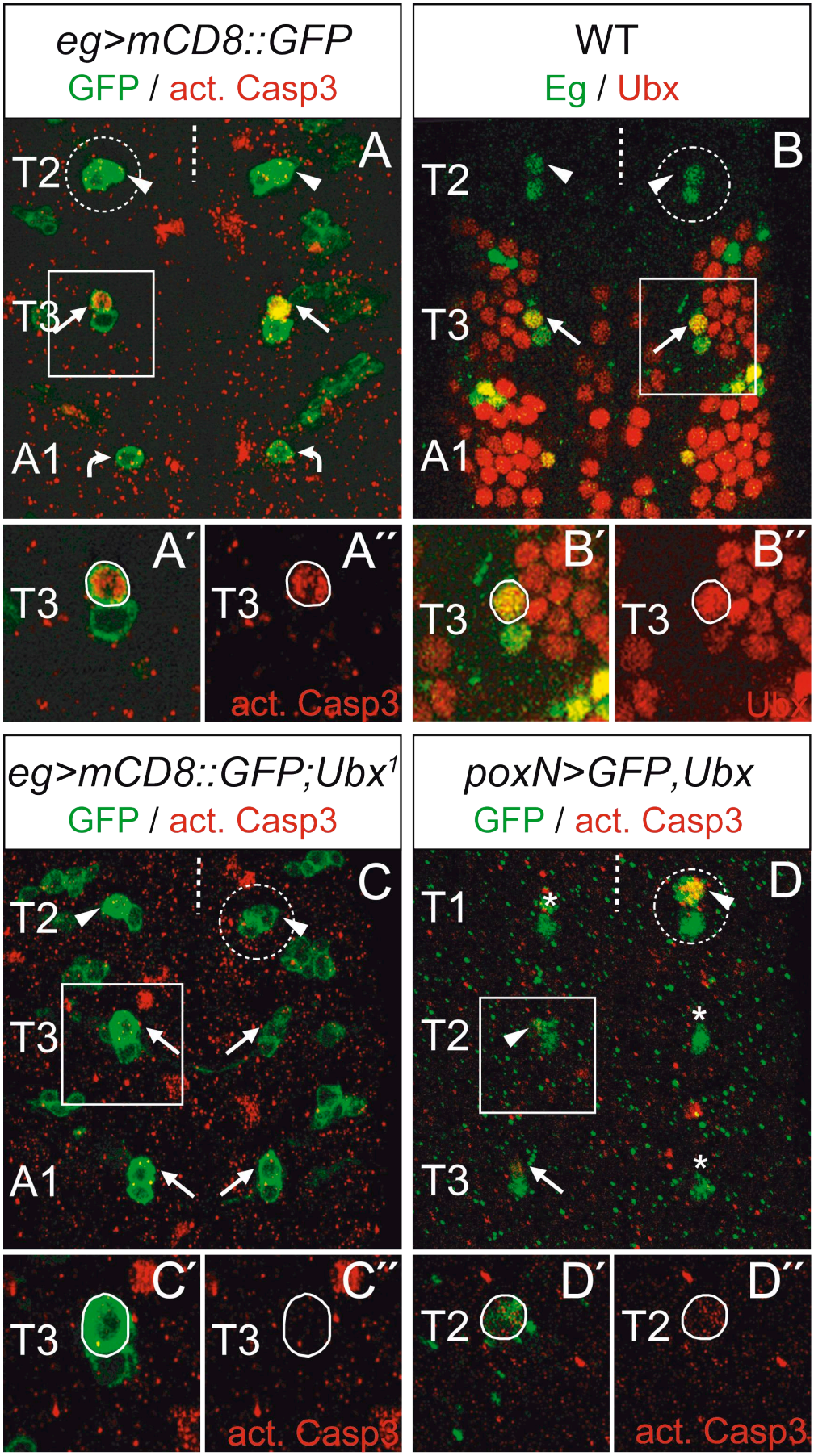
eg>mCD8::GFP
GFP / act. Casp3
WT
Eg / Ubx
A
B
T2
T3
A1
A´
A´´
B´
B´´
act. Casp3
Ubx
eg>mCD8::GFP;Ubx1
GFP / act. Casp3
poxN>GFP,Ubx
GFP / act. Casp3
C
D
T1
C´
C´´
D´
D´´

**Fig. 3-19.**

In *poxN>Ubx* embryos MNa underwent apoptosis in 75% of analyzed T3 hs (n=16), which was a slight increase compared to wt. In addition, segments T1 and T2 exhibited apoptotic MNas in 68.8% of cases (n=32) (Fig. 3-19D and Table 3-5). I conclude that *Ubx* is necessary and sufficient to induce apoptosis of the GW and the anterior NB2-4t motoneuron.

| Segment | Percentage of apoptotic MNas | | |
|---|---|---|---|
| | WT | *eg>UAS-mCD8::GFP;Ubx$^{1}$* | *poxN>GFP,Ubx* |
| T1-T2 | 0 % (n=29) | 0 % (n=20) | 68.8 % (n=32) |
| T3 | 64.7 % (n=17) | 0 % (n=11) | 75 % (n=16) |
| A1-A7 | 0 % (n=70) | 0 % (n=12, A1 only) | ND |

Table 3-5. Frequency of observed NB2-4t anterior motoneuron apoptosis in thoracic and abdominal segments of wild type (WT), *Ubx* loss of function (*eg>UAS-mCD8::GFP;Ubx$^{1}$*) and *Ubx* gain of function (*poxN>GFP,Ubx*) embryos at late stage 16. In *eg>UAS-mCD8::GFP;Ubx$^{1}$* embryos, only A1 was evaluated as this segment showed a transformation of the NB2-4a lineage into a NB2-4t lineage. n indicates the number of hemisegments analyzed. ND – no data.

**Fig. 3-19. *Ubx* is necessary and sufficient for apoptosis of the anterior NB2-4t motoneuron.**
A. NB2-4 motoneurons (stippled circle) in a late stage 16 *eg>mCD8::GFP* embryo are visualized with anti-GFP staining (green). MNa motoneurons in T3 (arrows) are positive for activated Caspase 3 (act. Casp3, red), indicating they are undergoing apoptosis. Their counterparts in T2 (arrowheads) survive. In A1, only the anterior motoneuron is visible in this position (curved arrows). A´ shows a magnified single scan of the T3 NB2-4t MNs boxed in A. The apoptotic MNa is outlined. A´´ shows only the activated Caspase 3 staining.
B. Co-expression of Eagle (Eg, green) and Ubx (red) in NB2-4 motoneurons (stippled circle) of a late stage 16 wild type embryo. In T2 neither MNa (arrowheads) nor MNp express *Ubx*. In T3, MNa (arrows) shows strong and MNp weak *Ubx* expression. In A1 only MNa is visible and expresses *Ubx* at high levels. B´ shows a magnified single scan of the T3 NB2-4t lineage boxed in B. MNa is outlined. B´´ shows only the Ubx staining.
C. Co-expression of GFP (green) and activated Caspase 3 (act. Casp3, red) in NB2-4 motoneurons (stippled circle) of a late stage 16 *eg>mCD8::GFP;Ubx$^{1}$* mutant embryo. In T2, MNa (arrowheads) and MNp are not changed. MNa in T3 and A1 (arrows) does not show Caspase 3 activation and appears intact. Both MNa and MNp are visible in the same section in A1, suggesting a transformation of the A1 NB2-4 lineage into a T3 one. C´ shows a magnified single scan of the T3 NB2-4 lineage boxed in C. MNa is outlined. C´´ shows only the activated Caspase 3 staining.
D. Co-expression of GFP (green) and activated Caspase 3 (act. Casp3, red) in NB2-4t motoneurons (stippled circle) of a late stage 16 *poxN>GFP,Ubx* embryo. MNa shows Caspase 3 activation in T1 and T2 (arrowheads), as well as in T3 (arrow). Asterisks indicate positions where the MNa motoneurons have lost *GFP* expression due to apoptosis. D´ shows a magnified single scan of the T2 NB2-4t lineage boxed in D. MNa is outlined. D´´ shows only the activated Caspase 3 staining.
Stippled lines mark the midline, anterior is up in all images.

### 3.6.1. Exploring the cell context-specific effect of *Ubx*

*Ubx* seemed to have a very specific effect on cells of NB7-3 in both wt and overexpression situations: while the GW motoneuron underwent apoptosis, the EW interneurons did not although they express *Ubx* at equally high levels. This implies that the apoptosis-inducing function of *Ubx* depends on cellular context. In order to gain more insight into the differences between GW and EWs, I tested the known cofactors of homeotic genes, *homothorax* (*hth*) (Pai et al., 1998; Rieckhof et al., 1997) and *extradenticle* (*exd*) (Peifer and Wieschaus, 1990; Rauskolb et al., 1993), which are required for some functions of *Ubx* and/or *Antp*. At late stage 16, *hth* is expressed in most NB7-3 cells in T1 and T2, although the expression levels in the EWs are weak (Fig. 3-20A). In T3 and A1 only some NB7-3 cells exhibit low Hth levels, and in A2-A7 NB7-3 cells are not immunopositive for Hth. Apoptosis of GW motoneurons in the abdominal segments was slightly reduced in $hth^{P2}$ mutants (61.8%, n=68) (Table 3-6), although I was not able to detect *hth* expression in NB7-3 posterior to A1. In T3 of $hth^{P2}$ mutants I found a slight increase in GW apoptosis (66.7%, n=12) as compared to wild type. Interestingly, 1 out of 24 analyzed T1 and T2 hemisegments (4.2%) showed an apoptotic GW. These results indicate a possible role for *hth* either in GW survival, or in correct specification of the early 7-3 neuroblast, in the thoracic segments. Exd protein is present at low levels in some NB7-3 cells in T1 to T3, and abdominal NB7-3 shows no *exd* expression (Fig. 3-20B). $exd^{B108}$ mutants showed an increase in GW apoptosis in T3 (90%, n=10), and no change in the abdomen (87.9%, n=66) (Table 3-6). T1 and T2 were not affected. These results are somewhat inconclusive, as *hth* seems to support activation of GW apoptosis in the abdomen despite of an apparent lack of expression, but it appears to play the opposite role in the thorax. *exd* does not seem to play a role in the abdomen, but may be required for proper timing of apoptosis in T3.

| Segment | Percentage of apoptotic GWs | | |
|---|---|---|---|
| | WT | $hth^{P2}$ | $exd^{B108}$ |
| T1-T2 | 0 % (n=19) | 4.2 % (n=24) | 0 % (n=20) |
| T3 | 55.6 % (n=27) | 66.7 % (n=12) | 90 % (n=10) |
| A1-A7 | 81.2% (n=69) | 61.8 % (n=68) | 87.9 % (n=66) |

Table 3-6. Frequency of observed GW motoneuron apoptosis in thoracic and abdominal segments of wild type (WT), and *hth* ($hth^{P2}$) and *exd* ($exd^{B108}$) loss of function mutant embryos at late stage 16. n indicates the number of hemisegments analyzed.

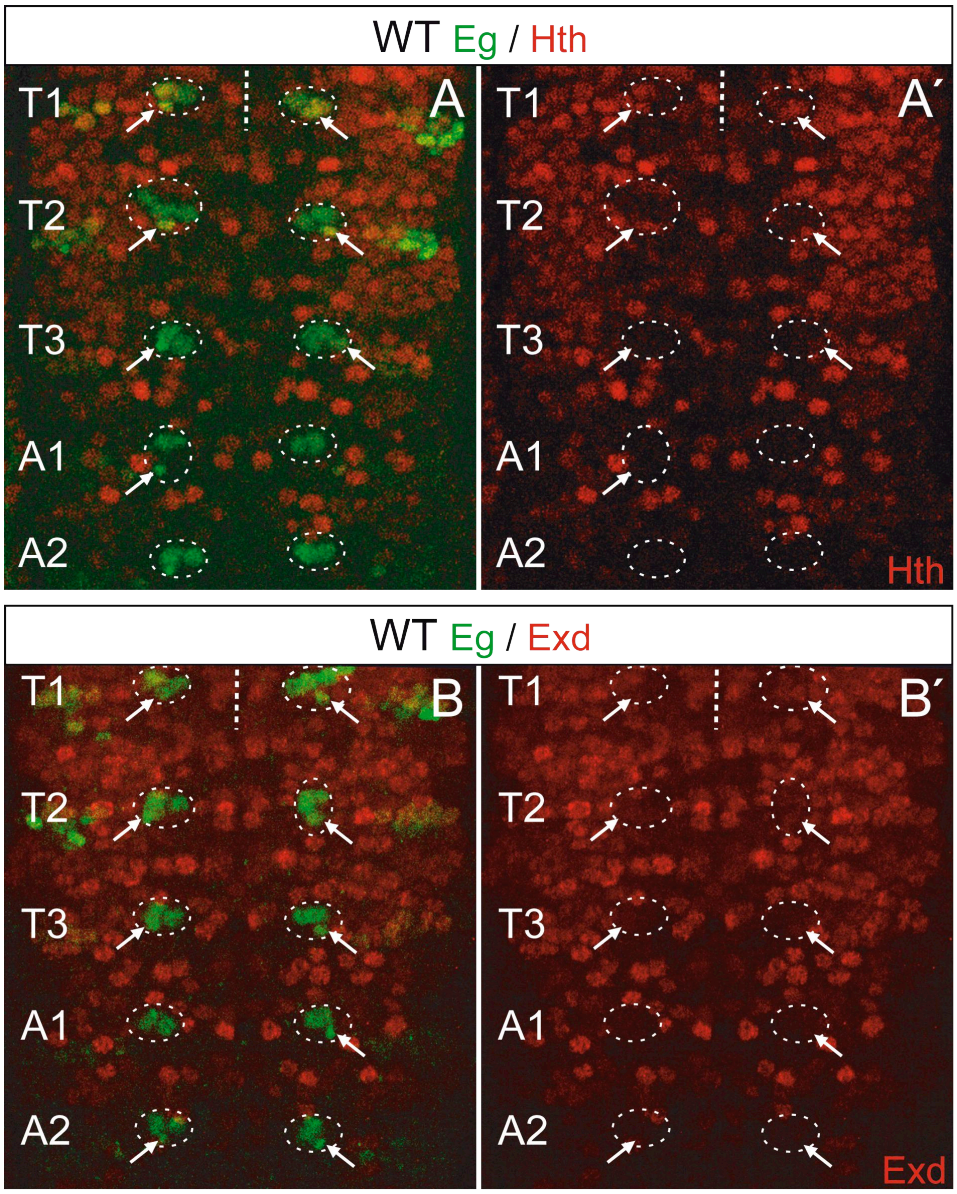


**Fig. 3-20. Expression of Homothorax and Extradenticle in the NB7-3 lineage.**
A. Co-expression of Eagle (Eg, green) and Homothorax (Hth, red) in a late stage 16 wild type embryo. NB7-3 progeny is shown (stippled circle), including GW (arrows). In T1 and T2, *hth* expression is weak in the interneurons and moderate in GW (arrows). In T3, A1 and A2 some NB7-3 cells may exhibit low Hth levels, but most show no *hth* expression. A´ shows only the Hth staining.
B. Co-expression of Eagle (Eg, green) and Extradenticle (Exd, red) in a late stage 16 wild type embryo. NB7-3 progeny is shown (stippled circle), including GW (arrows). Exd protein is expressed at low levels in some NB7-3 cells in T1 to T3. A1 and A2 show no *exd* expression in NB7-3 progeny. B´ shows only the Exd staining.
Stippled lines mark the midline, anterior is up in all images.

I then examined the NB7-3 expression of another *Hox* gene, *abdominal-A* (*abdA*) (Tiong et al., 1985; Whittle et al., 1986). In the ventral nerve cord, *abdA* is expressed in a broad domain extending from the posterior half of segment A1 to the posterior half of segment A7 (Hirth et al., 1998; Karch et al., 1990). In NB7-3, at

late stage 16 it is weakly expressed only in the EWs from A1 to A7, but not in GW (Fig. 3-21), which may suggest a possible role for *abdA* in survival of the abdominal EWs. To test this possibility, I examined the NB7-3 lineage in *abdA* mutants, and found an effect on EW survival (Table 3-7). In the wt I observed Caspase 3 activation excusively in EW3 of segment A7 (20% of analyzed A7 hs). In *abdA* mutants, segments A1 to A6 showed one apoptotic EW interneuron in 3.4% of analyzed hs. In A7 EW3 apoptosis increased to 80%, which would suggest either *abdA* involvement in the maintenance of EW3 in A7 until the end of embryonic development, or a transformation into a more anterior segment. *abdA* overexpression under control of the *en*-Gal4 driver results in 26.8% of hemisegments showing apoptotic EWs in A1 to A6 (Table 3-7), and 69.2% in A7. Thus, segments A1 to A6 show an increase of apoptosis compared to the *abdA* loss of function mutant, whereas a slight decrease is observed in A7. However, the percentages for *en>abdA* embryos shown in Table 3-7 include hemisegments showing one, two or all three EWs dying in all abdominal segments (A1 to A7). If one takes individual EWs into account, 13.9 % of the interneurons show Caspase 3 activation (n=252) when overexpressing *abdA*. This may be a consequence of wrong specification of these cells, since they show only weak *abdA* expression in wt embryos (Fig. 3-21).

Apoptosis of abdominal GWs increased somewhat, from 81.2% in wt to 98.6% in *abdA* mutants. In addition, GW apoptosis in T3 increased to 100% (Table 3-7), although, according to all known reports, *abdA* is not expressed in this segment at any time in development. Overexpression of *abdA* using the *en*-Gal4 driver resulted in a reduction in GW apoptosis: 50% in $abdA^{MX1}$ (n=84) compared to 81.2% in wt (n=69).

Thus, *abdA* may be required to allow EW3 survival in segment A7 until late stages, but generally increasing the amount of *abdA* in the interneurons rather induces than hinders apoptosis. Interestingly, I found the opposite effect on GW motoneuron apoptosis, where *abdA* removal increases, and overexpression reduces it.

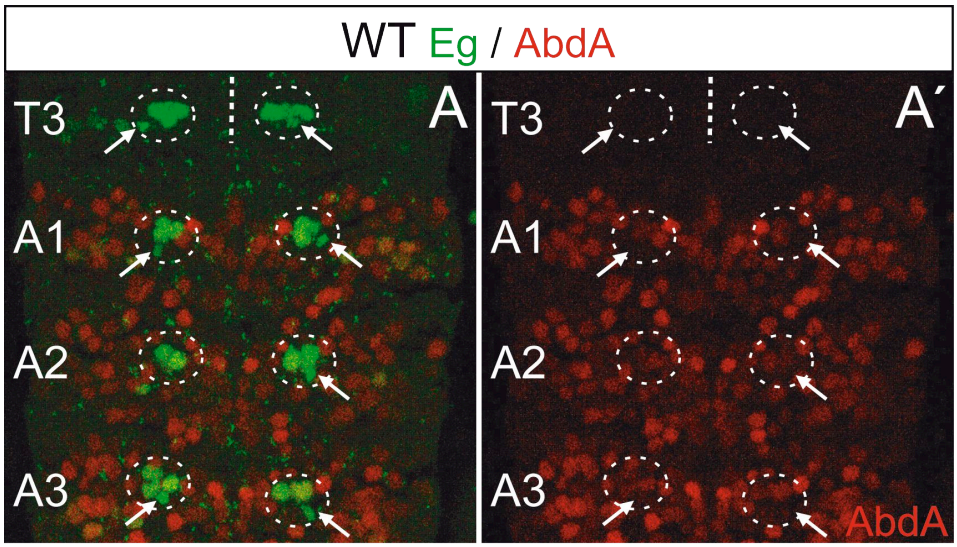


**Fig. 3-21. Abdominal-A expression in the NB7-3 lineage.**
A. Co-expression of Eagle (Eg, green) and Abdominal-A (AbdA, red) in a late stage 16 wild type embryo. NB7-3 progeny is shown (stippled circle), including GW (arrows). T3 NB7-3 cells show no *abdA* expression. In A1 to A3 only the interneurons express *abdA* weakly, whereas GWs show no expression. A´ shows only the AbdA staining.
Stippled lines mark the midline, anterior is up in all images.

| Segment | Neuron | Percenatge of apoptotic GWs | | |
|---|---|---|---|---|
| | | WT | *abdA*$^{MX1}$ | *en>abdA* |
| T1-T2 | GW | 0 % (n=19) | 0 % (n=15) | 0 % (n=26) |
| | EW | 0 % (n=19) | 0 % (n=15) | 23.1% (n=26) |
| T3 | GW | 55.6 % (n=27) | 100 % (n=10) | 25 % (n=12) |
| | EW | 0 % (n=27) | 0 % (n=10) | 33.3 % (n=12) |
| A1-A6 | GW | 79.7% (n=59) | 98.3 % (n=59) | 53.5 % (n=71) |
| | EW | 0% (n=59) | 3.4 % (n=59) | 26.8% (n=71) |
| A7 | GW | 90% (n=10) | 100% (n=10) | 30.8% (n=13) |
| | EW | 20 % (n=10) | 80% (n=10) | 69.2% (n=13) |

Table 3-7. Percentage of hemisegments showing GW motoneuron and EW interneuron apoptosis in the thorax and abdomen of wild type (WT), *abdA* loss of function (*abdA*$^{MX1}$) and *abdA* gain of function (*en>abdA*) embryos at late stage 16. n indicates the number of hemisegments analyzed.

I also examined mutants of other factors that are differentially expressed in the GW and EW neurons. One of these is the cytosolic signalling protein Numb, which is involved in specifying differential daughter cell fates through inhibition of the Notch signalling pathway (Spana and Doe, 1996; Uemura et al., 1989). During the NB7-3 GMCa division, Numb appears to be distributed asymmetrically into the EW1 daughter cell, and is not present in its sibling, GW (Karcavich and Doe,

2005). Accordingly, *numb* mutants show, albeit only partial, transformations of EW1 into GW fate, as judged by *zfh1* expression. EW2 and EW3 are also transformed into their respective siblings and hence undergo apoptosis right after birth, suggesting asymmetric distribution of Numb also in GMCb and GMCc (Karcavich and Doe, 2005; Lundell et al., 2003). Based on these findings it is conceivable that *numb* allows survival of the EWs despite high *Ubx* expression levels. This hypothesis cannot be tested for EW2 and EW3, since these cells anyway take on the apoptotic fate of their siblings in *numb* mutants, and this is not dependent on *Ubx*. One would therefore have to be able to knock out *numb* at a later developmental stage to test if it can suppress *Ubx*-induced apoptosis in these neurons. However, since GW normally undergoes apoptosis at a late developmental stage, and in the *numb* mutant EW1 appears transformed into GW, one would expect that, in the *numb* mutant, EW1 would also die at late stage 16. Contrary to this expectation, Lundell and colleagues have observed the dSert-positive EW1 interneuron in the ventral nerve cord of fully developed *numb* mutant embryos (Lundell et al., 2003). In agreement with this data, I did not observe Caspase-3 activation in EW1 of *numb* mutant embryos (n=80 hs), which indicates that *numb* is not the factor that allows EW survival in the presence of *Ubx*.

The last factor known to be expressed only in GW and not in the EWs, is the transcription factor *zfh1* (Isshiki et al., 2001; Novotny et al., 2002). *zfh1* mutants show GW apoptosis in 57.9% of T3 hs (n=9), indicating no change compared to wild type. In abdominal segments 61.8% of hemisegments show apoptotic GWs (n=68), which is lower than in the wild type. Thus, the question of how *Ubx* induces apoptosis in one neuron and not in its siblings still remains unanswered.

## 3.7. Initiation of apoptosis is a late function of *Ubx*

As both *en*-Gal4 and *poxN*-Gal4 drive *Ubx* expression from early stages of CNS development through to the end of embryogenesis, there are two ways to explain the results of the overexpression experiments. First, *Ubx* may be required only in the early neuroblast to specify its segmental identity and developmental program. Apoptotic fate of the progeny would then be specified already in the neuroblast, either intrinsically or as a response to an extrinsic apoptotic signal, and

would not require *Ubx* at a later point in development. In a second scenario, *Ubx* would be required specifically at a later developmental stage to induce the apoptotic program. In favor of the second hypothesis is the strong upregulation of *Ubx* at developmental stage 15 in both motoneurons, a few hours before detectable activation of Caspase-3. To test which of the above possibilities is true, *Ubx* was expressed under control of a heat-shock promoter. I reasoned that, since the early NB7-3 and NB2-4t neuroblasts and the GW and NB2-4t motoneurons show no *Ubx* expression in wild type T1 and T2, providing *Ubx* in these cells at relevant developmental time points should clarify whether it is required early (at the time of neuroblast determination) or late (in the differentiated neurons) to induce apoptosis. The heat-shock (HS) was given at two different timepoints in separate experiments: at 3.5 hrs after egg laying (AEL) (prior to NB7-3 delamination), and at 12 hrs AEL (when *Ubx* is normally upregulated in T3 to A7).

In the first experiment, following an early HS, in segments T1 and T2 *Ubx* is present at the time of neuroblast formation, but is degraded by the time of apoptosis initiation. This early *Ubx* expression in T1 and T2 may transform the NB7-3 lineage into a T3 identity, since the NB7-3 clusters in T1 and T2 in 96.3% of hs (n=27) contained only 4 cells instead of 5. In the wt I observed 4 cells in 80.6% of hs (n=36). In addition, a transformation of the thoracic NB6-4 lineage (contains neurons and glia) into an abdominal one (only glia) was observed, which indicates that ectopic *Ubx* expression can transform the tagma-specific identity of the neuroblasts. However, I observed no apoptotic GW motoneurons in T1 and T2 (n=27) following an early HS, which suggests that early *Ubx* expression is not sufficient to result in GW apoptosis (Fig. 3-22A, Table 3-8). This conclusion was supported by the fact that the percentage of apoptotic GW motoneurons in the abdomen of these embryos (82.4%, n=85) did not differ from that of wt ones (81.2%, n=69) (Table 3-8). In T3 however, I found an increase in apoptotic GW motoneurons (100%, n=12) as compared to the wt (55.6%, n=27) (Table 3-8), indicating that in this segment, *Ubx* may be required both early to specify apoptosis-susceptible progeny fate, and late to initiate apoptosis itself.

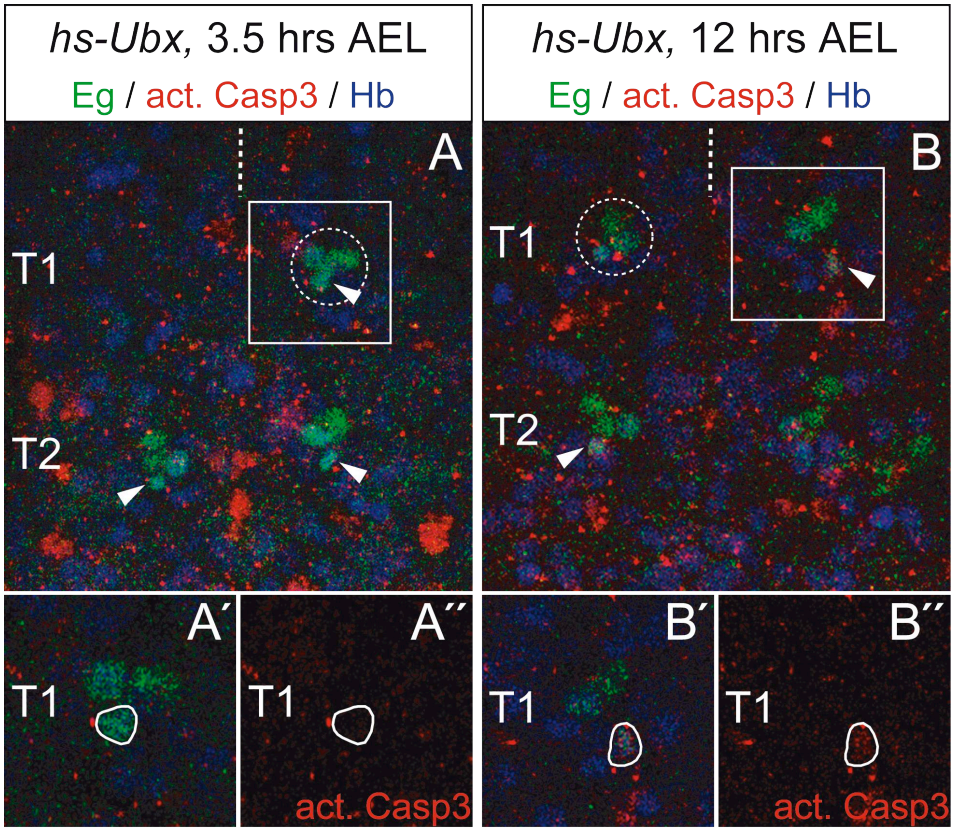


**Fig. 3-22. *Ubx* is required late in development to activate apoptosis.**
A. A late stage 16 *hs-Ubx* embryo following a heat shock early in development. Co-staining against Eagle (Eg, green), Hunchback (Hb, blue) and activated Caspase 3 (act. Casp3, red) in progeny of NB7-3 (stippled circle) is shown, including the GW motoneuron (arrowheads). No Caspase 3 activation can be seen in GWs of T1 or T2. A´ shows a magnified single scan of the T1 NB7-3 lineage boxed in A. GW is outlined. A´´ shows only the activated Caspase 3 staining.
B. A late stage 16 *hs-Ubx* embryo following a heat shock late in development. The progeny of NB7-3 (stippled circle) are shown, including the GW motoneuron (arrowheads). GWs positive for activated Caspase 3 can be seen in T1 and T2 (arrowheads). B´ shows a magnified single scan of the T1 NB7-3 lineage boxed in B. GW is outlined. B´´ shows only the activated Caspase 3 staining.
Stippled lines mark the midline, anterior is up in all images.

| Segment | Percentage of apoptotic GWs | | |
|---|---|---|---|
| | WT | *hs-Ubx* (3.5 hrs AEL) | *hs-Ubx* (12 hrs AEL) |
| T1-T2 | 0 % (n=19) | 0 % (n=27) | 21.9 % (n=64) |
| T3 | 55.6 % (n=27) | 100 % (n=12) | 90.6 % (n=32) |
| A1-A7 | 81.2% (n=69) | 82.4 % (n=85) | 98.8 % (n=84) |

Table 3-8. Frequency of observed GW motoneuron apoptosis in thoracic and abdominal segments of wild type (WT) and *hs-Ubx* embryos at late stage 16. The heat shock was administered at the indicated developmental time points. n indicates the number of hemisegments analyzed.

In the second experiment, all NB7-3 progeny cells were born and had begun to differentiate by the time the HS was administered (12 hrs AEL). Following such a treatment, I found apoptotic GW motoneurons in T1 and T2 in 21.9% of analyzed hs (n=64, Fig. 3-22B). Moreover, GW apoptosis was increased in T3 and in the abdominal segments (Table 3-8). These results lead to the conclusion that *Ubx* is required in the GW motoneuron at a late developmental stage to activate programmed cell death.

I could not analyze NB2-4t in these experiments, since expression of the marker protein Eg was not strong enough to reliably evaluate the data. However, I suggest it to be required late in this lineage as well, since *Ubx* is not expressed in the early NB2-4t neuroblast in T3 and thus probably does not participate in providing this neuroblast with its segment-specific identity. Moreover, constant ectopic *Ubx* expression using the *poxN*-Gal4 driver could not transform the thoracic NB2-4 into the abdominal lineage, but it could induce apoptosis of MNa in all thoracic segments (Fig. 3-18D), which further supports the notion that activation of apoptosis is a late function of the *Ubx* gene.

## 3.8. *Antp* is necessary and sufficient for survival of the GW motoneuron

To further explore the differences between GW motoneurons in different segments, I analyzed the expression of the more anteriorly expressed *Hox* genes, *Sex combs reduced* (*Scr*) (Kuroiwa et al., 1985) and *Antennapedia* (*Antp*) (Postlethwait and Schneiderman, 1969), in the NB7-3 lineage. *Scr* is expressed in the posterior half of the maxillary, and the anterior half of the labial segment (Carroll et al., 1988; Hirth et al., 1998; LeMotte et al., 1989; Mahaffey and Kaufman, 1987). Consequently, only the NB7-3 cells of the maxillary segment show *Scr* expression (Fig. 3-23), whereas the thoracic and abdominal ones do not, leading to the conclusion that *Scr* is not involved in the fate of NB7-3 progeny in these segments.

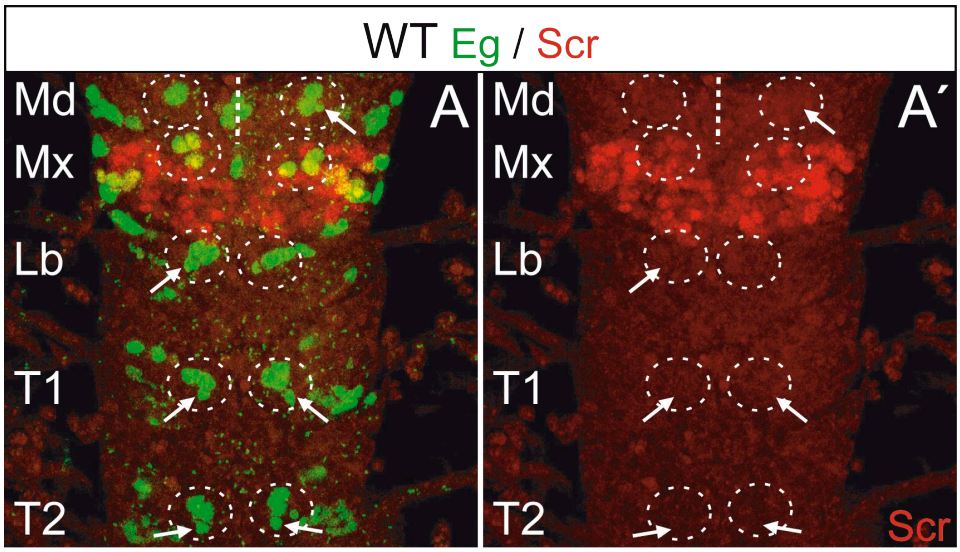


**Fig. 3-23. Sex combs reduced expression in the NB7-3 lineage.**
A. Co-expression of Eagle (Eg, green) and Sex combs reduced (Scr, red) in a late stage 16 wild type embryo. NB7-3 progeny is shown (stippled circle), including GW (arrows). *Scr* is expressed only in NB7-3 of the maxillary segment (Mx). A´ shows only the Scr staining. Md, Mx and Lb indicate the mandibular, maxillary and labial segments, respectively.
Stippled lines mark the midline, anterior is up in all images.

*Antp* is expressed in the embryonic CNS from the posterior half of the labial segment through to the anterior half of A8 (Carroll et al., 1986; Hirth et al., 1998), with strongest expression from the posterior half of T1 to the anterior half of T3. At the end of embryogenesis, *Antp* levels were high in all NB7-3 progeny cells in T1 (Fig. 3-24A). In T2 the EWs showed low *Antp* levels, but the GW motoneuron was strongly Antp-positive (Fig. 3-24A). In T3 and the abdomen of late stage 16 embryos NB7-3 progeny cells exhibited variably low *Antp* expression (Figs. 3-24A and summarized in Fig. 3-28). Considering the fact that *Antp* expression was high in surviving GW motoneurons of T1 and T2, and low in ones of T3 to A7 which undergo apoptosis, I wondered whether *Antp* might be required for GW motoneuron survival in T1 and T2. Indeed, in $Antp^{W10}$ mutant embryos, the GW motoneurons underwent cell death in T1 and T2 in 35% of analyzed hs (n=20) (Fig. 3-24B, Table 3-9). Additionally, in T3 the frequency of GW apoptosis increased from 55.6% (n=27) (in WT) to 90% (n=10). In the abdominal segments, the frequency of GW apoptosis was slightly decreased (Table 3-9). Together, these results indicated that *Antp* is necessary for survival of the GW motoneuron in T1 and T2.

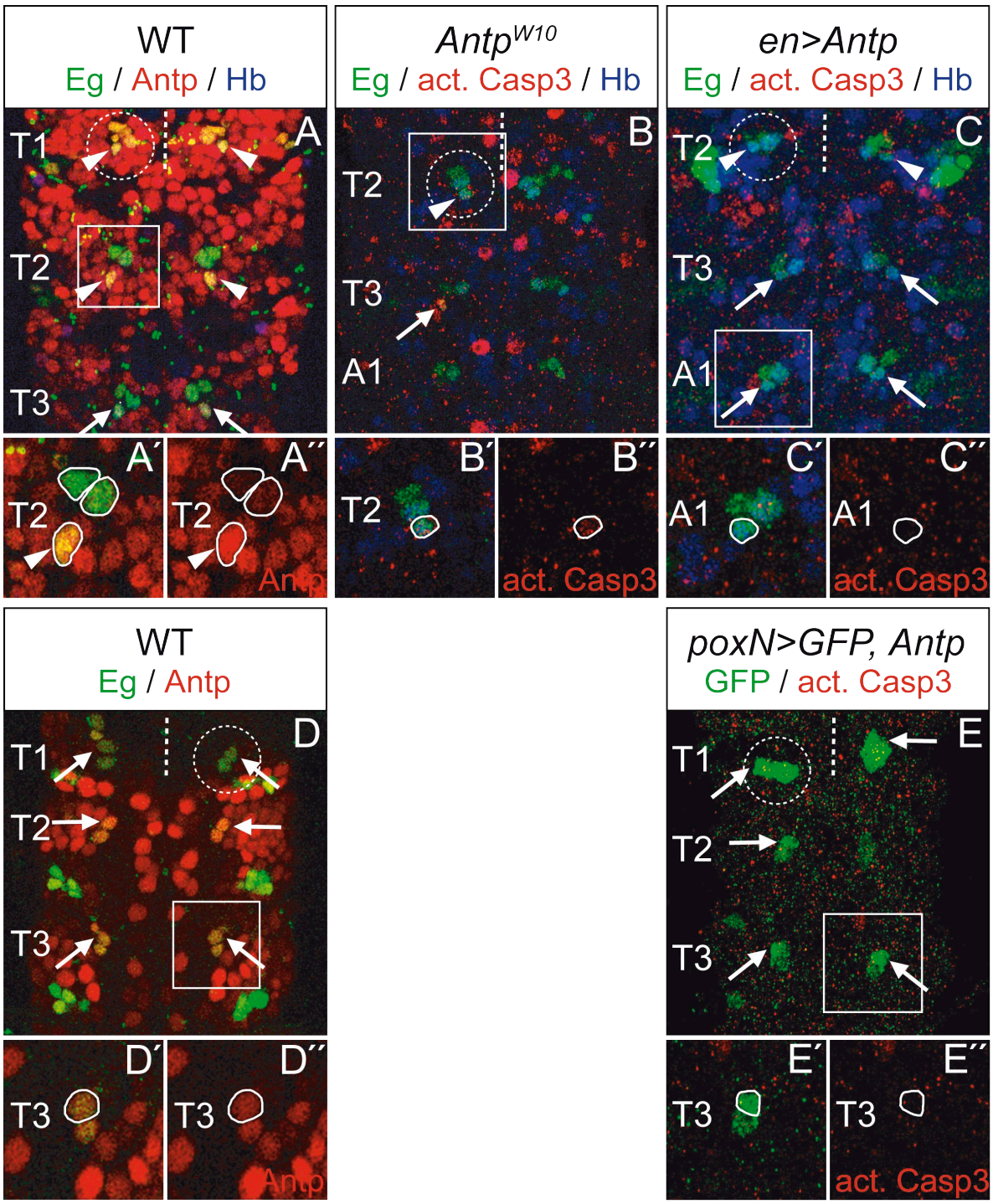
WT
Eg / Antp / Hb
A
T1
T2
T3
A´
A´´
Antp
Antp^W10
Eg / act. Casp3 / Hb
B
T2
T3
A1
B´
B´´
act. Casp3
en>Antp
Eg / act. Casp3 / Hb
C
T2
T3
A1
C´
C´´
act. Casp3
WT
Eg / Antp
D
T1
T2
T3
D´
D´´
Antp
poxN>GFP, Antp
GFP / act. Casp3
E
T1
T2
T3
E´
E´´
act. Casp3

**Fig. 3-24.**

| Segment | Percentage of apoptotic GWs | | |
|---|---|---|---|
| | WT | *Antp*$^{W10}$ | *en>Antp* |
| T1-T2 | 0 % (n=19) | 35 % (n=20) | 0 % (n=28) |
| T3 | 55.6 % (n=27) | 90 % (n=10) | 30.8 % (n=13) |
| A1-A7 | 81.2% (n=69) | 69 % (n=58) | 34.7 % (n=95) |

Table 3-9. Frequency of observed GW motoneuron apoptosis in thoracic and abdominal segments of wild type (WT), *Antp* loss of function (*Antp*$^{W10}$) and *Antp* gain of function (*en>Antp*) embryos at late stage 16. n indicates the number of hemisegments analyzed.

In order to test whether *Antp* could also rescue GW motoneurons from apoptosis, I performed *Antp* overexpression experiments using the *en*-Gal4 driver. In segments T1 and T2 of *en>Antp* embryos, I observed no apoptotic GW motoneurons (Table 3-9). In T3, only 30.8% of hs showed apoptotic GWs (n=13) compared to 55.6% in wt (n=27). In abdominal segments, only 34.7% of GW motoneurons (n=95) were apoptotic, which was significantly fewer than in wildtype (81.2%, n=69) (Fig. 3-24C, Table 3-9). In addition, one interneuron was often missing from the cluster: 7.1% of T1-T2 hs (n=28), 38.5% of T3 (n=13) and 72.8% of A1-A6 hs (n=81) showed only two EWs per hs. Based on the always visible Hb expression in EW1, and on the medial position of the other visible EW, I presume the missing cell to be EW3.

**Fig. 3-24. *Antennapedia* is required for survival of the GW and MNa motoneurons.**
A. Co-expression of Eg (green), Hb (blue) and Antennapedia (Antp, red) in NB7-3 (stippled circle) of a stage 16 wild type embryo. In T1, all NB7-3 progeny, including GW (arrowheads), show strong *Antp* expression. In T2, GW (arrowheads) also shows high and the interneurons low *Antp* levels. The T3 NB7-3 interneurons do not express *Antp*, whereas GW (arrows) does so at low levels. A´ shows a magnified single scan of the T2 NB7-3 lineage boxed in A. GW is outlined. A´´ shows only the Antp staining.
B. Co-expression of Eg (green), Hb (blue) and activated Caspase 3 (act. Casp3, red) in NB7-3 (stippled circle) of a late stage 16 *Antp*$^{W10}$ mutant embryo. One GW motoneuron in T2 (arrowhead) shows activation of Caspase 3. Caspase 3 is also activated in a GW of T3 (arrow). B´ shows a magnified single scan of the T2 NB7-3 lineage boxed in B. The apoptotic GW is outlined. B´´ shows only the activated Caspase 3 staining.
C. A late stage 16 *en>Antp* embryo, stained against Eg (green), Hb (blue) and activated Caspase 3 (act. Casp3, red). Progeny of NB7-3 are shown (stippled circle). The T2 NB7-3, including GW (arrowheads) is not changed compared to the wild type. In T3 and A1, GWs (arrows) show Caspase 3 activation less frequently. C´ shows a magnified single scan of the A1 NB7-3 lineage boxed in C. GW is outlined. C´´ shows only the activated Caspase 3 staining.
D. Co-expression of Eg (green) and Antp (red) in NB2-4t motoneurons (stippled circle) of a late stage 16 wild type embryo. In T1 both MNa (arrows) and MNp show weak *Antp* expression. In T2, both express *Antp* at high levels. The T3 MNa (arrow) and MNp show moderate *Antp* expression. D´ shows a magnified single scan of the T3 NB2-4t lineage boxed in D. MNa is outlined. D´´ shows only the Antp staining.
E. Co-expression of GFP (green) and activated Caspase 3 (act. Casp3, red) in NB2-4t motoneurons (stippled circle) of a late stage 16 *poxN>GFP,Antp* embryo. The T3 MNa (arrows) shows Caspase 3 activation less frequently than in the wild type. E´ shows a magnified single scan of the T3 NB2-4t lineage boxed in E. MNa is outlined. E´´ shows only the activated Caspase 3 staining.
Stippled lines mark the midline, anterior is up in all images.

MNa fate in the thorax could not be evaluated in *Antp* mutants due to extremely weak *eg* expression. However, driving *Antp* expression with *poxN*-Gal4 drastically reduced the percentage of apoptotic MNa motoneurons in T3 (Fig. 3-24F, Table 3-10). This suggested that *Ubx* may counteract *Antp* in a similar way as in NB7-3 to prevent it from promoting survival of this motoneuron.

| Segment | Percentage of apoptotic MNas | |
|---|---|---|
| | WT | *poxN>Antp* |
| T1-T2 | 0 % (n=29) | 0 % (n=41) |
| T3 | 64.7 % (n=17) | 5 % (n=20) |

Table 3-10. Frequency of observed MNa motoneuron apoptosis in thoracic segments of wild type (WT) and *Antp* gain of function (*poxN>Antp*) embryos at late stage 16. n indicates the number of hemisegments analyzed.

*Antp* mutant embryos showed another interesting phenotype in T1 and T2: in about 30% of analyzed hemisegments the NB7-3 cluster consisted of 6 to 7 cells (Fig. 3-29B), which is 1 to 2 cells more than in the wt (Fig. 3-29A). The additional cells were Hb-negative and occasionally showed Caspase 3 activation.

Taken together, these results suggested that *Antp* is necessary and sufficient for GW and possibly MNa motoneuron survival and that it can counteract the proapoptotic effect of *Ubx*. In addition, *Antp* appears to negatively affect NB7-3 cell number.

## 3.9. *Ubx* prevents *Antp* from promoting survival of the GW motoneuron

To examine how *Antp* counteracts the proapoptotic function of *Ubx*, I looked at *Ubx* and *Antp* expression in *Antp* and *Ubx* loss- and gain-of-function mutants, respectively. In $Antp^{W10}$ mutants *Ubx* expression was unchanged in late stage 16 embryos (Fig. 3-25B) and in *en>Antp* embryos of the same stage, *Ubx* expression in the NB7-3 cells occasionally appeared reduced (Fig. 3-25C) as compared to the wild type (Fig. 3-25A and summarized in Fig. 3-28). As above, *Ubx* expression in the MNa motoneuron of $Antp^{W10}$ mutants could not be evaluated due to low *eg* expression, but in *poxN>Antp* embryos *Ubx* expression was occasionally reduced

in MNa of segment T3 (Fig. 3-28). These results suggest that *Antp* overexpression reduces GW and MNa apoptosis either by downregulating *Ubx* expression or by sustaining cell survival, or by doing both. In the wild type, however, *Antp* probably cannot suppress *Ubx*, as *Antp* mutants show no change in *Ubx* expression (Fig. 3-25C) and no increase in abdominal GW apoptosis (Table 3-9).

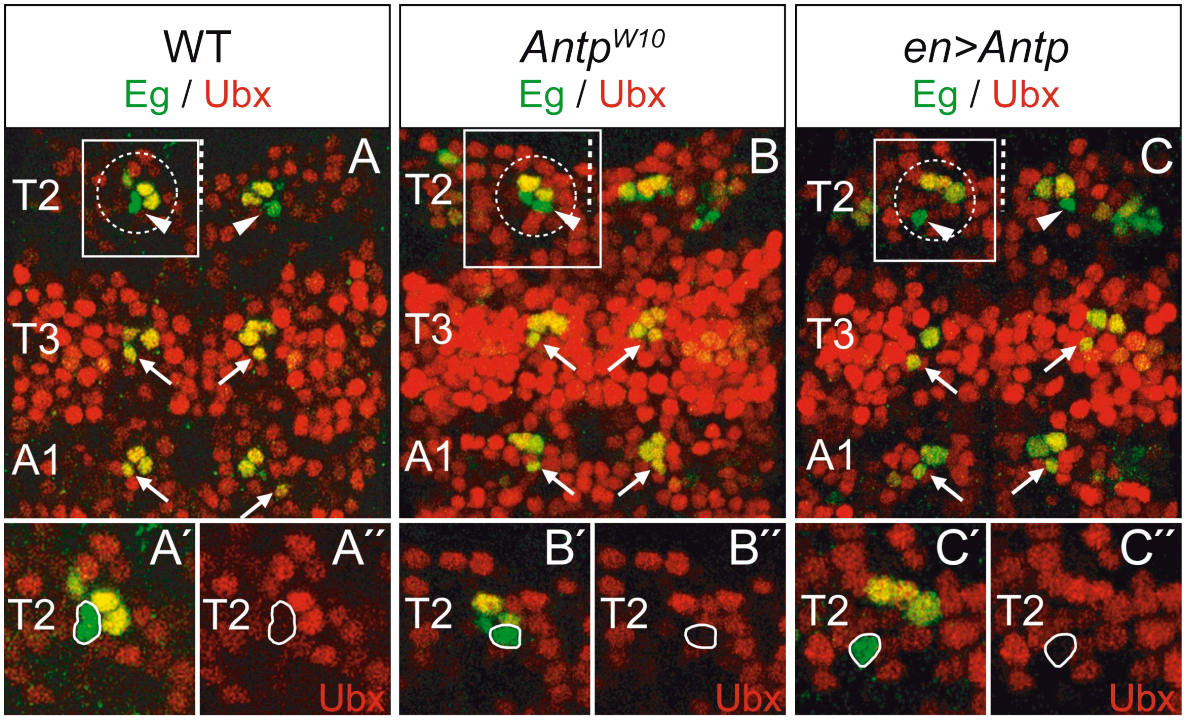


**Fig. 3-25. *Ubx* expression is not affected by changes in Antp levels.**
A. Co-expression of Eagle (Eg, green) and Ubx (red) in NB7-3 (stippled circle) of a late stage 16 wild type embryo. In T2 GW (arrowheads) does not express *Ubx*, whereas the interneurons show high *Ubx* levels. In T3 and A1 all progeny cells, including GW (arrows) show strong *Ubx* expression. A´ shows a magnified single scan of the T2 NB7-3 lineage boxed in A. GW is outlined. A´´ shows only the Ubx staining.
B. Co-expression of Eg (green) and Ubx (red) in NB7-3 (stippled circle) of a late stage 16 *Antp*$^{W10}$ mutant embryo. *Ubx* expression in GW of T2 (arrowhead), and T3 and A1 (arrows) does not differ from that in the wild type. B´ shows a magnified single scan of the T2 NB7-3 lineage boxed in B. GW is outlined. B´´ shows only the Ubx staining.
C. Co-expression of Eg (green) and Ubx (red) in NB7-3 (stippled circle) of a late stage 16 *en>Antp* mutant embryo. GW is indicated in T2 (arrowheads) and in T3 and A1 (arrows). *Ubx* expression is not significantly changed, although some cells appear to have slightly lower *Ubx* levels. C´ shows a magnified single scan of the T2 NB7-3 lineage boxed in C. GW is outlined. C´´ shows only the Ubx staining.
Stippled lines mark the midline, anterior is up in all images.

In *Ubx*$^{1}$ mutants, high Antp expression levels extend to the anterior half of segment A1, and in all NB7-3 cells *Antp* expression is equally strong from T1 to T3 (Fig. 3-26D,E,F). In the abdomen, in contrast, Antp levels in GWs do not differ from wt in most segments and *Antp* expression in the NB2-4t MNa is also unchanged (Fig. 3-28). In *en>Ubx* embryos *Antp* is downregulated in the whole NB7-3 cluster, both in thoracic and in abdominal segments (Fig. 3-26G,H,I and summarized in Fig. 3-28). *Antp* levels in *poxN>Ubx* embryos could not be analyzed. These results show that *Ubx* overexpression represses *Antp* (at least in GW) which contributes to an increase in thoracic and abdominal GW apoptosis. In *Ubx*$^{1}$ mutant embryos, however, NB7-3 *Antp* expression increases only in T2 and T3, but not in the abdominal segments (Fig. 3-28), although apoptosis is abolished in both tagmata (Table 3-4), which suggests that, in the wild type, high Antp levels are required to prevent activation of apoptosis in GWs. In the third thoracic and in abdominal segments, low *Antp* levels are not sufficient to counteract the proapoptotic effect of *Ubx*. Accordingly, *Antp* overexpression can significantly reduce GW and MNa apoptosis in all segments (Tables 3-9 and 3-10), without affecting Ubx protein levels (Fig. 3-28). Thus, *Antp* seems to be required to prevent activation of GW apoptosis, and *Ubx* appears to oppose this function of *Antp*.

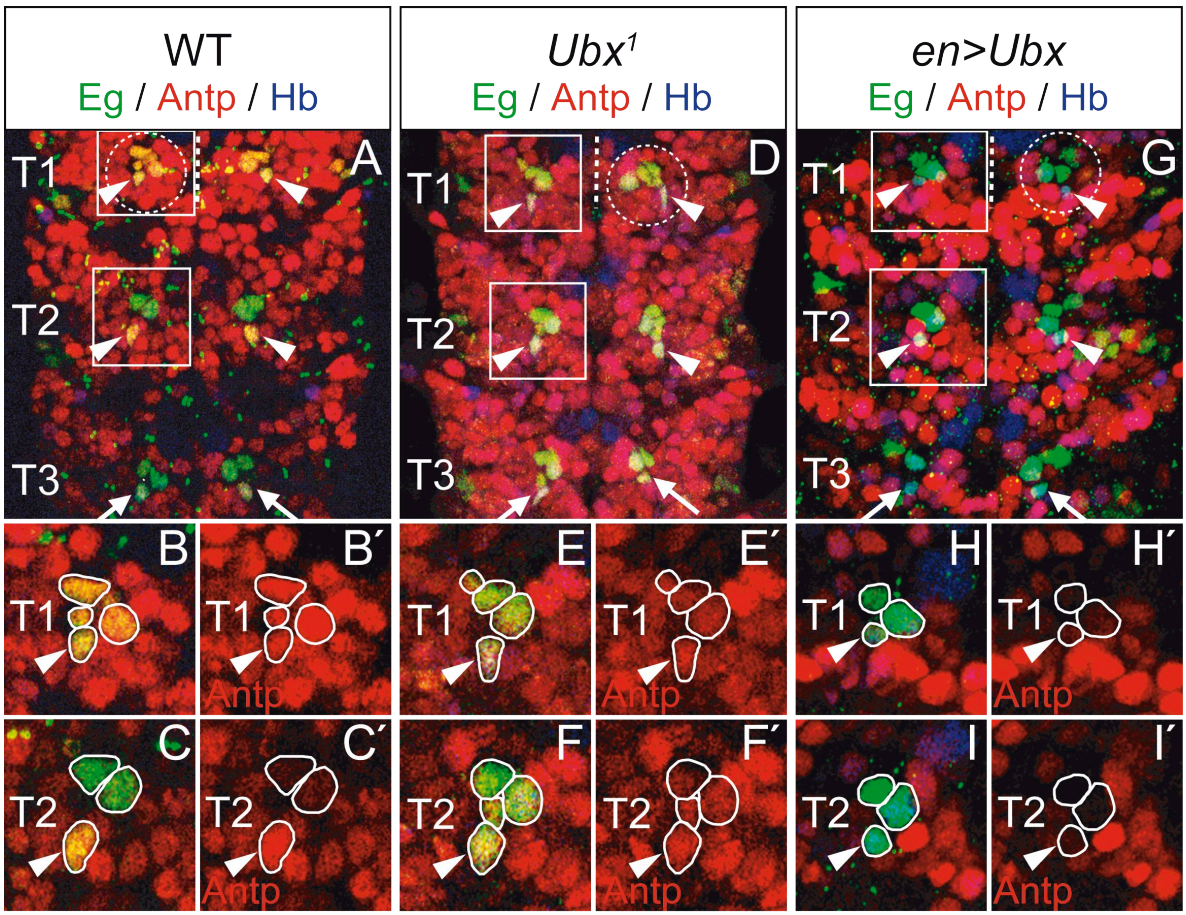


**Fig. 3-26. Changes in *Ubx* expression levels affect *Antp* expression.**
A. Co-expression of Eagle (Eg, green), Hunchback (Hb, blue) and Antennapedia (Antp, red) in NB7-3 (stippled circle) of a late stage 16 wild type embryo. In T1, all NB7-3 progeny, including GW (arrowheads), show strong *Antp* expression. In T2, GW (arrowheads) also shows high and the interneurons low *Antp* levels. The T3 NB7-3 interneurons do not express *Antp*, whereas GW (arrows) does so at low levels.
B. A magnified single scan of the T1 NB7-3 lineage boxed in A. All NB7-3 cells show equally strong *Antp* expression (outlined), GW is indicated by arrowhead. B´ shows only the Antp staining.
C. A magnified single scan of the T2 NB7-3 lineage boxed in A. NB7-3 cells are outlined. The interneurons show low *Antp* levels, whereas GW (arrowhead) expresses *Antp* strongly. C´ shows only the Antp staining.
D. Co-expression of Eg (green), Hb (blue) and Antp (red) in NB7-3 (stippled circle) of a late stage 16 *Ubx*$^{1}$ mutant embryo. The thoracic segments show equally high *Antp* levels in all NB7-3 cells, including GW in T1, T2 (arrowheads) and T3 (arrows).
E. A magnified single scan of the T1 NB7-3 lineage boxed in D. All NB7-3 cells show equally strong *Antp* expression (outlined), GW is indicated by arrowhead. E´ shows only the Antp staining.
F. A magnified single scan of the T2 NB7-3 lineage boxed in D. NB7-3 cells are outlined. The interneurons and GW (arrowhead) show equally high *Antp* levels. F´ shows only the Antp staining.
G. Co-expression of Eg (green), Hb (blue) and Antp (red) in NB7-3 (stippled circle) of a late stage 16 *en>Ubx* embryo. The thoracic segments show virtually no *Antp* expression in NB7-3 cells, including GW in T1, T2 (arrowheads) and T3 (arrows).
H. A magnified single scan of the T1 NB7-3 lineage boxed in G. None of the NB7-3 cells show *Antp* expression (outlined), GW is indicated by arrowhead. H´ shows only the Antp staining.
I. A magnified single scan of the T2 NB7-3 lineage boxed in G. NB7-3 cells are outlined. The interneurons and GW (arrowhead) all lack *Antp* expression. I´ shows only the Antp staining.
Stippled lines mark the midline, anterior is up in all images.

To confirm the opposing roles of *Antp* and *Ubx* in regulating GW survival, I examined *Antp*$^{W10}$,*Ubx*$^{1}$ double mutants and found that GW apoptosis was partly restored, with 19.6% of GWs dying in segments A1 to A7 (n=112) (Fig. 3-27 and Table 3-11, summarized in Fig. 3-28). In segment T3, 23.5% of counted hs (n=17) contained a cell triple-stained for Eg, activated-Caspase-3 and Hunchback, however thoracic segments of these mutants often showed strong overproliferation in the NB7-3 cluster, making it difficult to unambiguously identify the GW motoneuron.

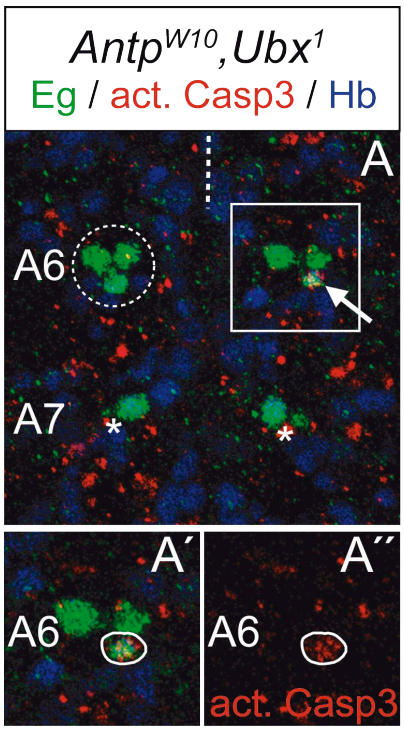


**Fig. 3-27. GW motoneuron apoptosis is restored in *Antp,Ubx* double mutants.**
A. A late stage 16 *Antp*$^{W10}$,*Ubx*$^{1}$ double mutant embryo, stained against Eagle (Eg, green), Hunchback (Hb, blue) and activated Caspase 3 (act. Casp3, red). In segment A6, a GW motoneuron shows Caspase 3 activation (arrow). Asterisks indicate positions where GW has already been removed. A´ shows a magnified single scan of the A6 NB7-3 lineage boxed in A. The apoptotic GW is outlined. A´´ shows only the activated Caspase 3 staining. Stippled line marks the midline, anterior is up.

| Segment | Percenatge of apoptotic GWs | | |
|---|---|---|---|
| | WT | *Ubx*$^{1}$ | *Antp*$^{W10}$,*Ubx*$^{1}$ |
| T1-T2 | 0 % (n=19) | 0 % (n=28) | ND |
| T3 | 55.6 % (n=27) | 0 % (n=14) | 23.5 % (n=17) |
| A1-A7 | 81.2% (n=69) | 0 % (n=98) | 19.6 % (n=112) |

Table 3-11. Frequency of observed GW motoneuron apoptosis in thoracic and abdominal segments of wild type (WT), *Ubx* loss of function (*Ubx*$^{1}$) and *Antp,Ubx* loss of function (*Antp*$^{W10}$,*Ubx*$^{1}$) embryos at late stage 16. n indicates the number of hemisegments analyzed. ND – no data.

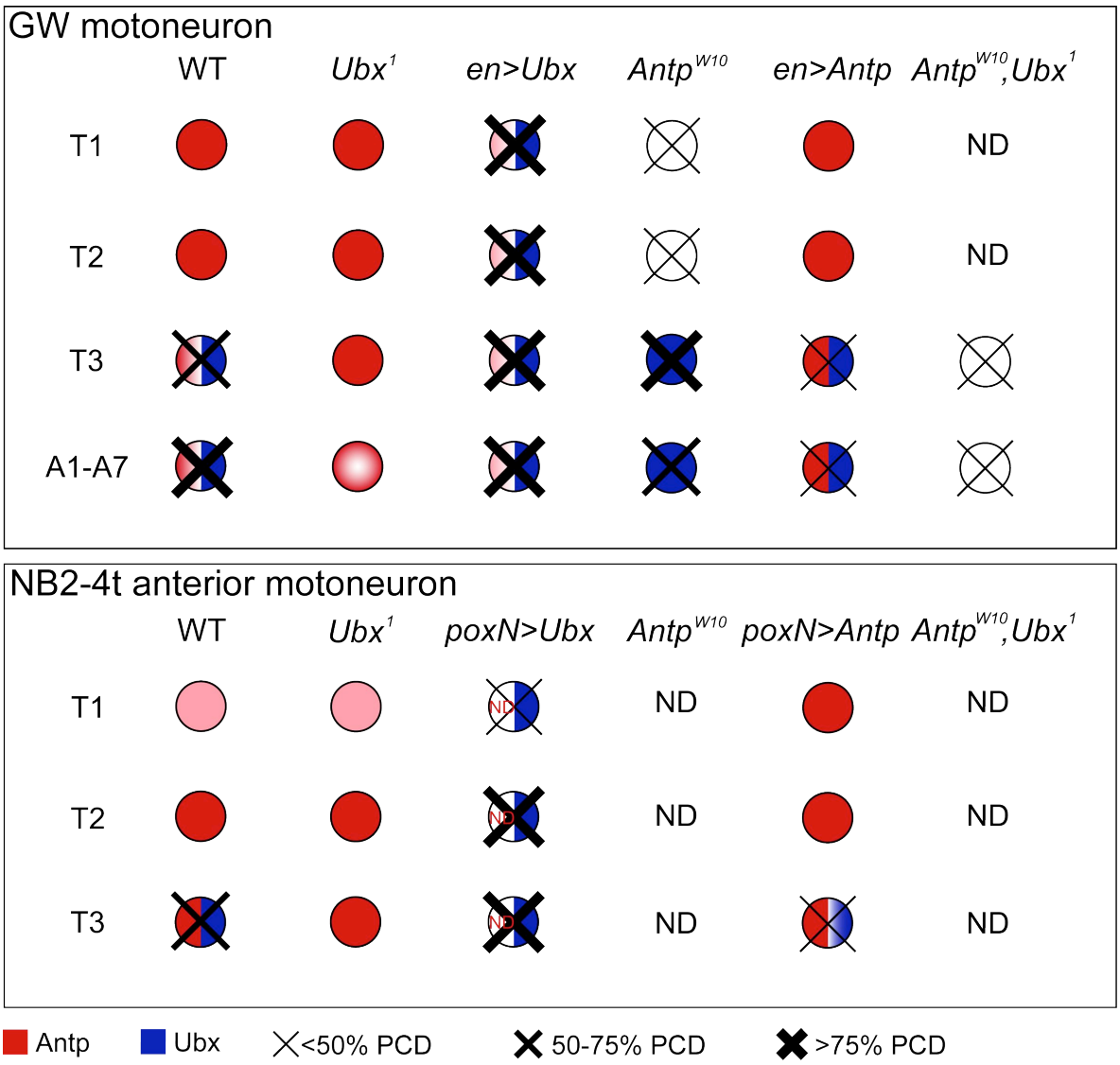


**Fig. 3-28. Summary of GW and NB2-4t MNa motoneuron apoptosis.**
Expression of *Antp* and *Ubx* is shown as observed in thoracic and abdominal segments of late stage 16 wild type or mutant embryos. *Antp* expression is represented in red (strong) or pink (weak) and *Ubx* expression in blue. Crosses indicate apoptotic cell death, with the different line widths reflecting its frequency as specified in the legend. ND - no data.

The overproliferation phenotype was present in 100% of T1 and T2 hemi-segments (n=29), and in 88.2% of T3 (n=17). In these cases NB7-3 comprised 12 to 13 cells, 3 to 4 of which were *hb*-positive (Fig 3-29C). This represents a further exaggeration of the *Antp* mutant phenotype, where NB7-3 comprised 6 to 7 cells (Fig 3-29B). As *Antp* overexpression results in a reduction in cell number, it is conceivable that *Antp* is required to stop NB proliferation after the birth of the 3 GMCs, either by inducing apoptosis of the NB or by promoting cell cycle exit. Removing *Antp* would then result in a few more divisions and a final cell number of 6 to 7 cells. Increasing *Antp* levels would result either in premature cell death or

cell cycle exit of the NB, before it can generate the last GMC, or in apoptosis of one EW. How the additional removal of *Ubx* can enhance this effect remains to be investigated.

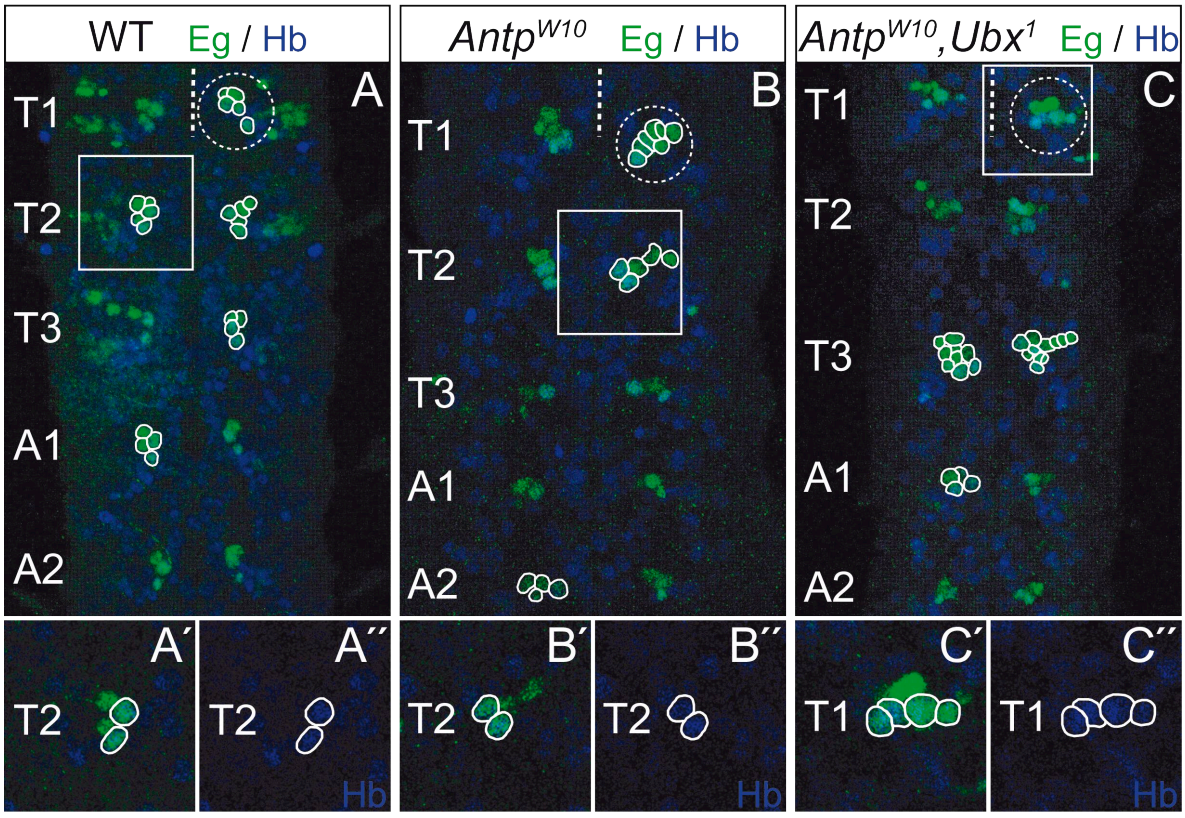


**Fig. 3-29. *Antp* mutants and *Antp,Ubx* double mutants show increased NB7-3 cell numbers.**
A. Anti-Eagle (Eg, green) and anti-Hunchback (Hb, blue) staining in a late stage 16 wild type embryo, showing 5 NB7-3 cells (outlined) in segments T1 and T2, and only 4 in T3 and the abdomen. There are only 2 Hb-positive cells per hemisegment. A´ shows a magnified single scan of the T2 NB7-3 lineage boxed in A. The two Hb-positive cells are outlined. A´´ shows only the Hb staining.
B. Shown is a late stage 16 $Antp^{W10}$ mutant embryo. NB7-3 (outlined) in T1 comprises 7 cells, and in T2 5 cells. T3-A2 show 4 cells like in the wild type. Only 2 cells per NB7-3 cluster are Hb-positive. B´ shows a magnified single scan of the T2 NB7-3 lineage boxed in B. The two Hb-positive cells are outlined. B´´ shows only the Hb staining.
C. In a late stage 16 $Antp^{W10},Ubx^{1}$ double mutant embryo, the overproliferation in the NB7-3 lineage is even more pronounced. The NB7-3 in T3 (outlined) comprises 9 and 11 cells in the left and right hemisegment, respectively. In addition, each hemisegment shows 3 to 4 Hb-positive cells. C´ shows a magnified single scan of the T1 NB7-3 lineage boxed in C. The four Hb-positive cells are outlined. C´´ shows only the Hb staining.
Stippled lines mark the midline, anterior is up in all images.

I also attempted co-expressing *Antp* and *Ubx* using the *en*-Gal4 driver. The NB7-3 cluster is severely affected in these embryos - it is completely missing in 20% of T3 (n=10) and 31.4% of abdominal segments (n=70), and in most other cases only 1 to 2 cells remain at stage 15, making it impossible to analyze GW fate. I therefore examined embryos in which the function of one or both of these

genes was partially or completely removed. I made use of the observation that, in *Ubx*$^{1}$/+ heterozygous embryos, GW apoptosis is reduced in T3 from 55.6% (in wt, n=27) to 7.1% (n=14), and in the abdomen from 81.2% (in wt, n=69) to 21.7% (n=97) (Fig. 3-30, Table 3-12), which confirms that *Ubx* is required for GW apoptosis, and that this effect is dose-dependent. Removing one copy of the *Antp* gene in these embryos (*Antp*$^{W10}$,*Ubx*$^{1}$/+) results in an increase in GW apoptosis to 16.7% (n=18) in T3 and 41.3% (n=126) in the abdomen. Moreover, completely removing *Antp* (*Antp*$^{W10}$,*Ubx*$^{1}$/*Antp*$^{W10}$,+) further increases the amount of dying GWs to 36.4% (n=22) in T3 and 52.2% (n=90) in abdomen (Fig. 3-30, Table 3-12).

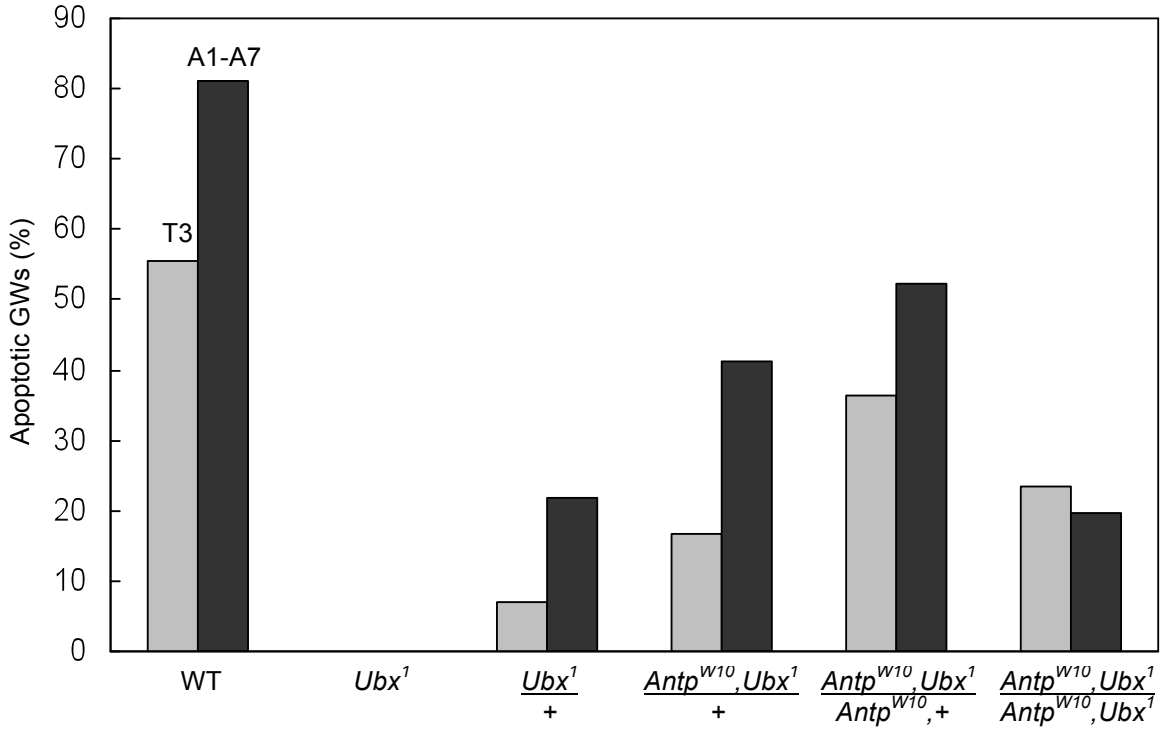


**Fig. 3-30. *Ubx* counteracts *Antp* in regulating GW motoneuron survival.**
The graph shows a comparison of GW motoneuron apoptosis in segments T3 and A1 to A7 between wild type (WT) and homozygous and heterozygous *Ubx* mutants and *Antp,Ubx* double mutants. Light gray bars represent segment T3 and dark gray bars segments A1 to A7. GW apoptosis is reduced in *Ubx*$^{1}$ heterozygotes, indicating that *Ubx*-induced apoptosis is dose-dependent. Progressively reducing the dose of *Antp* in a heterozygous *Ubx* mutant background increases the death rate of these motoneurons accordingly. When both *Antp* and *Ubx* are removed (*Antp*$^{W10}$,*Ubx*$^{1}$/*Antp*$^{W10}$,*Ubx*$^{1}$), the death rate of GW is again reduced.

| Segment | Percentage of apoptotic GWs | | | | | |
|---|---|---|---|---|---|---|
| | WT | *Ubx*$^{1}$ | *Ubx*$^{1}$ / + | *Antp*$^{W10}$,*Ubx*$^{1}$ / + | *Antp*$^{W10}$,*Ubx*$^{1}$ / *Antp*$^{W10}$,+ | *Antp*$^{W10}$,*Ubx*$^{1}$ / *Antp*$^{W10}$,*Ubx*$^{1}$ |
| T3 | 55.6 % (n=27) | 0% (n=14) | 7.1 % (n=14) | 16.7 % (n=18) | 36.4 % (n=22) | 23.5 % (n=17) |
| A1-A7 | 81.2% (n=69) | 0% (n=98) | 21.7 % (n=97) | 41.3 % (n=126) | 52.2 % (n=90) | 19.6 % (n=112) |

Table 3-12. Frequency of observed GW motoneuron apoptosis in segments T3 to A7 of wild type (WT), and homozygous and heterozygous *Ubx* loss of function (*Ubx*$^{1}$) and *Antp,Ubx* loss of function (*Antp*$^{W10}$,*Ubx*$^{1}$) mutant embryos at late stage 16. n indicates the number of hemisegments analyzed.

Taken together, these results demonstrate that, in abdominal segments, *Ubx* induces apoptosis of the GW motoneuron late in development, and it does so by counteracting the positive effect of *Antp* on cell survival. In anterior thoracic segments where *Ubx* expression is kept off by an unknown factor, *Antp* protects these neurons from apoptosis.

# 4. Discussion

One of the fundamental questions in biology is how morphological diversity is generated among the homologous body parts (segments). In the embryonic CNS of *Drosophila melanogaster*, clear differences emerge over the course of development between thoracic and abdominal segments in the form of specialized functional networks that support regional locomotion and sensory requirements. These differences are the result of region-specific division patterns of the NBs and of the different numbers and types of neural cells that the NBs generate (Technau et al., 2006). Regulation of CNS cell number is achieved through a controlled balance of cell proliferation and programmed cell death or apoptosis. Apoptosis is an integral part of animal development contributing to spatial patterning of tissues and organs. In the recent years, factors regulating developmental cell death in the CNS have begun to be identified using invertebrate (*C. elegans* and *Drosophila*) and vertebrate (mouse) model systems. These studies revealed the diversity of cellular signals involved, and have shown that cell death can be either a pre-determined cell fate or the result of insufficient survival-promoting interactions between cells (reviewed by Twomey and McCarthy, 2005). Despite these recent advances, we still know rather little about how the decision between life and death is made for a particular cell during development.

Since the incidence and pattern of apoptotic cells in the *Drosophila* CNS have been only poorly described to date, an effort was first made in our laboratory to describe the distribution of apoptosis throughout CNS development and thus establish a basis for further investigations into mechanisms of apoptosis regulation. My contribution to this effort comprises the first part of my thesis. The second part involves investigations into mechanisms that regulate developmental apoptosis of identified neurons in the CNS. My studies revealed that the *Drosophila Hox* genes *Ubx* and *Antp* regulate segment-specific survival of two differentiated motoneurons, and thus contribute to the patterning of neuromuscular networks along the antero-posterior body axis.

## 4.1. The CNS of apoptosis-deficient embryos does not appear grossly perturbed

In my analysis of the role of apoptosis in development of the embryonic CNS I compared the wt CNS with that of apoptosis-deficient (*H99*) embryos. I found that, macroscopically, they do not show large differences. The supernumerary cells found in *H99* embryos do not seem to disturb developmental events in the CNS, such as cell migration and axonal pathfinding, and the glial cells mostly find their appropriate positions accurately. The axonal projections appeared to form normally - they extend along their usual paths and find their targets in the periphery. In fact, the supernumerary cells themselves are capable of differentiating i.e. expressing differentiation markers and extending axons. In agreement with this data, the DiI-labeled NB lineages described in *H99* embryos were, in the majority of cases, easily identifiable based on their shape, position and axonal pattern, despite the supernumerary cells (Rogulja-Ortmann et al., 2007).

## 4.2. Specification of supernumerary neural cells in apoptosis-deficient embryos

The majority of the DiI-labelled NB lineages in *H99* embryos contained, as expected, supernumerary cells (Rogulja-Ortmann et al., 2007). Examination of the cell types and axonal projections in these lineages, as well as my analysis of marker gene expression in *H99* embryos showed that there were many additional neurons, but virtually no additional glia.

### 4.2.1. Supernumerary cells cannot be specified as glia

The finding that no additional glia were present in NB clones of *H99* embryos, and that there was no difference in numbers of Repo-expressing glial cells in wt and *H99*, suggests that lateral glia do not undergo apoptosis during embryonic CNS development. These results are not in agreement with a published report where the authors suggest that cells of one glial subtype, the longitudinal glia, are overproduced, and their numbers adjusted through axon contact (Hidalgo et al., 2001). Hidalgo et al. observed occasional apoptotic longitudinal glia (using TUNEL

staining) and it is possible that the counting method used in my experiments does not allow a resolution fine enough to account for an occasional additional Repo-positive cell in *H99* embryos. However, if glia of this subtype were consistently overproduced, I would expect to have observed a higher total number of glia in *H99* embryos. I therefore suggest that apoptosis of longitudinal glia may reflect a small variability in the number of cells needed, and not a general mechanism for adjusting glial cell numbers. In contrast, several of the Repo-negative midline glia in each segment have been shown to undergo apoptosis over the course of embryonic development (Sonnenfeld and Jacobs, 1995; Zhou et al., 1995).

A small difference does become apparent when one separates the total Repo-positive glia counts into those in the CNS and those in the periphery: 25.67±0.45 cells/hemisegment (hs) and 28.42±0.64 cells/hs for wt and *H99*, respectively, were counted in the CNS, whereas 8.50±0.28 cells/hs and 6.35±0.82 cells/hs for wt and *H99*, respectively, were found in the periphery. The reasons for this difference might be the greater width of the CNS in *H99* embryos, requiring more time for peripheral glia to reach their final positions. The cues required for proper migration of the peripheral glia may also be disturbed by additional cells. Alternatively, the difference might be due to differentiation defects in these cells.

### 4.2.2. Some supernumerary cells can differentiate into neurons

For the analysis of marker genes expressed in smaller groups of cells (Repo, Lbe, Eve and Eg), the chosen markers (apart from Repo) were expressed almost exclusively in neurons. The additional cells labelled by these markers in *H99* embryos could thus presumably also be specified as neurons. In support of this assumption, some of the NB clones with too many cells in *H99* embryos exhibited atypical axonal projection patterns, which unambiguously identifies these additional cells as neurons (Rogulja-Ortmann et al., 2007). The atypical projections were found to extend both within the CNS (“interneurons”) and into the periphery (“motoneurons”). The *H99* clones showing too many cells and normal projections also often showed thicker axonal bundles, suggesting additional axons. Thus, at least some of the supernumerary cells in *H99* embryos express differentiation markers and behave as typical neurons, i.e. they are capable of developing axons that can navigate through the CNS and extend as far as the periphery.

Based on the results obtained, one can in general conclude that apoptosis occurs almost exclusively in neurons and/or undifferentiated cells and that lateral glia are not produced in excess numbers in the embryo. It is interesting to speculate on the role of additional cells, if any, in the embryonic CNS and on the reasons for their removal. These cells may have an early function in development, and become superfluous once this function has been carried out. Such a role has been shown for the dMP2 and MP1 interneurons, which are born in all segments from head to abdomen and pioneer the longitudinal axon tracts early in development. At the end of embryogenesis these neurons undergo apoptosis in all segments except A6 to A8 (Miguel-Aliaga and Thor, 2004), where they survive due to expression of the *Hox* gene *Abdominal-B* (*AbdB*), are respecified into insulinergic neurons and innervate the hindgut (Miguel-Aliaga et al., 2008). Regarding the additional “motoneurons”, it would be interesting to determine their target(s) and thereby perhaps gain insight into physiological reasons for their death. Recently, two functional homologs of vertebrate Neurotrophins (NTs) have been identified in *Drosophila* as *DNT1* and *DNT2* (Zhu et al., 2008). In vertebrates neurons are produced in excess, and the surplus cells are eliminated via apoptosis in order to adjust innervation, targeting and connectivity to target size (Levi-Montalcini, 1987). In many of these cases, neuronal survival is promoted by NTs secreted by the target. Such a mechanism has been assumed to be absent in *Drosophila* until now. Zhu and colleagues found that limiting amounts of DNT1 produced by the midline intermediate target are required for neuronal survival, and targeting by the motor axons requires DNT1 at the muscle (Zhu et al., 2008). As the muscle pattern in the embryo shows segment-specific differences, one plausible reason for motoneuron elimination in the embryonic CNS could be a lack of the target(s), i.e. a lack of guidance or survival cues coming from these targets. This hypothesis would be difficult to test at the moment due to a lack of tools that allow specific labelling of these motoneurons in the *H99* mutant background.

### 4.2.3. On the origins of supernumerary cells in apoptosis-deficient embryos

Whether the observed supernumerary cells are normally born and undergo apoptosis, or originate from additional divisions of surviving NBs or GMCs, could not be determined from the experiments carried out in the course of these studies, but similar observations have been made for both cases. In their analysis of

apoptosis in the NB7-3 lineage, Lundell and colleagues have shown that, when cell death is prevented, the normally apoptotic progeny of NB7-3 can express the enzyme Dopa-decarboxylase (DDC) and the neuropeptide Corazonin, both of which indicate differentiation of these cells into secretory neurons (Lundell et al., 2003). Another study showed that the proapoptotic gene *reaper* (*rpr*) is responsible for the removal of the majority of abdominal NBs at the end of embryogenesis (Peterson et al., 2002). The progeny produced by continuing proliferation of the surviving NBs in the *reaper* mutant larvae express the neuronal marker Elav, showing that cells which are never born in the wt are capable of becoming neurons. In *H99* embryos, both cases are most likely occurring, since BrdU labeling experiments show additional divisions in about one half of analyzed *H99* embryos (Rogulja-Ortmann et al., 2007).

## 4.3. Involvement of *Hox* genes in developmental apoptosis in the CNS

In the wt embryo, only seven NB lineages show obvious tagma-specific differences in cell number and composition (Bossing et al., 1996; Schmidt et al., 1997). Tagma-specific differences among serially homologous CNS lineages have previously been shown to be controlled by homeotic genes (Berger et al., 2005; Prokop and Technau, 1994). Therefore, such lineages provide useful models for studying homeotic gene function in segment-specific apoptosis. In DiI labelling experiments in *H99* embryos, further lineages were observed that were differently affected in the thorax and abdomen (Rogulja-Ortmann et al., 2007), which may imply *Hox* gene involvement in their development as well.

The analysis of the distribution of activated Caspase-3-positive cells in wt embryos showed that some apoptotic cells appear rather randomly distributed, but many examples of regular, segmentally repeated apoptotic cells were found, which in turn suggested tight spatial and temporal control of apoptosis (Rogulja-Ortmann et al., 2007). In three cases where the apoptotic cells were precisely identified, the pattern of apoptosis can be brought in connection with the expression of *Hox* genes. The U motoneurons are removed in segments with the highest expression levels of *Abdominal-B* (*AbdB*), the NB2-4t motoneuron in the segment with highest

levels of *Ultrabithorax* (*Ubx*) expression and the GW motoneuron in all segments where *Ubx* is expressed. *Hox*-dependent apoptosis has been reported in all animal phyla and in various tissues, including the nervous system. For example, the mouse *Hoxb13* gene, an *AbdB* homolog, is required for finalizing tail development. *Hoxb13* mutant mice exhibit neural hyperplasia in the caudal extremity of the spinal cord, in part due to a defect in apoptosis induction (Economides et al., 2003). The *Antp* ortholog *mab-5* contributes to posterior ventral nerve cord patterning in *C. elegans* by directly activating transcription of *egl-1*, a BH3-domain encoding activator of apoptosis, in the P11 and P12 neuronal lineages (Liu et al., 2006). In *Drosophila* larvae, a*bdA* puts an end to neural proliferation in the abdomen by inducing apoptosis of postembryonic neuroblasts in this region of the ventral nerve cord (Bello et al., 2003). *abdA* and *Ubx* also control whether or not abdominal NBs undergo apoptosis in the CNS at the end of embryonic development (Prokop et al., 1998). In addition, the *Drosophila Hox* gene *Deformed* (*Dfd*) has been shown to directly activate transcription of the proapoptotic gene *rpr* in the head region, and thus shape the border between neighboring body segments (Lohmann et al., 2002). Thus, proapoptotic genes can also be direct effectors of *Hox* gene function, and it is possible that such interactions also take place in the CNS.

### 4.3.1. *Abdominal-B* may be involved in apoptosis of U motoneurons

The U motoneurons show a segment-specific cell death pattern in that a subset of these neurons undergoes apoptosis only in segments A7 and A8. Analysis of expression of the homeotic genes *Antp*, *Ubx*, *abdA* and *AbdB* did not clearly indicate involvement of any of these genes in U motoneuron apoptosis. Nevertheless, the difference in the strength of AbdB staining between Us of segments A5 to A6 and A7 to A8 may prove to be interesting. At the time of U apoptosis, these motoneurons exhibited low *AbdB* levels in segments A5 and A6, and very high levels in Us of A7 and A8. This would suggest that, at very high levels, *AbdB* may be able to induce apoptosis in a subset of U motoneurons, depending on cell context. Such cell-specific effects are typical of *Hox* genes, as has been shown in several studies (Brodu et al., 2002; Gaufo et al., 2003; Gaufo et al., 2004; Monier et al., 2005; Rozowski and Akam, 2002). Further experiments, examining the expression of known *Hox* cofactors, such as *extradenticle* (*exd*) (Peifer and Wieschaus, 1990; Rauskolb et al., 1993), *homothorax* (*hth*) (Pai et al.,

1998; Rieckhof et al., 1997), *engrailed* (*en*) (Gebelein et al., 2004; Morata and Lawrence, 1975) or *sloppy paired* (*slp*) (Cadigan et al., 1994; Gebelein et al., 2004; Grossniklaus et al., 1992), in U motoneurons would be necessary to clarify this point.

## 4.4. A dual requirement for *Ubx* in the development of the NB7-3 and NB2-4 lineages

The pattern of *Ubx* expression in the GW and NB2-4t motoneurons and their respective lineages is interesting. In early stages, beginning with NB delamination and ending with completion of proliferation within the lineage, the *Ubx* expression pattern conforms to its role as a homeotic gene: it is expressed from the posterior half of segment T3 to the anterior half of A7. The levels of Ubx protein in NB7-3 and NB2-4 and their progeny are not particularly high at these stages, but removal of both *Ubx* and *abdA* results in an NB7-3 lineage that is typical for T1 and T2, showing that they determine the segmental identity of this neuroblast. Following the completion of cell divisions within the lineage, *Ubx* expression is strongly upregulated in the NB7-3 and NB2-4 progeny in a segment- and cell-specific manner. This dynamic pattern of expression implies two roles for *Ubx* in these lineages: (1) an early role in establishing tagma-specific identity of the neuroblast, such as has already been shown for NB1-1 (Prokop and Technau, 1994); and (2) a late role in inducing apoptosis of the motoneurons. The results of the heat-shock experiments confirm that, at least in NB7-3, motoneuron apoptosis is not merely an outcome of segment-specific NB identity, but rather that specifically the late upregulation of *Ubx* leads to apoptosis. NB2-4t could not be tested for the proapoptotic function of *Ubx* in the heat-shock experiments. However, it likely plays a late role in this lineage as well: *Ubx* is not expressed in the early T3 NB2-4t neuroblast, meaning it does not play an early role in specifying its T3 identity. It cannot be excluded that *Ubx* is expressed in the presumptive T3 NB2-4t already in the neuroectoderm and is then downregulated upon delamination, although this is not very likely since *Ubx* is expressed in the posterior half of segment T3 and NB2-4 delaminates from an anterior position in the segment. Hence, motoneuron apoptosis is probably not a result of a specific NB identity, since the proapoptotic

function of *Ubx* must be executed at a later point in development. Also, ectopic *Ubx* expression in the NB2-4t lineage does not appear to transform it into its abdominal counterpart, as two closely positioned dorsal motoneurons were observed in thoracic segments. In these embryos, *Ubx* is still capable of inducing apoptosis of the anterior motoneuron in all thoracic segments, including T1 and T2 where *Ubx* is never expressed in early developmental stages. Taken together, these data indicate that, also in this lineage, *Ubx* is needed at a late developmental stage to induce apoptosis. Dual requirements for *Hox* genes have also been described in determining thoracic bristle patterns where *Ubx* blocks the development of the tibial apical bristle in segment T3 at two different timepoints: early in the second-order precursor cells, and again later in the sensory organ lineage (Akam, 1987; Rozowski and Akam, 2002). Another example was found in cardiac tube organogenesis, where *Hox* genes direct a posterior cardiac tube lineage early, and the differentiation of specific myocytes late in development (Perrin et al., 2004). It is not clear how the late expression of *Ubx* is regulated. It has been suggested that this might depend on genes that define the differences between cell types (Akam, 1987), and it will be interesting to see whether this is also the case for the NB7-3 and NB2-4 neurons.

## 4.5. The ability of *Ubx* to induce apoptosis is context dependent

Early expression of *Ubx* in NB7-3 stretches from the posterior half of segment T3 to the anterior half of A7. In late developmental stages *Ubx* expression in this lineage extends to the second thoracic segment, but in a cell-specific manner: the GW motoneuron does not activate *Ubx* expression, whereas the EW interneurons do. These findings evoke the following questions: (1) why is it that the EWs in T2 to A7 do not undergo apoptosis although they also upregulate *Ubx*? and (2) what represses *Ubx* expression in the T2 GW?

Regarding the first question, it is likely that the differentiation program of the EWs creates a different cellular context in which *Ubx* is unable to induce apoptosis. The results of the ectopic *Ubx* expression experiments support this assumption: whereas GW undergoes apoptosis, the EWs do so very rarely, although they

express *Ubx* at equally high levels. In addition, GW seems to acquire the competence to undergo *Ubx*-dependent apoptosis rather late, as *en*-Gal drives expression strongly from earlier stages but apoptosis does not occur until stage 15. This suggests that the susceptibility of these motoneurons to apoptosis is coupled to differentiation. The context-dependent ability of *Ubx* to activate apoptosis also holds true for the NB2-4t lineage: the anterior motoneuron is susceptible to *Ubx*-induced apoptosis, whereas the posterior one is not, even when *Ubx* is overexpressed.

The attempts made in this work to determine at least some of the factors contributing to apoptosis susceptibility were not successful. For the NB7-3 lineage, at the onset of GW apoptosis *abdA* appears to be weakly expressed only in the EWs from A1 to A7, but not in GW. However, the survival of the EWs is impaired when *abdA* expression levels are increased, and only EW3 in segment A7 appears to be affected in *abdA* loss of function mutants. This observation speaks against *abdA* being the factor that allows EW survival in presence of high Ubx protein levels. In addition, *abdA* appears necessary and sufficient for GW motoneuron survival, although the immunostaining with the available antibody shows no *abdA* expression in GW at any time in development. While these results hint toward an involvement of *abdA* in GW fate, they do not allow any clear conclusions. An improved anti-AbdA antibody would be necessary to re-examine *abdA* expression in the NB7-3 cluster.

Also no compelling evidence could be obtained for the involvement of the known *Hox* gene cofactors *homothorax* (*hth*) (Pai et al., 1998; Rieckhof et al., 1997) and *extradenticle* (*exd*) (Peifer and Wieschaus, 1990; Rauskolb et al., 1993), in cell-specific effects of *Ubx* expression. Mutants of other factors that show differential expression in GW and EWs [*numb* (Uemura et al., 1989), *zfh1* (Isshiki et al., 2001)] also showed no indication that any of these is involved in the effect of *Ubx* on cell survival. This issue could not be resolved in the course of this work and other *Ubx* cofactors, such as *engrailed* or *sloppy paired* (Gebelein et al., 2004), need to be examined in this context.

Regarding the question of differential *Ubx* expression in NB7-3 cells of T2, this is an intriguing observation that might prove to be key to determining the developmental signal that upregulates *Ubx* late in development. One candidate for

repressing *Ubx* expression in GW is the gap gene *hb* (White and Lehmann, 1986). It is known to repress *Ubx* in early embryonic development, and *hb* overexpression can suppress *Ubx* in the NB7-3 lineage. However, *hb* is also necessary to activate *Antp* expression and thereby specify the second thoracic segment (Wu et al., 2001). In *hb* mutants, T2 is not present which did not permit testing whether this is the factor repressing *Ubx* expression in GW. Other obvious candidates are the Polycomb group (PcG) proteins, well-known repressors of *Hox* genes (Ringrose and Paro, 2007). It has recently been shown that, contrary to what had been believed for a long time, target gene repression by these proteins is not necessarily maintained throughout development. In one report, *Drosophila* homologs of testis-specific TAF (TBP-associated factor) have been found to activate their target genes in part by counteracting repression by Polycomb (Chen et al., 2005). Another group has found that during tissue regeneration in *Drosophila* imaginal discs, cells activate the JNK signaling pathway which in turn downregulates transcription of several PcG proteins. In this way cells seem to shift their chromatin to a reprogrammable state in order to allow a change in cell identity (Lee et al., 2005). It is conceivable that such a downregulation of PcG repression could take place in some cells (e.g. EWs in T2) and not in others (e.g. GW). However, the question would still remain as to how the difference between the GW and EW neurons is established specifically in this segment. Alternatively, differential *Ubx* regulation might be affected by non-coding RNAs (ncRNAs). Evidence for post-transcriptional regulation of *Hox* gene expression, both in verterbrate systems and in *Drosophila*, has been accumulating for some time (Pearson et al., 2005). Several ncRNAs have been observed from the *bithorax* complex (BX-C) of *Drosophila* (Bae et al., 2002; Cumberledge et al., 1990; Lipshitz et al., 1987; Sanchez-Herrero and Akam, 1989), and a regulatory function for them has been inferred from their role in recruitment of the Trithorax transcriptional activator complex near the *Ubx* promoter (Sanchez-Elsner et al., 2006). Although their expression patterns have been also described, no direct function for BX-C ncRNAs has been established to date (Lempradl and Ringrose, 2008).

## 4.6. *Ubx* counteracts *Antp* to induce programmed cell death

The obtained results also showed that *Antp* is required for GW survival in all segments, and that *Ubx* counteracts *Antp* in T3 to A7 to induce apoptosis. Although the lower percentage of dying abdominal GWs in *Antp* mutants (69%) as compared with wild type (81.2%) might indicate a proapoptotic function of *Antp* in the abdomen, this is most likely not the case because *Antp* overexpression actually reduced the amount of abdominal GW apoptosis more than twofold. Moreover, removing *Antp* function in a *Ubx* heterozygous background increased GW apoptosis (both in T3 and in abdomen) in a dose-dependent manner, and removing both *Ubx* and *Antp* resulted in a recurrence of GW apoptosis, albeit with low penetrance, lending further support to a pro-survival function of *Antp*.

The other phenotype observed in *Antp* loss and gain of function experiments suggests that it may also control proliferation within the NB7-3 lineage. *Antp* mutants show one to two additional cells per cluster and *Antp* overexpression results in a reduction in cell number. It is conceivable that *Antp* is required to stop NB proliferation after the birth of the 3 GMCs, either by inducing apoptosis of the NB or by promoting cell cycle exit. Removing *Antp* would then result in a few more divisions and a final cell number of 6 to 7 cells, instead of 4 to 5. Increasing *Antp* levels would result either in premature apoptosis or cell cycle exit of the NB, before it can generate the last GMC, or in apoptosis of one EW. *Antp* has recently been reported to be required for quiescence entry of the thoracic NB3-3 following the birth of the last GMC (Tsuji et al., 2008), which indicates that it can promote cell cycle exit of the NB. How *Antp* influences NB7-3 cell number, and how the additional removal of *Ubx* can enhance this effect of *Antp* remains to be investigated.

Regarding their antagonistic functions in regulation of cell survival, it is not clear at which level *Ubx* and *Antp* interact. GW apoptosis was inhibited both in T3 and in abdominal segments of *Ubx* mutants. However, *Antp* expression in *Ubx* mutants was upregulated only in T3, and remained low in abdominal segments, suggesting that here *Ubx* did not induce apoptosis through *Antp* repression. In addition, the pattern and levels of *Ubx* expression did not change at all in *Antp*

mutants, indicating that in this context *Antp* does not promote survival via *Ubx* regulation. I therefore propose that in the wild type, Antp and Ubx might compete for a co-factor or for a target enhancer, rather than cross-regulating each other. The proapoptotic gene *rpr* (White et al., 1996), which is transcriptionally activated in both GW and MNa motoneurons, is a candidate target. In fact, several binding sites for both Ubx and Antp are present in the enhancer of the *rpr* gene (Fig. 4-1). It will be interesting to see whether *Antp* can prevent activation of the apoptotic machinery by affecting an upstream factor or through direct repression of *rpr*. The presence of two Antp binding sites in the *rpr* enhancer permits such speculation, and although it awaits experimental validation, this does suggest a model for the antagonistic effects of *Antp* and *Ubx* on cell survival. According to this model, Ubx and Antp would compete for sites in the *rpr* enhancer. In cells that express *Antp* at high levels and show no *Ubx* expression, it would repress *rpr* transcription. In cells that express *Ubx*, it would overcome repression by Antp and activate *rpr* transcription to induce apoptosis. Such positive *Hox* regulation of *rpr* has already been demonstrated in shaping segment borders in *Drosophila* embryos, where Deformed directly activates *rpr* transcription through binding sites found on the same 4kb enhancer fragment as the Ubx and Antp sites (Lohmann et al., 2002) (Fig. 4-1). In addition, antagonistic transcriptional regulation of the P2 *Antp* promoter in the embryonic ventral nerve cord has been demonstrated for Antp and Ubx (Appel and Sakonju, 1993). In this case, Antp positively autoregulates its own P2 promoter in the thoracic segments, and Ubx competes with Antp for the same binding sites and thus prevents high-level expression of *Antp* in the more posterior segments.

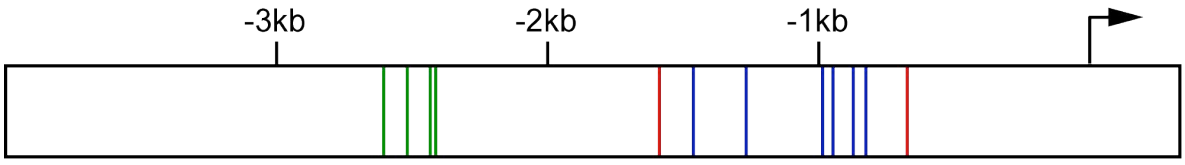


**Fig. 4-1. Ubx and Antp binding sites are found in the *rpr* enhancer.**
Schematic drawing of a 4kb rpr enhancer fragment just upstream of the transcription start site (arrow). Binding sites for the following *Hox* genes are shown: Dfd (green) (Lohmann et al., 2002), Ubx (blue) and Antp (red).

## 4.7. *Hox* gene dependent apoptosis as a mechanism for CNS patterning

The analysis of apoptotic cells in the CNS revealed that most of the identified cells were presumable motoneurons. This finding is relatively surprising, since there are only about 30 motoneurons born in each hemineuromere in the embryo, and they are required for locomotion of the hatched larva. In a recent study, *Hox* genes have been shown to affect locomotor behavior in larval crawling, suggesting they "provide positional information for neurons and thus regulate the formation of neuromuscular networks that control region-specific peristaltic locomotion" (Dixit et al., 2008). One of the outputs of this positional information may be the death of specific outward-projecting neurons in order to selectively remove cells that may disturb the highly refined circuitry required for control of locomotion. A requirement for *Hox* genes in segment-specific cell survival has already been shown for the MP2 and MP1 pioneer neurons (Miguel-Aliaga and Thor, 2004), where *AbdB* expression is required postmitotically for survival of these neurons in the three posterior-most abdominal segments.

The exact function and targets of the GW and the anterior NB2-4t motoneurons in the first and second thoracic segment are unclear (Bossing et al., 1996; Schmid et al., 1999; Schmidt et al., 1997), as is the reason for their removal in the abdominal and posterior thoracic segments. They both project axons out of the CNS, but there have been inconclusive reports about their targets. The GW neuron of segment T2 has been reported to contact muscles 15, 16 and 17 (ventral oblique muscles 4, 5 and 6) in segment T3 (Schmid et al., 1999). However, the description of thoracic muscle patterns depicts these muscles only in segments A2 to A7, whereas they do not develop in the thoracic segments (Bate, 1993). Another description of the NB7-3 lineage suggests that the GW neuron projection ends in the root of the intersegmental (ISN) or the segmental (SN) nerve (Bossing et al., 1996). The abdominal NB2-4 motoneuron was reported to project contralaterally out the posterior root of the ISN to muscle 8 (segment border muscle, SBM) (Schmid et al., 1999). However this muscle is missing in the first and second thoracic segment (Bate, 1993). In another description of the thoracic NB2-4 lineage, the two motoneurons exit the nerve cord through the anterior root of the

ISN (Schmidt et al., 1997) but endplates were not detected. The muscle pattern in the thorax differs considerably from the abdominal one in that many muscles do not develop in the thoracic segments (e.g. ventral acute muscles 2 and 3), and others are present only in the thorax (e.g. dorsal acute muscle 4 or the ventral intersegmental muscles 2-5) (Bate, 1993). Moreover, there are T1-specific muscles which are not found in other segments, such as the dorsal and ventral mouthparts muscles. It is therefore conceivable that the elimination of certain outward-projecting neurons in the posterior thoracic and/or abdominal segments ensures adjustment of the neuronal pattern to the pattern of muscle fibers. Alternatively, the surviving GW and NB2-4t neurons could have other functions. They may, for example, exert a region-specific neurosecretory function and thus modulate neuronal or muscle activity. Such a function has been described for neurosecretory cells in the larval brain, whose processes arborize on the wall of the anterior aorta adjacent to the ring gland (Johnson et al., 2003). They may also be interneurons that synapse peripherally with a motor axon, as has been shown for the PSI interneuron which synapses with the dorsal longitudinal motoneuron in the adult fly (King and Wyman, 1980).

Regardless of the function of neurons described in this work, it is clear that *Hox* genes regulate segment-specific patterns in the CNS not just by specifying segment-specific NB identites, but also by more directly regulating survival of individual neurons. It can be said that *Hox*-regulated segment-specific neuron survival is a part of the patterning process that enables formation of region-specific, functional neuromuscular networks.

# 5. Summary

This study deals with the function and regulation of programmed cell death, or apoptosis, in the development of the embryonic central nervous system of *Drosophila melanogaster*. The first part provides a description of apoptosis-deficient embryos, which showed that preventing apoptosis does not cause gross morphological defects in the CNS, as it appears well organized despite the presence of too many cells. An analysis of the incidence and pattern of apoptosis over the course of development discloses a partly very orderly pattern suggesting tight spatio-temporal control, but also reveals random apoptotic cells, which suggests a certain amount of plasticity in the embryo. This analysis also allowed precise identification of some of the dying neural cells in the embryo, and establishment of single cell models for studying regulation of segment-specific apoptosis in the embryonic CNS. In the second part of the work, further investigations into mechanisms controlling segment-specific apoptosis revealed the involvement of two *Hox* genes, *Antennapedia* (*Antp*) and *Ultrabithorax* (*Ubx*), in this process. *Hox* genes control the formation of segment-specific structures in their domains of expression, but also regulate organ and tissue morphogenesis. The study presented here shows that *Antp* and *Ubx* play antagonistic roles in motoneuron survival in the embryo. *Ubx* expression in the CNS is strongly upregulated at a late point in development, when most cells have begun to differentiate. This upregulation shortly precedes *Ubx*-dependent, segment-specific apoptosis of two differentiated motoneurons. It could further be demonstrated that *Antp* is required for proper development of the NB7-3 lineage and for survival of the NB7-3 motoneuron in the anterior thoracic segments. In segments where *Antp* and *Ubx* expression overlaps, *Ubx* counteracts the anti-apoptotic function of *Antp*, resulting in cell death. Thus, these two *Hox* genes play opposing roles in the survival of differentiated neurons in the late developing nervous system. They thereby contribute to establishment of correct connections between outward-projecting neurons and their targets, which is crucial for the assembly of functional

neural circuits, as these have to fulfill region-specific locomotion and sensory requirements along the antero-posterior body axis.

# 6. References

**Abbott, M. K. and Lengyel, J. A.** (1991). Embryonic head involution and rotation of male terminalia require the *Drosophila* locus *head involution defective*. *Genetics* **129**, 783-9.

**Abrams, J. M., White, K., Fessler, L. I. and Steller, H.** (1993). Programmed cell death during Drosophila embryogenesis. *Development* **117**, 29-43.

**Akam, M.** (1987). The molecular basis for metameric pattern in the Drosophila embryo. *Development* **101**, 1-22.

**Appel, B. and Sakonju, S.** (1993). Cell-type-specific mechanisms of transcriptional repression by the homeotic gene products UBX and ABD-A in Drosophila embryos. *Embo J* **12**, 1099-109.

**Arama, E., Agapite, J. and Steller, H.** (2003). Caspase activity and a specific cytochrome C are required for sperm differentiation in Drosophila. *Dev Cell* **4**, 687-97.

**Artavanis-Tsakonas, S. and Simpson, P.** (1991). Choosing a cell fate: a view from the Notch locus. *Trends Genet* **7**, 403-8.

**Bae, E., Calhoun, V. C., Levine, M., Lewis, E. B. and Drewell, R. A.** (2002). Characterization of the intergenic RNA profile at abdominal-A and Abdominal-B in the Drosophila bithorax complex. *Proc Natl Acad Sci U S A* **99**, 16847-52.

**Bangs, P., Franc, N. and White, K.** (2000). Molecular mechanisms of cell death and phagocytosis in Drosophila. *Cell Death Differ* **7**, 1027-34.

**Bangs, P. and White, K.** (2000). Regulation and execution of apoptosis during Drosophila development. *Dev Dyn* **218**, 68-79.

**Bastiani, M. J., Harrelson, A. L., Snow, P. M. and Goodman, C. S.** (1987). Expression of fasciclin I and II glycoproteins on subsets of axon pathways during neuronal development in the grasshopper. *Cell* **48**, 745-55.

**Bate, M.** (1993). The mesoderm and its derivatives. In *The Development of Drosophila Melanogaster*, vol. 2 (ed. M. Bate and A. Martinez-Arias), pp. 1013-1090. New York: Cold Spring Harbor Laboratory Press.

**Beachy, P. A., Helfand, S. L. and Hogness, D. S.** (1985). Segmental distribution of bithorax complex proteins during Drosophila development. *Nature* **313**, 545-51.

**Bello, B. C., Hirth, F. and Gould, A. P.** (2003). A pulse of the *Drosophila* Hox protein Abdominal-A schedules the end of neural proliferation via neuroblast apoptosis. *Neuron* **37**, 209-19.

**Berger, C., Pallavi, S. K., Prasad, M., Shashidhara, L. S. and Technau, G. M.** (2005). A critical role for cyclin E in cell fate determination in the central nervous system of Drosophila melanogaster. *Nat Cell Biol* **7**, 56-62.

**Bergmann, A., Agapite, J., McCall, K. and Steller, H.** (1998a). The Drosophila gene hid is a direct molecular target of Ras-dependent survival signaling. *Cell* **95**, 331-41.

**Bergmann, A., Agapite, J. and Steller, H.** (1998b). Mechanisms and control of programmed cell death in invertebrates. *Oncogene* **17**, 3215-23.

**Boll, W. and Noll, M.** (2002). The Drosophila Pox neuro gene: control of male courtship behavior and fertility as revealed by a complete dissection of all enhancers. *Development* **129**, 5667-81.

**Bopp, D., Burri, M., Baumgartner, S., Frigerio, G. and Noll, M.** (1986). Conservation of a large protein domain in the segmentation gene paired and in functionally related genes of Drosophila. *Cell* **47**, 1033-40.
**Bossing, T., Udolph, G., Doe, C. Q. and Technau, G. M.** (1996). The embryonic central nervous system lineages of *Drosophila melanogaster*. I. Neuroblast lineages derived from the ventral half of the neuroectoderm. *Dev Biol* **179**, 41-64.
**Brand, A. H. and Perrimon, N.** (1993). Targeted gene expression as a means of altering cell fates and generating dominant phenotypes. *Development* **118**, 401-15.
**Brennecke, J., Hipfner, D. R., Stark, A., Russell, R. B. and Cohen, S. M.** (2003). *bantam* encodes a developmentally regulated microRNA that controls cell proliferation and regulates the proapoptotic gene *hid* in *Drosophila*. *Cell* **113**, 25-36.
**Broadie, K. S. and Bate, M.** (1993). Development of the embryonic neuromuscular synapse of Drosophila melanogaster. *J Neurosci* **13**, 144-66.
**Broadus, J., Skeath, J. B., Spana, E. P., Bossing, T., Technau, G. and Doe, C. Q.** (1995). New neuroblast markers and the origin of the aCC/pCC neurons in the *Drosophila* central nervous system. *Mech Dev* **53**, 393-402.
**Brodsky, M. H., Nordstrom, W., Tsang, G., Kwan, E., Rubin, G. M. and Abrams, J. M.** (2000). Drosophila p53 binds a damage response element at the reaper locus. *Cell* **101**, 103-13.
**Brodu, V., Elstob, P. R. and Gould, A. P.** (2002). abdominal A specifies one cell type in Drosophila by regulating one principal target gene. *Development* **129**, 2957-63.
**Brody, T. and Odenwald, W. F.** (2002). Cellular diversity in the developing nervous system: a temporal view from Drosophila. *Development* **129**, 3763-70.
**Broihier, H. T. and Skeath, J. B.** (2002). *Drosophila* homeodomain protein dHb9 directs neuronal fate via crossrepressive and cell-nonautonomous mechanisms. *Neuron* **35**, 39-50.
**Cadigan, K. M., Grossniklaus, U. and Gehring, W. J.** (1994). Localized expression of sloppy paired protein maintains the polarity of Drosophila parasegments. *Genes Dev* **8**, 899-913.
**Campos-Ortega, J.** (1993). Early neurogenesis in *Drosophila melanogaster*. In *Development of Drosophila melanogaster*, vol. II (ed. M. Bate and A. Martinez-Arias), pp. 1091-1130. Cold Spring Harbor, NY: Cold Spring Harbor Laboratory Press.
**Campos-Ortega, J. and Hartenstein, V.** (1997). The embryonic development of *Drosophila melanogaster*. Berlin, Heidelberg, New York: Springer Verlag.
**Carlson, S. D., Hilgers, S. L. and Juang, J. L.** (1997). First developmental signs of the scolopale (glial) cell and neuron comprising the chordotonal organ in the Drosophila embryo. *Glia* **19**, 269-74.
**Carroll, S. B., DiNardo, S., O'Farrell, P. H., White, R. A. and Scott, M. P.** (1988). Temporal and spatial relationships between segmentation and homeotic gene expression in Drosophila embryos: distributions of the fushi tarazu, engrailed, Sex combs reduced, Antennapedia, and Ultrabithorax proteins. *Genes Dev* **2**, 350-60.
**Carroll, S. B., Laymon, R. A., McCutcheon, M. A., Riley, P. D. and Scott, M. P.** (1986). The localization and regulation of Antennapedia protein expression in Drosophila embryos. *Cell* **47**, 113-22.
**Casanova, J., Sanchez-Herrero, E. and Morata, G.** (1986). Identification and characterization of a parasegment specific regulatory element of the abdominal-B gene of Drosophila. *Cell* **47**, 627-36.

**Challa, M., Malladi, S., Pellock, B. J., Dresnek, D., Varadarajan, S., Yin, Y. W., White, K. and Bratton, S. B.** (2007). Drosophila Omi, a mitochondrial-localized IAP antagonist and proapoptotic serine protease. *Embo J* **26**, 3144-56.
**Chen, P., Nordstrom, W., Gish, B. and Abrams, J. M.** (1996). grim, a novel cell death gene in Drosophila. *Genes Dev* **10**, 1773-82.
**Chen, X., Hiller, M., Sancak, Y. and Fuller, M. T.** (2005). Tissue-specific TAFs counteract Polycomb to turn on terminal differentiation. *Science* **310**, 869-72.
**Christich, A., Kauppila, S., Chen, P., Sogame, N., Ho, S. I. and Abrams, J. M.** (2002). The damage-responsive Drosophila gene sickle encodes a novel IAP binding protein similar to but distinct from reaper, grim, and hid. *Curr Biol* **12**, 137-40.
**Cryns, V. and Yuan, J.** (1998). Proteases to die for. *Genes Dev* **12**, 1551-70.
**Cumberledge, S., Zaratzian, A. and Sakonju, S.** (1990). Characterization of two RNAs transcribed from the cis-regulatory region of the abd-A domain within the Drosophila bithorax complex. *Proc Natl Acad Sci U S A* **87**, 3259-63.
**Dasen, J. S., Liu, J. P. and Jessell, T. M.** (2003). Motor neuron columnar fate imposed by sequential phases of Hox-c activity. *Nature* **425**, 926-33.
**Dasen, J. S., Tice, B. C., Brenner-Morton, S. and Jessell, T. M.** (2005). A Hox regulatory network establishes motor neuron pool identity and target-muscle connectivity. *Cell* **123**, 477-91.
**De Graeve, F., Jagla, T., Daponte, J. P., Rickert, C., Dastugue, B., Urban, J. and Jagla, K.** (2004). The *ladybird* homeobox genes are essential for the specification of a subpopulation of neural cells. *Dev Biol* **270**, 122-34.
**Delorenzi, M. and Bienz, M.** (1990). Expression of Abdominal-B homeoproteins in Drosophila embryos. *Development* **108**, 323-9.
**Deveraux, Q. L., Takahashi, R., Salvesen, G. S. and Reed, J. C.** (1997). X-linked IAP is a direct inhibitor of cell-death proteases. *Nature* **388**, 300-4.
**DiNardo, S., Kuner, J. M., Theis, J. and O'Farrell, P. H.** (1985). Development of embryonic pattern in D. melanogaster as revealed by accumulation of the nuclear engrailed protein. *Cell* **43**, 59-69.
**Dittrich, R., Bossing, T., Gould, A. P., Technau, G. M. and Urban, J.** (1997). The differentiation of the serotonergic neurons in the *Drosophila* ventral nerve cord depends on the combined function of the zinc finger proteins Eagle and Huckebein. *Development* **124**, 2515-25.
**Dixit, R., Vijayraghavan, K. and Bate, M.** (2008). Hox genes and the regulation of movement in Drosophila. *Dev Neurobiol* **68**, 309-16.
**Doe, C. Q.** (1992). Molecular markers for identified neuroblasts and ganglion mother cells in the Drosophila central nervous system. *Development* **116**, 855-63.
**Doe, C. Q., Smouse, D. and Goodman, C. S.** (1988). Control of neuronal fate by the *Drosophila* segmentation gene *even-skipped*. *Nature* **333**, 376-8.
**Dong, R. and Jacobs, J. R.** (1997). Origin and differentiation of supernumerary midline glia in *Drosophila* embryos deficient for apoptosis. *Dev Biol* **190**, 165-77.
**Economides, K. D., Zeltser, L. and Capecchi, M. R.** (2003). Hoxb13 mutations cause overgrowth of caudal spinal cord and tail vertebrae. *Dev Biol* **256**, 317-30.
**Frasch, M., Hoey, T., Rushlow, C., Doyle, H. and Levine, M.** (1987). Characterization and localization of the even-skipped protein of *Drosophila*. *Embo J* **6**, 749-59.
**Garcia-Bellido, A.** (1975). Genetic control of wing disc development in Drosophila. *Ciba Found Symp* **0**, 161-82.

**Gaufo, G. O., Thomas, K. R. and Capecchi, M. R.** (2003). Hox3 genes coordinate mechanisms of genetic suppression and activation in the generation of branchial and somatic motoneurons. *Development* **130**, 5191-201.
**Gaufo, G. O., Wu, S. and Capecchi, M. R.** (2004). Contribution of Hox genes to the diversity of the hindbrain sensory system. *Development* **131**, 1259-66.
**Gebelein, B., McKay, D. J. and Mann, R. S.** (2004). Direct integration of Hox and segmentation gene inputs during Drosophila development. *Nature* **431**, 653-9.
**Giraldez, A. J. and Cohen, S. M.** (2003). Wingless and Notch signaling provide cell survival cues and control cell proliferation during wing development. *Development* **130**, 6533-43.
**Goodman, C. S., Bastiani, M. J., Doe, C. Q., du Lac, S., Helfand, S. L., Kuwada, J. Y. and Thomas, J. B.** (1984). Cell recognition during neuronal development. *Science* **225**, 1271-9.
**Grenningloh, G., Rehm, E. J. and Goodman, C. S.** (1991). Genetic analysis of growth cone guidance in Drosophila: fasciclin II functions as a neuronal recognition molecule. *Cell* **67**, 45-57.
**Grether, M. E., Abrams, J. M., Agapite, J., White, K. and Steller, H.** (1995). The head involution defective gene of Drosophila melanogaster functions in programmed cell death. *Genes Dev* **9**, 1694-708.
**Grossniklaus, U., Pearson, R. K. and Gehring, W. J.** (1992). The Drosophila sloppy paired locus encodes two proteins involved in segmentation that show homology to mammalian transcription factors. *Genes Dev* **6**, 1030-51.
**Gutjahr, T., Patel, N. H., Li, X., Goodman, C. S. and Noll, M.** (1993). Analysis of the gooseberry locus in Drosophila embryos: gooseberry determines the cuticular pattern and activates gooseberry neuro. *Development* **118**, 21-31.
**Halter, D. A., Urban, J., Rickert, C., Ner, S. S., Ito, K., Travers, A. A. and Technau, G. M.** (1995). The homeobox gene *repo* is required for the differentiation and maintenance of glia function in the embryonic nervous system of *Drosophila melanogaster*. *Development* **121**, 317-32.
**Hassan, B. and Vaessin, H.** (1996). Regulatory interactions during early neurogenesis in Drosophila. *Dev Genet* **18**, 18-27.
**Hidalgo, A., Kinrade, E. F. and Georgiou, M.** (2001). The Drosophila neuregulin vein maintains glial survival during axon guidance in the CNS. *Dev Cell* **1**, 679-90.
**Higashijima, S., Shishido, E., Matsuzaki, M. and Saigo, K.** (1996). *eagle*, a member of the steroid receptor gene superfamily, is expressed in a subset of neuroblasts and regulates the fate of their putative progeny in the *Drosophila* CNS. *Development* **122**, 527-36.
**Hirth, F., Hartmann, B. and Reichert, H.** (1998). Homeotic gene action in embryonic brain development of Drosophila. *Development* **125**, 1579-89.
**Hombria, J. C. and Lovegrove, B.** (2003). Beyond homeosis--HOX function in morphogenesis and organogenesis. *Differentiation* **71**, 461-76.
**Igaki, T., Suzuki, Y., Tokushige, N., Aonuma, H., Takahashi, R. and Miura, M.** (2007). Evolution of mitochondrial cell death pathway: Proapoptotic role of HtrA2/Omi in Drosophila. *Biochem Biophys Res Commun* **356**, 993-7.
**Isshiki, T., Pearson, B., Holbrook, S. and Doe, C. Q.** (2001). Drosophila neuroblasts sequentially express transcription factors which specify the temporal identity of their neuronal progeny. *Cell* **106**, 511-21.
**Ito, K., Urban, J. and Technau, G. M.** (1995). Distribution, classification, and development of *Drosophila* glial cells in the late embryonic and early larval ventral nerve cord. *Roux's Arch. Dev. Biol.* **204**, 284-307.

**Jacobs, J. R. and Goodman, C. S.** (1989). Embryonic development of axon pathways in the Drosophila CNS. II. Behavior of pioneer growth cones. *J Neurosci* **9**, 2412-22.
**Jagla, K., Frasch, M., Jagla, T., Dretzen, G., Bellard, F. and Bellard, M.** (1997). *ladybird*, a new component of the cardiogenic pathway in *Drosophila* required for diversification of heart precursors. *Development* **124**, 3471-9.
**Jagla, K., Stanceva, I., Dretzen, G., Bellard, F. and Bellard, M.** (1994). A distinct class of homeodomain proteins is encoded by two sequentially expressed *Drosophila* genes from the 93D/E cluster. *Nucleic Acids Res* **22**, 1202-7.
**Jagla, T., Bellard, F., Lutz, Y., Dretzen, G., Bellard, M. and Jagla, K.** (1998). *ladybird* determines cell fate decisions during diversification of *Drosophila* somatic muscles. *Development* **125**, 3699-708.
**Jiang, C., Lamblin, A. F., Steller, H. and Thummel, C. S.** (2000). A steroid-triggered transcriptional hierarchy controls salivary gland cell death during Drosophila metamorphosis. *Mol Cell* **5**, 445-55.
**Johnson, E. C., Garczynski, S. F., Park, D., Crim, J. W., Nassel, D. R. and Taghert, P. H.** (2003). Identification and characterization of a G protein-coupled receptor for the neuropeptide proctolin in Drosophilamelanogaster. *Proc Natl Acad Sci U S A* **100**, 6198-203.
**Kambadur, R., Koizumi, K., Stivers, C., Nagle, J., Poole, S. J. and Odenwald, W. F.** (1998). Regulation of POU genes by castor and hunchback establishes layered compartments in the Drosophila CNS. *Genes Dev* **12**, 246-60.
**Karcavich, R. and Doe, C. Q.** (2005). *Drosophila* neuroblast 7-3 cell lineage: a model system for studying programmed cell death, Notch/Numb signaling, and sequential specification of ganglion mother cell identity. *J Comp Neurol* **481**, 240-51.
**Karch, F., Bender, W. and Weiffenbach, B.** (1990). abdA expression in Drosophila embryos. *Genes Dev* **4**, 1573-87.
**Kaufman, T. C., Seeger, M. A. and Olsen, G.** (1990). Molecular and genetic organization of the antennapedia gene complex of Drosophila melanogaster. *Adv Genet* **27**, 309-62.
**Khan, F. S., Fujioka, M., Datta, P., Fernandes-Alnemri, T., Jaynes, J. B. and Alnemri, E. S.** (2008). The interaction of DIAP1 with dOmi/HtrA2 regulates cell death in Drosophila. *Cell Death Differ* **15**, 1073-83.
**King, D. G. and Wyman, R. J.** (1980). Anatomy of the giant fibre pathway in Drosophila. I. Three thoracic components of the pathway. *J Neurocytol* **9**, 753-70.
**Klambt, C. and Goodman, C. S.** (1991). The diversity and pattern of glia during axon pathway formation in the Drosophila embryo. *Glia* **4**, 205-13.
**Kornberg, T., Siden, I., O'Farrell, P. and Simon, M.** (1985). The engrailed locus of Drosophila: in situ localization of transcripts reveals compartment-specific expression. *Cell* **40**, 45-53.
**Kurada, P. and White, K.** (1998). Ras promotes cell survival in Drosophila by downregulating hid expression. *Cell* **95**, 319-29.
**Kuroiwa, A., Kloter, U., Baumgartner, P. and Gehring, W. J.** (1985). Cloning of the homeotic Sex combs reduced gene in Drosophila and in situ localization of its transcripts. *Embo J* **4**, 3757-3764.
**Lee, N., Maurange, C., Ringrose, L. and Paro, R.** (2005). Suppression of Polycomb group proteins by JNK signalling induces transdetermination in Drosophila imaginal discs. *Nature* **438**, 234-7.

**LeMotte, P. K., Kuroiwa, A., Fessler, L. I. and Gehring, W. J.** (1989). The homeotic gene Sex Combs Reduced of Drosophila: gene structure and embryonic expression. *Embo J* **8**, 219-27.
**Lempradl, A. and Ringrose, L.** (2008). How does noncoding transcription regulate Hox genes? *Bioessays* **30**, 110-21.
**Levi-Montalcini, R.** (1987). The nerve growth factor 35 years later. *Science* **237**, 1154-62.
**Lewis, E. B.** (1978). A gene complex controlling segmentation in Drosophila. *Nature* **276**, 565-70.
**Lipshitz, H. D., Peattie, D. A. and Hogness, D. S.** (1987). Novel transcripts from the Ultrabithorax domain of the bithorax complex. *Genes Dev* **1**, 307-22.
**Liu, H., Strauss, T. J., Potts, M. B. and Cameron, S.** (2006). Direct regulation of egl-1 and of programmed cell death by the Hox protein MAB-5 and by CEH-20, a C. elegans homolog of Pbx1. *Development* **133**, 641-50.
**Lohmann, I., McGinnis, N., Bodmer, M. and McGinnis, W.** (2002). The Drosophila Hox gene deformed sculpts head morphology via direct regulation of the apoptosis activator reaper. *Cell* **110**, 457-66.
**Lundell, M. J., Lee, H. K., Perez, E. and Chadwell, L.** (2003). The regulation of apoptosis by Numb/Notch signaling in the serotonin lineage of *Drosophila*. *Development* **130**, 4109-21.
**Maelfait, J. and Beyaert, R.** (2008). Non-apoptotic functions of caspase-8. *Biochem Pharmacol* **76**, 1365-73.
**Mahaffey, J. W. and Kaufman, T. C.** (1987). Distribution of the Sex combs reduced gene products in Drosophila melanogaster. *Genetics* **117**, 51-60.
**Mann, R. S. and Hogness, D. S.** (1990). Functional dissection of Ultrabithorax proteins in D. melanogaster. *Cell* **60**, 597-610.
**Mann, R. S. and Morata, G.** (2000). The developmental and molecular biology of genes that subdivide the body of Drosophila. *Annu Rev Cell Dev Biol* **16**, 243-71.
**Marois, E., Mahmoud, A. and Eaton, S.** (2006). The endocytic pathway and formation of the Wingless morphogen gradient. *Development* **133**, 307-17.
**Martin-Bermudo, M. D., Martinez, C., Rodriguez, A. and Jimenez, F.** (1991). Distribution and function of the lethal of scute gene product during early neurogenesis in Drosophila. *Development* **113**, 445-54.
**Martin, D. N. and Baehrecke, E. H.** (2004). Caspases function in autophagic programmed cell death in Drosophila. *Development* **131**, 275-84.
**McGinnis, W. and Krumlauf, R.** (1992). Homeobox genes and axial patterning. *Cell* **68**, 283-302.
**Mettler, U., Vogler, G. and Urban, J.** (2006). Timing of identity: spatiotemporal regulation of hunchback in neuroblast lineages of Drosophila by Seven-up and Prospero. *Development* **133**, 429-37.
**Miguel-Aliaga, I. and Thor, S.** (2004). Segment-specific prevention of pioneer neuron apoptosis by cell-autonomous, postmitotic Hox gene activity. *Development* **131**, 6093-105.
**Miguel-Aliaga, I., Thor, S. and Gould, A. P.** (2008). Postmitotic specification of Drosophila insulinergic neurons from pioneer neurons. *PLoS Biol* **6**, e58.
**Monier, B., Astier, M., Semeriva, M. and Perrin, L.** (2005). Steroid-dependent modification of Hox function drives myocyte reprogramming in the Drosophila heart. *Development* **132**, 5283-93.
**Morata, G. and Lawrence, P. A.** (1975). Control of compartment development by the engrailed gene in Drosophila. *Nature* **255**, 614-7.

**Murray, T. V., McMahon, J. M., Howley, B. A., Stanley, A., Ritter, T., Mohr, A., Zwacka, R. and Fearnhead, H. O.** (2008). A non-apoptotic role for caspase-9 in muscle differentiation. *J Cell Sci* **121**, 3786-93.
**Novotny, T., Eiselt, R. and Urban, J.** (2002). Hunchback is required for the specification of the early sublineage of neuroblast 7-3 in the *Drosophila* central nervous system. *Development* **129**, 1027-36.
**Pai, C. Y., Kuo, T. S., Jaw, T. J., Kurant, E., Chen, C. T., Bessarab, D. A., Salzberg, A. and Sun, Y. H.** (1998). The Homothorax homeoprotein activates the nuclear localization of another homeoprotein, extradenticle, and suppresses eye development in Drosophila. *Genes Dev* **12**, 435-46.
**Patel, N. H., Schafer, B., Goodman, C. S. and Holmgren, R.** (1989). The role of segment polarity genes during Drosophila neurogenesis. *Genes Dev* **3**, 890-904.
**Pearson, J. C., Lemons, D. and McGinnis, W.** (2005). Modulating Hox gene functions during animal body patterning. *Nat Rev Genet* **6**, 893-904.
**Peifer, M. and Wieschaus, E.** (1990). Mutations in the Drosophila gene extradenticle affect the way specific homeo domain proteins regulate segmental identity. *Genes Dev* **4**, 1209-23.
**Perrin, L., Monier, B., Ponzielli, R., Astier, M. and Semeriva, M.** (2004). Drosophila cardiac tube organogenesis requires multiple phases of Hox activity. *Dev Biol* **272**, 419-31.
**Peterson, C., Carney, G. E., Taylor, B. J. and White, K.** (2002). *reaper* is required for neuroblast apoptosis during *Drosophila* development. *Development* **129**, 1467-76.
**Postlethwait, J. H. and Schneiderman, H. A.** (1969). A clonal analysis of determination in Antennapedia a homoeotic mutant of Drosophila melanogaster. *Proc Natl Acad Sci U S A* **64**, 176-83.
**Poulson, D. F.** (1950). Histogenesis, organogenesis and differentiation in the embryo of *Drosophila melanogaster* Meigen. In *Biology of Drosophila*, (ed. M.Demerec), pp. 168-274. New York: Wiley.
**Primrose, D. A., Chaudhry, S., Johnson, A. G., Hrdlicka, A., Schindler, A., Tran, D. and Foley, E.** (2007). Interactions of DNR1 with the apoptotic machinery of Drosophila melanogaster. *J Cell Sci* **120**, 1189-99.
**Prokop, A., Bray, S., Harrison, E. and Technau, G. M.** (1998). Homeotic regulation of segment-specific differences in neuroblast numbers and proliferation in the Drosophila central nervous system. *Mech Dev* **74**, 99-110.
**Prokop, A. and Technau, G. M.** (1994). Early tagma-specific commitment of Drosophila CNS progenitor NB1-1. *Development* **120**, 2567-78.
**Rauskolb, C., Peifer, M. and Wieschaus, E.** (1993). extradenticle, a regulator of homeotic gene activity, is a homolog of the homeobox-containing human proto-oncogene pbx1. *Cell* **74**, 1101-12.
**Rieckhof, G. E., Casares, F., Ryoo, H. D., Abu-Shaar, M. and Mann, R. S.** (1997). Nuclear translocation of extradenticle requires homothorax, which encodes an extradenticle-related homeodomain protein. *Cell* **91**, 171-83.
**Ringrose, L. and Paro, R.** (2007). Polycomb/Trithorax response elements and epigenetic memory of cell identity. *Development* **134**, 223-32.
**Rogulja-Ortmann, A., Luer, K., Seibert, J., Rickert, C. and Technau, G. M.** (2007). Programmed cell death in the embryonic central nervous system of Drosophila melanogaster. *Development* **134**, 105-16.
**Rogulja-Ortmann, A., Renner, S. and Technau, G. M.** (2008). Antagonistic roles for Ultrabithorax and Antennapedia in regulating segment-specific apoptosis of

differentiated motoneurons in the Drosophila embryonic central nervous system. *Development* **135**, 3435-45.
**Rogulja-Ortmann, A. and Technau, G. M.** (2008). Multiple roles for Hox genes in segment-specific shaping of CNS lineages. *Fly (Austin)* **2**.
**Rozowski, M. and Akam, M.** (2002). Hox gene control of segment-specific bristle patterns in Drosophila. *Genes Dev* **16**, 1150-62.
**Ryoo, H. D., Gorenc, T. and Steller, H.** (2004). Apoptotic cells can induce compensatory cell proliferation through the JNK and the Wingless signaling pathways. *Dev Cell* **7**, 491-501.
**Sanchez-Elsner, T., Gou, D., Kremmer, E. and Sauer, F.** (2006). Noncoding RNAs of trithorax response elements recruit Drosophila Ash1 to Ultrabithorax. *Science* **311**, 1118-23.
**Sanchez-Herrero, E. and Akam, M.** (1989). Spatially ordered transcription of regulatory DNA in the bithorax complex of Drosophila. *Development* **107**, 321-9.
**Sanchez-Herrero, E. and Crosby, M. A.** (1988). The Abdominal-B gene of Drosophila melanogaster: overlapping transcripts exhibit two different spatial distributions. *Embo J* **7**, 2163-2173.
**Sanchez-Herrero, E., Vernos, I., Marco, R. and Morata, G.** (1985). Genetic organization of Drosophila bithorax complex. *Nature* **313**, 108-13.
**Schmid, A., Chiba, A. and Doe, C. Q.** (1999). Clonal analysis of *Drosophila* embryonic neuroblasts: neural cell types, axon projections and muscle targets. *Development* **126**, 4653-89.
**Schmidt, H., Rickert, C., Bossing, T., Vef, O., Urban, J. and Technau, G. M.** (1997). The embryonic central nervous system lineages of *Drosophila melanogaster*. II. Neuroblast lineages derived from the dorsal part of the neuroectoderm. *Dev Biol* **189**, 186-204.
**Seeger, M., Tear, G., Ferres-Marco, D. and Goodman, C. S.** (1993). Mutations affecting growth cone guidance in Drosophila: genes necessary for guidance toward or away from the midline. *Neuron* **10**, 409-26.
**Sink, H. and Whitington, P. M.** (1991). Location and connectivity of abdominal motoneurons in the embryo and larva of Drosophila melanogaster. *J Neurobiol* **22**, 298-311.
**Skeath, J. B.** (1999). At the nexus between pattern formation and cell-type specification: the generation of individual neuroblast fates in the Drosophila embryonic central nervous system. *Bioessays* **21**, 922-31.
**Skeath, J. B. and Carroll, S. B.** (1992). Regulation of proneural gene expression and cell fate during neuroblast segregation in the Drosophila embryo. *Development* **114**, 939-46.
**Sonnenfeld, M. J. and Jacobs, J. R.** (1995). Macrophages and glia participate in the removal of apoptotic neurons from the *Drosophila* embryonic nervous system. *J Comp Neurol* **359**, 644-52.
**Spana, E. P. and Doe, C. Q.** (1996). Numb antagonizes Notch signaling to specify sibling neuron cell fates. *Neuron* **17**, 21-6.
**Srinivasula, S. M., Datta, P., Kobayashi, M., Wu, J. W., Fujioka, M., Hegde, R., Zhang, Z., Mukattash, R., Fernandes-Alnemri, T., Shi, Y. et al.** (2002). sickle, a novel Drosophila death gene in the reaper/hid/grim region, encodes an IAP-inhibitory protein. *Curr Biol* **12**, 125-30.
**Sun, Y. H., Tsai, C. J., Green, M. M., Chao, J. L., Yu, C. T., Jaw, T. J., Yeh, J. Y. and Bolshakov, V. N.** (1995). White as a reporter gene to detect transcriptional

silencers specifying position-specific gene expression during Drosophila melanogaster eye development. *Genetics* **141**, 1075-86.
**Tabata, T., Schwartz, C., Gustavson, E., Ali, Z. and Kornberg, T. B.** (1995). Creating a Drosophila wing de novo, the role of engrailed, and the compartment border hypothesis. *Development* **121**, 3359-69.
**Technau, G. M., Berger, C. and Urbach, R.** (2006). Generation of cell diversity and segmental pattern in the embryonic central nervous system of Drosophila. *Dev Dyn* **235**, 861-9.
**Tenev, T., Zachariou, A., Wilson, R., Paul, A. and Meier, P.** (2002). Jafrac2 is an IAP antagonist that promotes cell death by liberating Dronc from DIAP1. *Embo J* **21**, 5118-29.
**Tiong, S., Bone, L. M. and Whittle, J. R.** (1985). Recessive lethal mutations within the bithorax-complex in Drosophila. *Mol Gen Genet* **200**, 335-42.
**Tsuji, T., Hasegawa, E. and Isshiki, T.** (2008). Neuroblast entry into quiescence is regulated intrinsically by the combined action of spatial Hox proteins and temporal identity factors. *Development* **135**, 3859-69.
**Twomey, C. and McCarthy, J. V.** (2005). Pathways of apoptosis and importance in development. *J Cell Mol Med* **9**, 345-59.
**Udolph, G., Luer, K., Bossing, T. and Technau, G. M.** (1995). Commitment of CNS progenitors along the dorsoventral axis of Drosophila neuroectoderm. *Science* **269**, 1278-81.
**Uemura, T., Shepherd, S., Ackerman, L., Jan, L. Y. and Jan, Y. N.** (1989). numb, a gene required in determination of cell fate during sensory organ formation in Drosophila embryos. *Cell* **58**, 349-60.
**Villares, R. and Cabrera, C. V.** (1987). The achaete-scute gene complex of D. melanogaster: conserved domains in a subset of genes required for neurogenesis and their homology to myc. *Cell* **50**, 415-24.
**von Hilchen, C. M., Beckervordersandforth, R. M., Rickert, C., Technau, G. M. and Altenhein, B.** (2008). Identity, origin, and migration of peripheral glial cells in the Drosophila embryo. *Mech Dev* **125**, 337-52.
**Vucic, D., Kaiser, W. J., Harvey, A. J. and Miller, L. K.** (1997). Inhibition of reaper-induced apoptosis by interaction with inhibitor of apoptosis proteins (IAPs). *Proc Natl Acad Sci U S A* **94**, 10183-8.
**Vucic, D., Kaiser, W. J. and Miller, L. K.** (1998). Inhibitor of apoptosis proteins physically interact with and block apoptosis induced by Drosophila proteins HID and GRIM. *Mol Cell Biol* **18**, 3300-9.
**Wakimoto, B. T., Turner, F. R. and Kaufman, T. C.** (1984). Defects in embryogenesis in mutants associated with the antennapedia gene complex of Drosophila melanogaster. *Dev Biol* **102**, 147-72.
**White, K., Grether, M. E., Abrams, J. M., Young, L., Farrell, K. and Steller, H.** (1994). Genetic control of programmed cell death in *Drosophila*. *Science* **264**, 677-83.
**White, K., Tahaoglu, E. and Steller, H.** (1996). Cell killing by the Drosophila gene reaper. *Science* **271**, 805-7.
**White, R. A. and Lehmann, R.** (1986). A gap gene, hunchback, regulates the spatial expression of Ultrabithorax. *Cell* **47**, 311-21.
**White, R. A. and Wilcox, M.** (1984). Protein products of the bithorax complex in Drosophila. *Cell* **39**, 163-71.
**White, R. A. and Wilcox, M.** (1985). Distribution of Ultrabithorax proteins in Drosophila. *Embo J* **4**, 2035-2043.

**Whittle, J. R., Tiong, S. Y. and Sunkel, C. E.** (1986). The effect of lethal mutations and deletions within the bithorax complex upon the identity of caudal metameres in the Drosophila embryo. *J Embryol Exp Morphol* **93**, 153-66.
**Wichmann, A., Jaklevic, B. and Su, T. T.** (2006). Ionizing radiation induces caspase-dependent but Chk2- and p53-independent cell death in Drosophila melanogaster. *Proc Natl Acad Sci U S A* **103**, 9952-7.
**Wilson, R., Goyal, L., Ditzel, M., Zachariou, A., Baker, D. A., Agapite, J., Steller, H. and Meier, P.** (2002). The DIAP1 RING finger mediates ubiquitination of Dronc and is indispensable for regulating apoptosis. *Nat Cell Biol* **4**, 445-50.
**Wimmer, E. A., Carleton, A., Harjes, P., Turner, T. and Desplan, C.** (2000). Bicoid-independent formation of thoracic segments in Drosophila. *Science* **287**, 2476-9.
**Wing, J. P., Karres, J. S., Ogdahl, J. L., Zhou, L., Schwartz, L. M. and Nambu, J. R.** (2002). Drosophila sickle is a novel grim-reaper cell death activator. *Curr Biol* **12**, 131-5.
**Wu, X., Vasisht, V., Kosman, D., Reinitz, J. and Small, S.** (2001). Thoracic patterning by the Drosophila gap gene hunchback. *Dev Biol* **237**, 79-92.
**Xiong, W. C., Okano, H., Patel, N. H., Blendy, J. A. and Montell, C.** (1994). *repo* encodes a glial-specific homeo domain protein required in the *Drosophila* nervous system. *Genes Dev* **8**, 981-94.
**Xu, D., Woodfield, S. E., Lee, T. V., Fan, Y., Antonio, C. and Bergmann, A.** (2009). Genetic control of programmed cell death (apoptosis) in Drosophila. *Fly (Austin)* **3**.
**Yu, S. Y., Yoo, S. J., Yang, L., Zapata, C., Srinivasan, A., Hay, B. A. and Baker, N. E.** (2002). A pathway of signals regulating effector and initiator caspases in the developing Drosophila eye. *Development* **129**, 3269-78.
**Zhang, Y., Ungar, A., Fresquez, C. and Holmgren, R.** (1994). Ectopic expression of either the Drosophila gooseberry-distal or proximal gene causes alterations of cell fate in the epidermis and central nervous system. *Development* **120**, 1151-61.
**Zhou, L., Hashimi, H., Schwartz, L. M. and Nambu, J. R.** (1995). Programmed cell death in the *Drosophila* central nervous system midline. *Curr Biol* **5**, 784-90.
**Zhu, B., Pennack, J. A., McQuilton, P., Forero, M. G., Mizuguchi, K., Sutcliffe, B., Gu, C. J., Fenton, J. C. and Hidalgo, A.** (2008). Drosophila neurotrophins reveal a common mechanism for nervous system formation. *PLoS Biol* **6**, e284.

# 7. Appendix

## Abbreviation index

| | |
|---|---|
| A1-A9 | abdominal segment one to nine |
| aCC | anterior corner cell |
| AEL | after egg laying |
| AP | anterio-posterior |
| C1-C3 | gnathal segments one to three |
| cDNA | copy DNA |
| CNS | central nervous system |
| DEPC-$H_2O$ | diethlpyrocarbonate-treated water |
| *Def* | deficiency |
| DIG | Digoxigenin |
| DiI | 1,1'-Dioctadecyl-3,3,3',3'-tetramethylindocarbocyanideperchlorate |
| DNA | deoxyribonucleic acid |
| DSHB | Developmental Studies Hybridoma Bank |
| DV | dorso-ventral |
| et al. | and others |
| Fig. | figure |
| FITC | Fluorescein-isothiocyanate |
| g | gram |
| Gal | galactosidase |
| GB | glioblast |
| GFP | green fluorescent protein |
| GMC | ganglion mother cell |
| hr(s) | hour(s) |
| HRP | horseradish peroxidase |
| hs | hemisegment |
| HS | heat shock |
| Hyb | hybridization |

| | |
|---|---|
| ISN | intersegmental nerve |
| kb | kilobases |
| L | liter |
| Lb | labial segment |
| M | molar |
| Md | mandibular segment |
| mg | milligram |
| min | minutes |
| ml | milliliter |
| µl | microliter |
| mM | millimolar |
| mRNA | messenger RNA |
| Mx | maxillary segment |
| n | number of samples |
| NB | neuroblast |
| ON | overnight |
| pCC | posterior corner cell |
| pNR | procephalic neurogenic region |
| PNS | peripheral nervous system |
| RNA | ribonucleic acid |
| RP2 | Royal Prawn 2 |
| RT | room temperature |
| S1-S5 | segregation wave one to five |
| SN | segmental nerve |
| ssDNA | single-stranded DNA, salmon sperm DNA |
| St. | developmental stage |
| T1-T3 | thoracic segment one to three |
| TN | transversal nerve |
| UAS | upstream activating sequence |
| UTP | uridine triphosphate |
| VNC | ventral nerve cord |
| vNE | ventral neuroectoderm |
| vNR | ventral neurogenic region |
| WT | wild type |

# Declaration

Versicherung gemäß §11, Abs.3d der Promotionsordnung

1. Ich habe die als Dissertation vorgelegte Arbeit selbst angefertigt und alle benutzten Hilfemittel (Literatur, Apparaturen, Material) in der Arbeit angegeben.

2. Ich habe und hatte die als Dissertation vorgelegte Arbeit nicht als Prüfungsarbeit für eine staatliche oder andere wissenschaftliche Prüfung eingereicht.

3. Ich hatte weder die als Dissertation vorgelegte Arbeit noch Teile einer Abhandlung davon bei einer anderen Fakultät bzw. einem anderen Fachbereich als Dissertation eingereicht.

Mainz, den _____

Ana Rogulja-Ortmann